International Journal of Computer Science in Sport

Volume 9/Edition 1

ISSN 1684-4769

TABLE OF CONTENTS

Editorial

Arnold Baca

Department of Biomechanics, Kinesiology and Applied Computer Science,

ZSU, University of Vienna

Dear readers:

Welcome to the summer 2010 issue of the **International Journal of Computer Science in Sport (IJCSS)**.

Two full papers and three project reports have been included within this issue.

B. Eskofier, M. Wagner, I. Munson and **M. Oleson** present classifiers for speed and inclination during running based on features, which can be calculated on microprocessors embedded in a shoe.

In the paper by **P. Lamb, R. Bartlett** and **A. Robins** self organizing maps (SOMs) are used to classify the coordination patterns of four participants performing three different types of basket ball shot from different distances. The authors conclude that SOMs may be helpful in recognizing aspects that are not obvious from more traditional approaches.

N. Hirotsu, M. Ito, C. Miyaji, K. Hamano and **A. Taguchi** analyze tactical conflicts between attacking formations and blocking formations in the phase of reception attack in volleyball by using a zero-sum game model. They resume that their method could be a promising alternative in volleyball match analysis.

A Genetic Algorithm is applied by **S. Lenjan-nejadian** and **M. Rostami** in order to optimize the motion of a weightlifter snatching.

N. Roznawski and **J. Wiemeyer** report an experimental pilot study which tested e-learning units with different degrees of interactivity. No significant impact on knowledge improvement could be found.

I hope you enjoy this issue.

If you have any questions, comments, suggestions and points of criticism, please send them to me.

Enjoy the summer!

Arnold Baca, Editor in Chief

University of Vienna, arnold.baca@univie.ac.at

Embedded Classification of Speed and Inclination during Running

Bjoern Eskofier[1], Martin Wagner[2], Ian Munson[3] and Mark Oleson[3]

[1]Human Performance Lab, Faculty of Kinesiology, University of Calgary, Canada

[2]Pattern Recognition Lab, University of Erlangen-Nuremberg, Germany

[3]adidas innovation team ait., adidas AG, Portland OR, USA

Abstract

This paper presents methods for classifying speed and track inclination groups during recreational runs using input data from the "adidas_1" running shoe. Running speed, altitude and shoe heel compression were recorded continuously while athletes ran freely outdoors. A total of 84 one-hour-runs were collected in order to have sufficient ground truth as well as sensor data for classification. The data was analyzed using features computed for each step of the athlete.

The goal of this work was to distinguish three speed and three surface inclination classes, respectively. The speed and inclination classes were established using the collected ground truth data.

The results showed that surface inclination classification was only possible with an accuracy of 67.2% due to measurement restrictions. However, it is also demonstrated that speed classification was feasible with up to 89.2% accuracy.

The developed classification system for speed classification was implemented and verified on the embedded microprocessor of the "adidas_1". Such a system can be used to support sportsmen, for example by adapting their equipment to the specific running speed. The employed pattern recognition methods are general in nature and can thus be applied to other embedded classification applications as well.

KEYWORDS: EMBEDDED CLASSIFICATION, TRACK INCLINATION CLASSIFICATION, SPEED CLASSIFICATION, DIGITAL SPORTS, ADIDAS_1

Introduction

Smart sensors embedded in clothes and equipment for sports open novel opportunities to support and guide athletes. An example is the "adidas_1" running shoe, which is the first shoe that features an embedded system (see Figure 1). This shoe was built to adapt to various running conditions. Examples for conditions that have to be taken into account include the prevailing surface situation, the fatigue state and the speed of the runner.

The adaptation was performed by changing the cushioning of the sole by a motor driven cable system inside the shoe. In order to recognize the current running situation, the heel compression of the shoe was continuously measured. The embedded microprocessor of the "adidas_1" processed this signal and performed a classification of the prevailing situation. Based on this classification result, a decision for a cushioning adaptation was made.

Pattern recognition methods in general were frequently used in recent locomotion related research (e.g. Schöllhorn, 2004; Wu & Wang, 2008). For example, a wavelet transformation was applied to electromyographic signals of runners (von Tscharner & Goepfert, 2003) for feature extraction. The resulting multi-muscle pattern could be employed for gender classification with high classification rate of 95%. In another study, the authors calculated three types of features (basic temporal/spatial, kinetic and kinematic) on human walking gait data (Begg & Kamruzzaman, 2005). The resulting set of 24 features was utilized to distinguish the gait of young and elderly subjects with a classification rate of 91.7%. Those application examples illustrated that pattern recognition algorithms can contribute considerably to data analysis tasks in locomotion related projects.

To the best of our knowledge, the embedded classification of running speed and surface inclination using the described compression measurements has previously not been investigated in the literature. Previous publications with the purpose of classifying these two variables used different sensor input and were not focused on embedded implementation. For example, a method for walking gait that was based on accelerometer measurements was presented (Aminian et al., 1995). For classification, the authors applied a neural network. The methodology was subsequently extended (Herren et al., 1999) for outdoor running. However, these approaches were based on triaxial accelerometry. The acceleration signal had implicitly included the running speed in its signal. Thus, the results from these studies could not be compared to results derived from compression measurements that were the basis for the running speed and surface inclination classification system that was developed in the present paper. Moreover, the measured signals were evaluated on PC hardware only. The complex mathematical calculations used for the complex neural networks that were employed (Aminian, et al., 1995; Herren, et al., 1999) may not have been possible with an embedded microprocessor. Nevertheless, the embedded classification of the speed and the track inclination variables were important in the "adidas_1" application scenario. Hence, the primary purpose of this paper was to use methods from pattern recognition to identify a classification system that distinguished three speed and three inclination classes based on the heel compression measurements.

In general, athletes can benefit from embedded classification systems. In the particular case of running with the "adidas_1", the shoe could be adapted accordingly, setting itself into a cushioning state that was considered optimal for the given situation. However, the "adidas_1" shoe was just one example of smart sensors embedded in apparel and sport equipment. Comparable systems could be useful in other sports where an athlete can be actively supported by adapting the equipment to the prevailing situation. In a previous publication (Eskofier et al., 2009), it was already demonstrated that accurate classification on an embedded microprocessor in sports was feasible. For this purpose, a framework for embedded classification was developed. This framework aimed at calculating features that described the originally measured signal well, while being at the same time efficiently calculable on embedded hardware. It was also discussed, which types of classifiers are suited for implementation on embedded hardware. The key idea that was followed was to conduct the various experiments on computationally powerful desktop computers, and to implement and validate only the most promising solution on the embedded hardware. Comparable systems could be useful in other sports where an athlete can be actively supported by adapting the equipment to the prevailing situation. Therefore, the secondary purpose of this paper was to further develop the previously employed (Eskofier, et al., 2009) general methods for embedded classification, so that the developed methodology could be more straightforwardly applied to other similar embedded classification tasks.

Methods

Data Collection

A total of 84 runners (30 female, 54 male) participated in a one-hour outdoor data collection. The age of the subjects was 32.9 ± 7.9 years (average, standard deviation). The subjects were not specifically chosen according to running experience; instead, the group contained runners of all activity levels. The measurement system consisted of three separate devices. Firstly, a "Polar RS800 Running Computer" (Polar Electro Oy, 2010) was used, which included an "S3 stride sensor" and a chest strap. This system was capable of measuring running speed, stride frequency and barometric height. The sampling interval for the collected signals was set to 5 s. These measurements formed the ground truth data, which means that the classes for the subsequent classification experiments were assigned according to these measurements.

Secondly, the heel compression signal f[t] of the runners was continuously measured using the "adidas_1" shoe (DiBenedetto et al., 2004; Eskofier, et al., 2009). The heel part of the shoe contained an adjustable cushioning element (Figure 1). The amount of vertical compression that this element allowed was regulated by a motor-driven cable system (DiBenedetto, et al., 2004). For the purpose of the data collection for this study, the cushioning element was manually put in a setting that allowed maximal heel compression and was not changed subsequently. This setting was chosen because the resulting compression signal had the highest possible signal-to-noise ratio. A hall sensor mounted at the top of the cushioning element detected the magnetic field strength induced by a small magnet at the bottom of the element. The sensor was sampled with a rate f_s = 342 Hz by the embedded microprocessor. The sensor-magnet distance d_m was computed from the measured field strength with an accuracy of ± 0.1 mm (Figure 3).

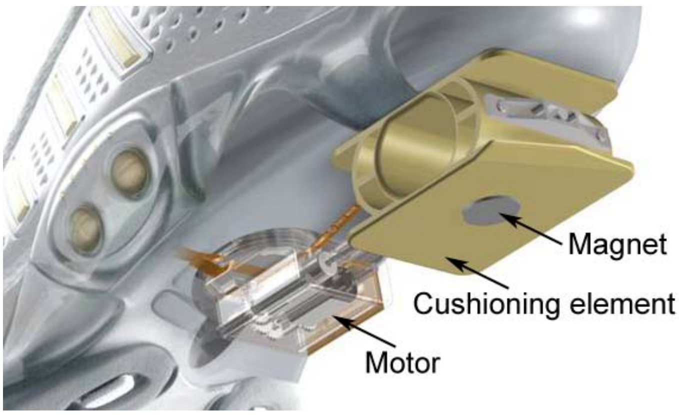

Figure 1. The "adidas_1" shoe, its cushioning element, magnet and motor unit (DiBenedetto, et al., 2004; Eskofier, et al., 2009)

Lastly, a specially programmed mobile phone (Eskofier et al., 2008) was used to store the GPS position of the runner in intervals of 1 s. This allowed reconstructing all running situations after data collection. An example run is visualized in Figure 2 based on the Google Earth (Google Inc., Mountain View, CA, USA) software. In this illustration, running speed is displayed as the height of the orange band along the running track. The software (Eskofier & Melzer, 2009) that was utilized to generate Figure 2 is available for download from http://tinyurl.com/gervit.

After completion of the run, each participant was asked to fill in a questionnaire. Among other information, the questionnaire asked the test subjects whether they thought that the amount of equipment was in any way hindering to their run. Only two out of the 84 runners perceived a notable impediment by the equipment while running. This indicated that the collected data represented a free outdoor run very well (Eskofier, et al., 2008).

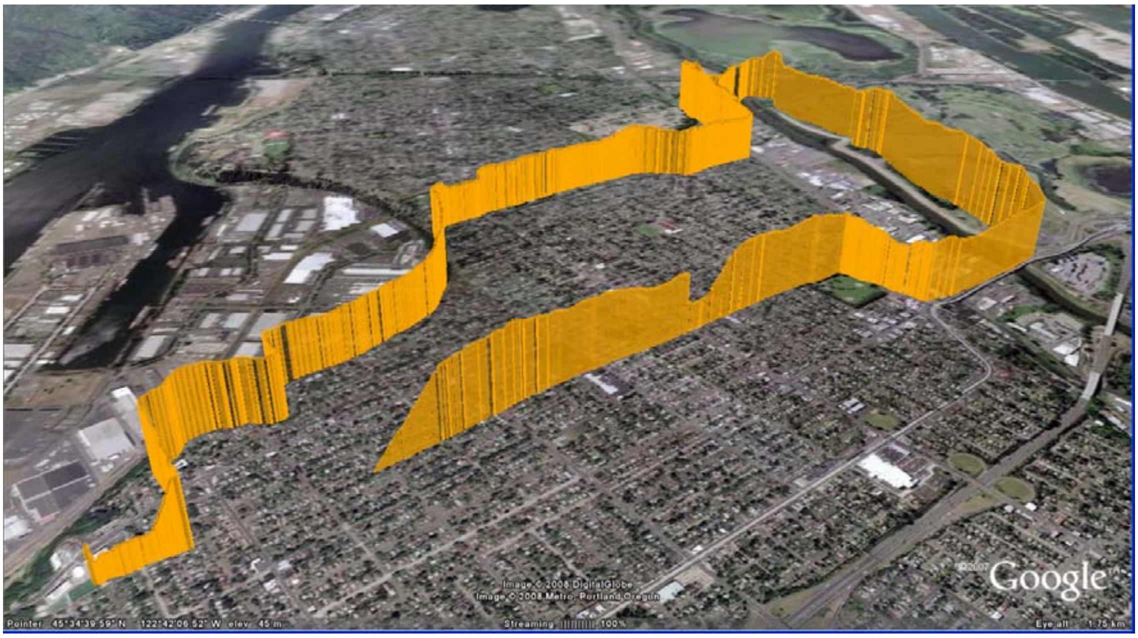

Figure 2. Visualization of an example run in Portland, OR, USA. The height of the band represents the running speed.

Data Processing

Out of the 84 study participants, 28 had to be excluded from further processing for various reasons. More specifically, five runners had incomplete data from the Polar RS800 system. The remaining 23 participants had to be excluded because of unusable data from the "adidas_1" shoe. In eight of these cases, data collection was not possible because the "adidas_1" was not present in all shoe sizes at the beginning of the study, and therefore the runners had to use other shoe models. In the remaining 15 cases (about 18% of all subjects), the runners were mid- or forefoot strikers. The measurement system of the "adidas_1" is located at the heel of the shoe and can therefore only capture meaningful data for rearfoot strikers, which represent more than 80% of the running population (Kerr et al., 1983).

Step Segmentation

Prior to feature extraction, the single strides were segmented by finding the deflection of the respective compression phases. Figure 3 shows an example representation of the heel compression signal. The task of step segmentation was to find the beginning of the compression phase, i.e. the point in time when the runners started to compress the heel. A linear filter with the convolution vector

$$v_{con} = (-1, -1, -1, -1, -1, -1, -1, -1, 0, 1, 1, 1, 1, 1, 1, 1) \quad (1)$$

was used for this purpose. It was implemented with a moving window strategy in order to minimize the number of multiplications. That means that when a new sample was measured, the multiplication with the filter was only computed once. The multiplication result was stored in a ring buffer which contained only the preceding results according to the filter length. For each new sample, the filter output was then updated according to the elements in the buffer.

The filter was chosen for two reasons. First, noise was present in the signal during the time that the foot was in the air (Figure 3). The filter had sufficient length to avoid misdetecting this noise as beginning of compression. Second, the filter yielded maxima for the beginning of the compression phase. The respective maxima after filtering marked the beginnings of the compression phase. In Figure 3, the points where the maxima were located are depicted as red crosses.

The beginnings of each compression phase were defining the starts of consecutive strides $t_{s,i}$ and $t_{s,i+1}$, with i and i+1 indicating the respective stride number. Within the boundaries of one single stride, the point of maximum compression $t_{m,i}$ was identified by a linear search. The points of maximum compression are depicted as red circles in Figure 3. The end of the compression phase $t_{c,i}$ (depicted with red stars in Figure 3) was defined by the first sample value after maximum compression that was greater than the mean value before the actual compression phase minus two sample units. The reliability of this method was tested by visual inspection of 449 measured strides from 6 subjects (Eskofier, et al., 2009). The end of the compression phase was always identified at the correct position.

Feature Extraction

From every step, eleven hand-selected features were calculated (Table 1 and Figure 3). These basic features were denoted by $F_1 \ldots F_{11}$. In order to add context information, the means μ_N and standard deviations σ_N over the features of the preceding $N = \{4, 8, 16\}$ steps were also calculated. These features were denoted $\mu_N(F_n)$ and $\sigma_N(F_n)$, and were calculated from the $n = 1, \ldots, 11$ basic features. For standard deviation calculation the unbiased version given in Equation 2 was used. In this equation, c_m denotes a single calculated feature value for stride number m and $\overline{c}$ is the mean value of the respective feature values.

$$\sigma_N = \left(\frac{1}{N-1} \sum_{m=1}^{N} \left(c_m - \overline{c} \right) \right) \tag{2}$$

The gradients of all 11 basic features using N = 16 steps were also calculated and were denoted $g_{16}(F_n)$. Consequently, a total of N_f = 88 features were calculated. For feature extraction, the first five minutes of each run were not considered to ensure that the runners were warmed up and accustomed to data collection.

The obvious redundancy that was contained in these 88 extracted features was volitional. It was a goal from the start to use only a subset of the originally computed features in order to reduce complexity and to use only features with small or no mutual dependence. The feature subset selection algorithm will be presented below.

When conducting the speed classification experiments, it was noticed that a runner dependent feature rescaling considerably improved the result. A rescaling to the [0, 1] interval for each feature F_n of a runner according to

$$\hat{F}_n = \frac{F_n - \min(F_n)}{\max(F_n) - \min(F_n)} \tag{3}$$

was therefore implemented for each of the $n = 1, \ldots, N_f, = 88$ features for the speed classification experiments. In this equation, $\hat{F}_n$ denominates the rescaled feature value.

Table 1. Definition of the eleven basic features. From these, additional features were derived by computing context information over multiple steps. The resulting feature vector had 88 dimensions.

Nr.	Name	Formula
F_1	Inter step time	$t_{s,i+1} - t_{s,i}$
F_2	Time to peak	$t_{m,i} - t_{s,i}$
F_3	Maximum compression	$f[t_{m,i}]$ (measured value at $t_{m,i}$)
F_4	Compression time	$t_{c,i} - t_{s,i}$
F_5	Mean compression	$1/F_{4,i} \sum_{m=t_{s,i}}^{t_{c,i}} f[m]$
F_6	Step mass center	$1/F_{7,i} \sum_{m=t_{s,i}}^{t_{c,i}} \left(\left(m - t_{s,i}\right) f[m]\right)$
F_7	Step energy	$\sum_{m=t_{s,i}}^{t_{c,i}} f[m]$
F_8	Normalized compression time	F_4 / F_1
F_9	Normalized time to peak	F_2 / F_4
F_{10}	Compression gradient	$(f[t_{m,i}] - f[t_{s,i}]) / F_{2,i}$
F_{11}	Decompression gradient	$(f[t_{c,i}] - f[t_{m,i}]) / (t_{c,i} - t_{m,i})$

Labeling

After consulting four sports experts, three classes according to running speed v and surface inclination, respectively, were defined (Table 2, Table 3). The class definition was chosen in a way that the resulting ranges of running speeds and inclinations covered an approximately equal amount of the distribution of the respective values for a typical training run. For this definition, an internal adidas report was used that had investigated relevant running speed and inclination distributions. In Table 2 and Table 3, $k = 1 \ldots 3$ indicates the class number. Each detected step was labeled for the subsequent classification experiments according to these classes using the measured ground truth speed and surface inclination signals.

Table 2. Definition of the three classes according to running speed v.

Class	Class definition in m/s	
$\omega_{1,v}$	$0 \leq v$	< 2.5
$\omega_{2,v}$	$2.5 \leq v$	< 3.6
$\omega_{3,v}$	$3.6 \leq v$	

Table 3. Definition of the three classes according to surface inclination α. A negative value indicates that the athlete was running downhill.

Class	Class definition in deg.
$\omega_{1,\alpha}$	$\alpha < -3°$
$\omega_{2,\alpha}$	$-3° \leq \alpha \leq 3°$
$\omega_{3,\alpha}$	$3° < \alpha$

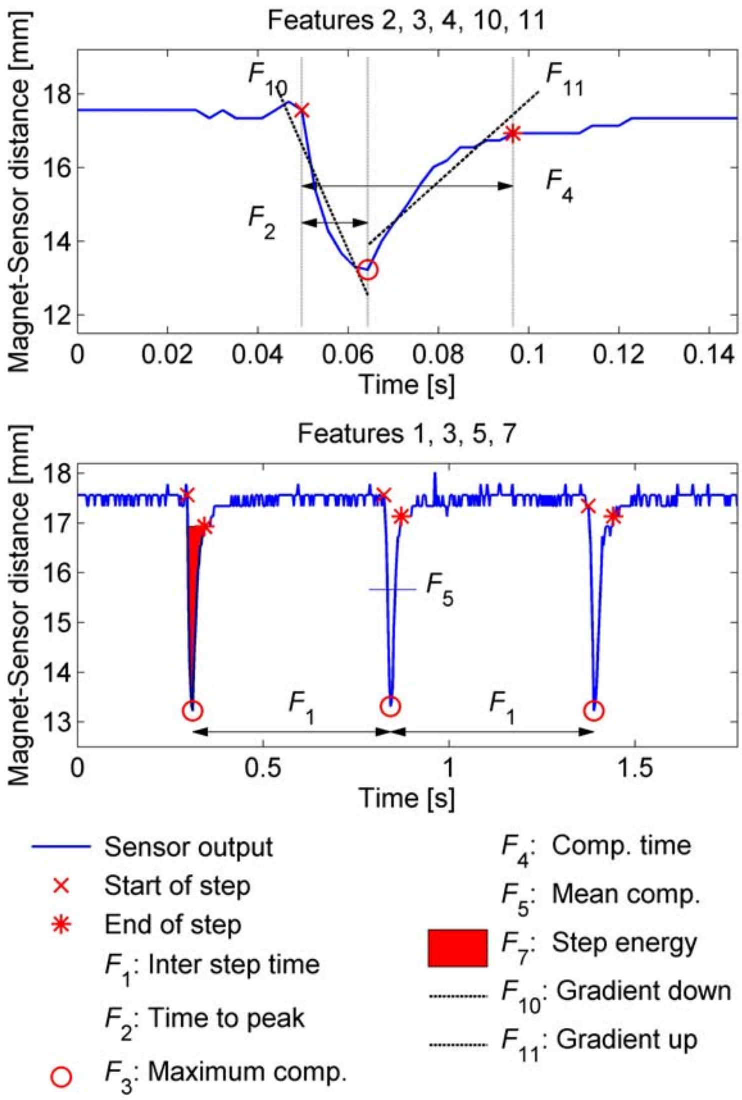

Figure 3. Illustration of the eleven basic features. From these, additional features were derived by computing context information over multiple steps. The resulting feature vector had 88 dimensions.

Classifiers

In the classification experiments, five different classifiers were compared in order to evaluate their performance on the measured data. The selected classifiers were chosen because each of them can be implemented on an embedded microprocessor. More specifically, the following classifiers were used for the evaluation:

- Bayes Classifier (BC). The BC makes use of the assumption that all features are mutually independently distributed (Niemann, 1983). This assumption allows a straightforward estimation of the classifier parameters from the samples that are used for classifier training by direct mean and variance computation. The resulting linear discriminant function g_k can be computed by a multiplication of each feature with a weight factor, adding the results of the multiplications and comparing the sum against a threshold. Due to this simplicity, the BC is well suited for embedded implementation. The BC has been proven to perform well in many classification tasks (Domingos & Pazzani, 1997; Langley et al., 1992).
- Linear Discriminant Analysis (LDA). The LDA classifier is based on Fisher's (Fisher, 1936) work on discriminant methods. It is a transformation that aims at minimizing the variability within a class, and maximizing the distance between classes. When LDA is applied for classification, the feature space is effectively projected onto a single axis. On this single axis, a linear decision boundary is applied for differentiation. In contrast to BC, the full covariance of the distribution is considered. However, the resulting linear discriminant function g_k can be implemented in the same simple way as for the BC. Applications of LDA can be found in a variety of fields, including face recognition (Lu et al., 2003) and document classification (Ye & Li, 2005).
- Polynomial Classifier (PC). The PC does, in contrast to BC and LDA, not use the parameters of the distribution of the features in the sample used for classifier training, but estimates the discriminant function g_k directly from this training sample (Niemann, 1983)). Different polynomial degrees can be used. In the present study, given that a simple classification rule for the embedded system had to be used, a linear polynomial was chosen. The estimation of the discriminant function g_k is then performed by solving a least squares systems of equations. The discriminant function g_k that results is again linear and can be implemented in the same simple way as for the BC and LDA classifiers. The PC has been shown to obtain good classification results in a variety of studies (e.g. Franke, 1997; Liu & Sako, 2006).
- Support Vector Machine (SVM). Support Vector Machines operate by first transforming the features into a high dimensional space (Vapnik, 1998). This transformation can be computed quite efficiently by different kernel functions (Schölkopf & Smola, 2002). In the present study a linear kernel was chosen, again due to reasons of computational simplicity. After the kernel transformation, a linear decision boundary with maximum margin is established in the resultant high dimensional space. While the process of training is complex, it is computed on a desktop PC and therefore not relevant for the implementation of the classifier on the embedded system. A standard SVM implementation was used throughout the present study ("libSVM" (Chang & Lin, 2001), freely available on the web). Support Vector Machines obtain high classification rates in many pattern recognition tasks (Sapankevych & Sankar, 2009). Numerous applications of this classifier exist, including image classification (Chapelle et al., 1999) and email categorization (Drucker et al., 1999).
- Multilayer Perceptron Classifier (MLP). The MLP is built to simulate neuron interaction in the human brain (Specht, 1990). The neurons are implemented by multiple single nodes that are connected in multilayer nets (Duda et al., 2001). Each

node has an input and an output. A feature value that is input into the node is subjected to a specified nonlinear function, e.g. a sigmoid function. Weights specify the contribution of individual nodes to the classification result. These weights are adjusted during classifier training according to different learning strategies (Hagan & Menhaj, 1994). The resulting discriminant function g_k is nonlinear. For the classifier implementation, the complete weight structure multiplication and the evaluation of the nonlinear (e.g. sigmoid) function needs to be performed on the embedded system. While this is still practicable, considerable higher computational demands are posed to the embedded system. MLP classifiers are frequently applied and several survey articles cover them (e.g. Baxt, 1995; Chua & Yang, 1988; Hunt et al., 1992).

With these classifiers, each vector of observed features $\boldsymbol{x} = (F_1 \ldots F_{88})$ was assigned to the class ω_k for that the discriminant function g_k of the respective classifier is maximal. In the experiments, five-fold cross-validation was performed in order to ensure generalizability of the results. In each of the cross-validation iterations the classifier was trained using all but the feature vectors from one specific fold. Subsequently, the feature vectors from the remaining fold (the test set) was classified according to maximum g_k. The mean classification accuracy was then computed as the average over all cross-validation iterations. To ensure that feature vectors were equally distributed over all classes, 10,000 vectors from each class were randomly selected from the collected data. The equal distribution of feature vectors per class allowed using equal priors for example for the Bayes Classifier.

Classification accuracies were deemed significant if the null hypothesis that classification was random could be rejected using a binomial test with significance level $\alpha = 0.01$.

Feature Selection

Due to the requirement that all computations had to be made in real-time on the employed microprocessor of the "adidas_1", it was impossible to implement a classifier based on the complete set of 88 features. A feature selection algorithm was therefore implemented, the dynamic programming algorithm (Niemann, 1983). It required that the initial feature set was rather small, and that the scoring metric was monotone and separable. This is true for the Mahalanobis distance (Mahalanobis, 1936)

$$G_{k,l} = (\mu_k - \mu_l)^T \Sigma^{-1} (\mu_k - \mu_l) \tag{4}$$

between two classes ω_k and ω_l. In Equation 3, μ_k and μ_l denote the class means and Σ^{-1} is the common inverse covariance matrix of all features. The dynamic programming algorithm was applied in multiple iterations using the Mahalanobis distance criterion. In each iteration, one single feature was added that gave the highest improvement for the worst class pair.

Microprocessor Implementation

The number of features that was possible to be computed in real-time on the employed microprocessor of the "adidas_1" was empirically found to be only two. Therefore, for the microprocessor implementation, the best performing two features had to be chosen. However, combinations of more features were also evaluated, because they could be implemented in future "adidas_1" versions that employ computationally more powerful microprocessors.

In order to demonstrate the ability of the developed methodology to perform accurately on the embedded microprocessor of the "adidas_1" shoe, the best classification system (according to the results on a desktop PC) was implemented on this microprocessor. The first important framework requirement for this implementation was the limited size of the internal memory (256 bytes). This meant that the program had to be as short as possible to save ROM and that it had to economize on variables. Moreover the classification had to be done in real-time with the available computing power. The microprocessor of the "adidas_1" was clocked with 24 MHz, which posed considerable demands to the embedded classification algorithm. Finally, a floating point unit was lacking and therefore all computations had to work with integer operations only.

Considering this different hardware architecture, a final evaluation of the performance of the classification system on the embedded microprocessor was made. For this purpose, the classification decisions made by the microprocessor were compared with those of a desktop PC. For the multi-class decision system a one-against-one approach was used, where the decision for every class against each other was calculated. The one class that won the most decisions was the selected class. If two classes won exactly the same number of comparisons, the selection depended on the iteration sequence, and a decision for the first considered class was always made. In the case of a three class problem this was equal to a decision tree of depth 2. Therefore, two decision functions per step were calculated.

Results

Inclination Classification

The resulting classification rates for the inclination classification are given in Figure 4. Figure 4 shows the class-wise averaged classification rates that were obtained using one to six features that were selected according to the feature selection algorithm for each classifier.

The results of the feature selection algorithms showed that the most important features for this task were μ_{16} (F_2), μ_{16} (F_9) and μ_{16} (F_{11}). These are the mean values over 16 steps computed from time to peak, normalized time to peak and decompression gradient, respectively. Those features were, in the given order, selected in almost all cases for the classification. It can be seen that by using more features, better classification results were achieved in general. The best accuracy of 67.2 % class-wise mean accuracy was reached by using six features and the MLP classifier. This classification result is significantly different from random ($p < 0.001$). The confusion matrix for this case is given in Table 4.

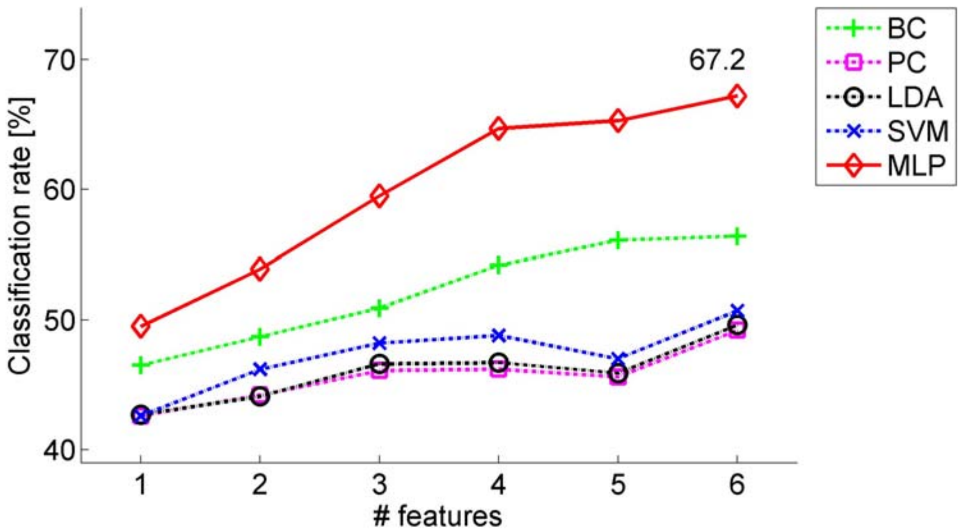

Figure 4. Resulting inclination classification rates. For each classifier, the results using one to six features according to the feature selection algorithm are shown. Depicted are the class-wise averaged accuracies in %.

Table 4. Confusion matrices for six features when using the MLP classifier for inclination classification. The classification accuracy values are given in %.

Classified as	$\omega_{1,\alpha}$	$\omega_{2,\alpha}$	$\omega_{3\ \alpha}$
labeled $\omega_{1,\alpha}$	**54.6**	22.6	22.8
labeled $\omega_{2,\alpha}$	5.5	**87.8**	6.7
labeled $\omega_{3,\alpha}$	19.7	21.1	**59.2**

Speed Classification

The resulting classification rates for the speed classification are given in Figure 5. Figure 5 shows the class-wise averaged classification rates that were obtained using one to six features that were selected according to the feature selection algorithm for each classifier.

The results of the feature selection algorithms showed that the most important features for this task were μ_{16} (F_3) and μ_{16} (F_1). These are the mean values over 16 steps computed from maximum compression and inter step time, respectively. Those features were, in the given order, selected in almost all cases for the classification. It can again be seen that by using more features, better classification results were achieved in general. The classification accuracies showed a noteworthy rise when using two features for all classification approaches. For some approaches (BC, SVM, MLP), another considerable rise in the classification accuracies was noticed when using four features. The best accuracy of 89.2 % class-wise mean accuracy was reached by calculating six features and applying the MLP classifier. This classification result is significantly different from random ($p < 0.001$).

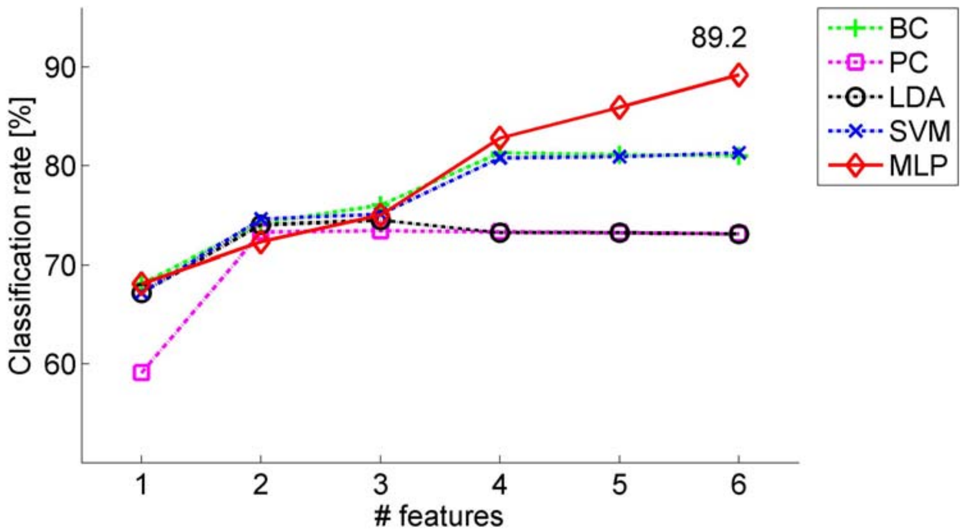

Figure 5. Resulting speed classification rates. For each classifier, the results using one to six features according to the feature selection algorithm are shown. Depicted are the class-wise averaged accuracies in %.

For the two-feature case (the number of features that could be computed on the currently employed microprocessor of the "adidas_1") the best results were found using the SVM classifier and features μ_{16} (F_3) and μ_{16} (F_1). The class-wise mean accuracy was 74.6%, which is significantly different from random ($p < 0.001$). The confusion matrix for the SVM two-feature case is given in Table 5.

Table 5. Confusion matrices for two features when using the SVM classifier for speed classification. The classification accuracy values are given in %.

Classified as	$\omega_{1,v}$	$\omega_{2,v}$	$\omega_{3,v}$
labeled $\omega_{1,v}$	**73.7**	11.7	14.7
labeled $\omega_{2,v}$	4.0	**74.9**	21.1
labeled $\omega_{3,v}$	7.7	17.0	**75.2**

Microprocessor Evaluation

Due to the low classification rates of the surface inclination system, only the SVM two-feature speed classification system was implemented on the product version of the "adidas_1" shoe. For the speed classification case, the classification decisions made by the microprocessor were compared with those of a desktop PC. The tests showed that 99.2% of the classification decisions were the same.

Discussion

The inclination classification (Figure 4) could not be performed with high classification rate. A major reason for this result was the fact that the quality of the signal measured with the "adidas_1" was decreasing with increasing inclination (both up- and downhill). This can be seen in the confusion matrix (Table 4) for this case, which showed to be unbalanced with a preference for the class for the low inclination range. Further examination of the data revealed that the reason for this unbalance was that the measurement sensor was located in the heel part of the shoe. When running up- or downhill at certain inclinations many runners tended to land more on the mid- or forefoot. In consequence, less overall compression was sensed. This resulted in a reduced signal to noise ratio and thus in a lower classification accuracy. To resolve this issue, at least a second sensor would have been needed in the front part of the shoe. Using such a sensor, additional information would have been available for classification. The incorporation of a second or even more sensors, therefore, is part of the future research work within this project.

The speed classification accuracies showed a considerable rise when using two features for all classification approaches (see Figure 5). Another noteworthy rise was noticed when using four features for some approaches (BC, SVM, MLP). The result that adding more features, and therefore more information, to the classification process and to then obtain higher classification rates is often observed in pattern recognition (Duda, et al., 2001; Theodoridis & Koutroumbas, 2009). The particular result in this study suggested using either two or four features for the final implementation on the microprocessor. Because of the limited hardware of the microprocessor, only the two feature approach was possible. In a future implementation on a computationally more powerful microprocessor, more features might also be implemented based on the results. The two selected features for classification were μ_{16} (F_3) and μ_{16} (F_1), as these were performing best.

Although the MLP classifier delivered results that were among the best for all conducted classification experiments, it was not chosen for the final implementation. First, it is computationally more demanding in a working classification system than the other classifiers. The BC, LDA, PC and SVM classifiers all have a different approach to classifier training, with typically increasing complexity. In the working classification system, however, all these classifiers pose a similar demand to the system they are implemented on. Only the MLP classifier is computationally considerably more demanding with its necessity of a more complex incorporation of the neuron weights and the requirement of the evaluation of the nonlinear function. Second, in the two feature case, the SVM classifier obtained the highest accuracies in any case. Thus, a decision was made to use SVM in the final microprocessor implementation. The confusion matrix in Table 5 for this case showed that the SVM yielded nearly equally good results for all classes. This meant that no speed class was considerable favored over another. This is an advantage of the system, because it prevents an overestimation of a certain prevailing speed condition.

The runner dependent feature rescaling was needed in order to obtain more accurate classification results. This rescaling thus had to implemented on the microprocessor, which might be considered a disadvantage due to the additional calculational effort. However, the additional computational effort was low because only the current extreme values of the two features selected for implementation had to be stored in memory. Those were updated regularly, this way the shoe adapted to different runners. Moreover, the actual computation of the rescaling could be efficiently implemented and thus the real-time requirements could still be met.

The fact that the microprocessor classification results were the same as the results on a desktop computer in 99.2% of classified steps showed that it was feasible to do all the evaluations that require high computational effort on desktop computers while only evaluating the final product solution on the embedded microprocessor. The obtained classification results were practically the same on both systems. This confirms the results shown in a previous study (Eskofier, et al., 2009). The 0.8% of steps that were not classified in the same way as on the desktop computer were a negligible minority. Although a deficient implementation of the classification algorithms on the desktop PC could, in principle, also be the reason for the discrepancy, the different classification results were mainly ascribed to the different hardware architectures of both systems, e.g. a missing floating point unit on the microprocessor.

The core idea for enabling embedded classification was using computationally simple features and classifiers that could also be implemented on embedded microprocessors. Furthermore, all comparative experiments were performed on computationally powerful desktop computers, and only the best solution was implemented and validated on the embedded hardware. This approach was again successful, and an accurate embedded speed classification system could be developed. The proposed methodology will be helpful in many tasks in sports where classification on embedded systems has to be performed.

Summary

This research demonstrated the application of pattern recognition methods to detect running surface inclination and running speed using heel compression measured with the “adidas_1” running shoe. A set of 88 features was manually designed that was suited for the classification task at hand. The features were computationally inexpensive and could be calculated using the embedded microprocessor of the “adidas_1” shoe. Several classifiers that are suited for embedded implementation were compared with respect to their classification rate. Subsequently, it was shown how a subset of the original 88 features, which were most important for the classification task, could be identified. The applicability of the developed speed classification system was demonstrated by implementing and evaluating it on the embedded microprocessor of the “adidas_1”. Thus, a classification of the prevailing running speed was performed directly on the embedded system.

It was shown that in the three-class inclination case, a classification rate of 67.2% could be obtained using six features and a MLP classifier. Better performance was not possible due to the fact that only the heel compression was measured, and for the classification of some track inclinations this available sensor information was insufficient. However, it was demonstrated that if continuously good heel compression signals were available, as it was in the three-class speed classification case, acceptable classification rates of 74.6% could be achieved using only two and even 89.2% using six features. This result suggested that a trained automatic system could quite precisely support the athlete, for example by providing more shoe stiffness and thus more stability by the “adidas_1” running shoe when the sportsman was running faster.

Acknowledgments

The authors would like to thank the adidas innovation team *ait*. for the financial and technical support of this research. We are indebted to Pascal Kühner from the University of Koblenz-Landau for his help in data collection, and also thank the participants of the running study. Special thanks go to our colleagues that were proofreading this manuscript for their time and support.

References

Aminian, K., Robert, P., Jéquier, E., & Schutz, Y. (1995). Estimation of speed and incline of walking using neural network. *IEEE Transactions on Instrumentation and Measurement, 44*(3), 743-746.

Baxt, W. G. (1995). Application of artificial neural networks to clinical medicine. *Lancet, 346*(8983), 1135-1138.

Begg, R., & Kamruzzaman, J. (2005). A machine learning approach for automated recognition of movement patterns using basic, kinetic and kinematic gait data. *Journal of Biomechanics, 38*(3), 401-408.

Chang, C., & Lin, C. (2001). LIBSVM: a Library for Support Vector Machines. Software available at http://www.csie.ntu.edu.tw/~cjlin/libsvm.

Chapelle, O., Haffner, P., & Vapnik, V. N. (1999). Support vector machines for histogram-based image classification. *IEEE Transactions on Neural Networks, 10*(5), 1055-1064.

Chua, L. O., & Yang, L. (1988). Cellular neural networks: Applications. *IEEE Transactions on Circuits and Systems, 35*(10), 1273-1290.

DiBenedetto, C., Oleson, M. A., Roth, C., & Thompson, M. C. (2004). United States Patent No. 20040177531.

Domingos, P., & Pazzani, M. (1997). On the Optimality of the Simple Bayesian Classifier under Zero-One Loss. *Machine Learning, 29*(2-3), 103-130.

Drucker, H., Wu, D., & Vapnik, V. N. (1999). Support vector machines for spam categorization. *IEEE Transactions on Neural Networks, 10*(5), 1048-1054.

Duda, R. O., Hart, P. E., & Stork, D. G. (2001). *Pattern classification* (2nd ed.). New York, NY: Wiley & Sons.

Eskofier, B. M., Hartmann, E., Kühner, P., Griffin, J., Schlarb, H., Schmitt, M., et al. (2008). Real time surveying and monitoring of athletes using mobile phones and GPS. *International Journal of Computer Science in Sports, 7*(1), 18-27.

Eskofier, B. M., & Melzer, D. (2009). GERVIT - A tool for sports data visualization employing Google Earth. *International Journal of Computer Science in Sports, 8*(2), 32-39.

Eskofier, B. M., Oleson, M., DiBenedetto, C., & Hornegger, J. (2009). Embedded surface classification in digital sports. *Pattern Recognition Letters, 30*(16), 1448-1456.

Fisher, R. A. (1936). The use of multiple measurements in taxonomic problems. *Annals of Eugenics, 7*(2), 179-188.

Franke, J. (1997). *A Comparison of Gaussian Distribution and Polynomial Classifiers in a Hidden Markov Model Based System for the Recognition of Cursive Script*.

Hagan, M. T., & Menhaj, M. B. (1994). Training feedforward networks with the Marquardt algorithm. *IEEE Transactions on Neural Networks, 5*(6), 989-993.

Herren, R., Sparti, A., Aminian, K., & Schutz, Y. (1999). The prediction of speed and incline in outdoor running in humans using accelerometry. *Medicine and Science in Sports and Exercise, 31*(7), 1053-1059.

Hunt, K. J., Sbarbaro, D., Zbikowski, R., & Gawthrop, P. J. (1992). Neural networks for control systems - A survey. *Automatica, 28*(6), 1083-1112.

Kerr, B. A., Beauchamp, L., Fisher, V., & Neil, R. (1983). Footstrike patterns in distance running. In B. M. Nigg & B. A. Kerr (Eds.), *Biomechanical Aspects of Sport Shoes and Playing Surfaces* (1st ed., pp. 135-142). Calgary, AB: University Printing Calgary.

Langley, P., Iba, W., & Thompson, K. (1992). *An analysis of bayesian classifiers*. Paper presented at the Proceedings of the 10th National Conference on Artificial Intelligence (AAAI-92), San Jose, CA. http://citeseerx.ist.psu.edu/viewdoc/summary?doi=10.1.1.55.1659

Liu, C.-L., & Sako, H. (2006). Class-specific feature polynomial classifier for pattern classification and its application to handwritten numeral recognition. *Pattern Recognition, 39*(4), 669-681.

Lu, J., Plataniotis, K. N., & Venetsanopoulos, A. N. (2003). Face recognition using LDA-based algorithms. *IEEE Transactions on Neural Networks, 14*(1), 195-200.

Mahalanobis, P. C. (1936). On the generalized distance in statistics. *Proceedings of the National Institute of Sciences of India, 2*(1), 49-55.

Niemann, H. (1983). *Klassifikation von Mustern*. Berlin: Springer.

Polar Electro Oy. (January 2010). RS800 Training Computer. Retrieved January 15, 2010, from http://www.polar.fi/en/products/earlier_products/RS800.

Sapankevych, N., & Sankar, R. (2009). Time series prediction using support vector machines: A survey. *IEEE Computational Intelligence Magazine, 4*(2), 24-38.

Schölkopf, B., & Smola, A. J. (2002). *Learning with kernels: support vector machines, regularization, optimization, and beyond* (1st ed.). Cambridge, MA: MIT Press.

Schöllhorn, W. I. (2004). Applications of artificial neural nets in clinical biomechanics. *Clinical Biomechanics, 19*(9), 876-898.

Specht, D. F. (1990). Probabilistic neural networks. *Neural Networks, 3*(1), 109-118.

Theodoridis, S., & Koutroumbas, K. (2009). *Pattern recognition* (4th ed.). Amsterdam: Elsevier Academic Press.

Vapnik, V. N. (1998). *Statistical learning theory* (1st ed.). New York, NY: Wiley & Sons.

von Tscharner, V., & Goepfert, B. (2003). Gender dependent EMGs of runners resolved by time/frequency and principal pattern analysis. *Journal of Electromyography and Kinesiology, 13*(3), 253-272.

Wu, J., & Wang, J. (2008). PCA-based SVM for automatic recognition of gait patterns. *Journal of Applied Biomechanics, 24*(1), 83-87.

Ye, J., & Li, Q. (2005). A two-stage linear discriminant analysis via QR-decomposition. *IEEE Transactions on Pattern Analysis and Machine Intelligence, 27*(6), 929-941.

Self-Organising Maps: An Objective Method for Clustering Complex Human Movement

Peter Lamb, Roger Bartlett, Anthony Robins

University of Otago, Dunedin, New Zealand

Abstract

In this study self-organising maps (SOM) were used to classify the coordination patterns of four participants performing three different types of basketball shot from different distances. The shots were the free throw, the three-point and the hook shot. The free throw and three-point shot were hypothesised to be more similar to one another than to the hook shot. The first analysis involved an analysis of trial trajectories visualised on a U-matrix. Two of the participants, unexpectedly, showed more similarity between the three-point shot and the hook shot, instead of the free throw. Where the first analysis was useful in showing aspects of the movement that were not obvious from viewing the computer animation of the original movement, a second SOM was trained on the appearance of the original trajectories and used to produce an output that shows the variability in coordination between all trials in the study. The second SOM showed groupings of the three shooting conditions which were unexpected. The second SOM technique may provide a more objective method than visual technique analysis for explaining movement patterning and structuring practice routines.

KEYWORDS: NEURAL NETWORKS, KOHONEN, SOM, COORDINATION, BASKETBALL.

Introduction

The data used for this study were generated from four players performing three different types of basketball shot from different distances. The shots were the three-point shot, the free throw and the hook shot. The free throw and three-point shot were hypothesised to be more similar to one another than to the hook shot. A free throw is commonly awarded when an offensive player is fouled during shooting. Each foul usually results in the offended player being awarded two free throw shots, which makes the free throw shot an important skill. The three-point shot is more strategic; the probability of successfully scoring with this shot is much less but the reward is higher. The three-point shot is taken from further away than the free throw shot and is often performed in the presence of defenders. Subsequently, the three-point shot is almost always performed as a jump shot, both to afford more power for the shot and to release the ball higher thus reducing the chance of being blocked. During the study, the hook shot was performed starting with the player’s back to the net then turning and shooting with a one-handed release. The hook shot has a lower percentage success rate but, because of the release point, it is a difficult shot to defend. A good hook shot involves the shooter’s body being positioned between the ball and the defender. Typically the hook shot is used as a last resort and, therefore, occurs less frequently than the other two shots.

A likely practice routine would reflect the hook shot's infrequent use. The hook shot is often assumed to be a different movement pattern compared to the similar patterns used for the free throw and the three-point shot, which are often thought of as modifications of the 'set shot' movement pattern. Consider why these assumptions exist. The observational learning literature suggests the motion of distal segments as one of the most influential factors when learning new skills (Hodges, Williams, Hayes, & Breslin, 2007). The typical one-handed release of the hook shot makes the kinematics of the distal segments a plausible explanation for its distinction as a unique shot. If such visual information negatively influences the observer, the opportunity exists for a new method of structuring practice and thinking about movement patterning to come to light. The purpose of this study was to show that SOMs are an objective tool for movement analysis.

Methods

Data Collection and Processing

A 12-camera, three-dimensional motion capture system (Motion Analysis Corporation Inc, Santa Rosa, CA, USA) was used to collect the data for this study. Using post-processing software (Visual3D, C-Motion), a 12-segment body model was established. Based on the Euler convention, motion in the sagittal plane for the right and left ankles, knees, hips (Bell, Pedersen, & Brand, 1990) and shoulders (Rab, Petuskey, & Bagley, 2002) were processed for the SOM analysis.

Trials were time normalised to 101 data points. Within each trial, each variable was range normalised to maximum and minimum values of +1 and -1, respectively. The trials were appended one after the other to create one block of data used for training the neural network.

SOM Outline

The SOM can be thought of as a layer of nodes with associated weight vectors, fed forward by a layer of inputs. Weight vectors of the map nodes are adjusted based on an unsupervised learning strategy to represent relevent information in the input. The output node whose weight vector has the smallest Euclidean distance to a given input is declared that input's best matching node. Convergence to the input is acheived by iteratively updating the weights of the best matching node and its neighbours, within a specified radius, according to the neighbourhood function and learning rate (Kohonen, 2001). Because of such non-linear properties, the SOM is able to remove redundancies in high-dimensional input data and produce a low-dimensional mapping of the output while preserving topological relationships in the data. The neighbourhood function effectively allows local interactions between map nodes to coalesce into states of global order and to achieve self-organisation.

Network Architecture

The SOM toolbox for MATLAB was integrated into the software tool (Vesanto, Himberg, Alhoniemi, & Parkankangas, 2000) for the analysis. A PCA-based initialisation process was used to create a two-dimensional hexagonal lattice output map (Table 6). The neighbourhood sizes were selected according to the principal components of the data (Barton, Lees, Lisboa, & Attfield, 2006).

A second SOM, inspired by Barton (1999), was trained on the trajectories from the original SOM. Inputs for the second SOM were created from projecting the weight vectors into weight space using Sammon's mapping (Sammon, 1969). The two-dimensional coordinates of each consecutive best matching node were used to create an input vector representative of an individual trial. This process was repeated for the best matching nodes of all trials in the study. The result of the second map is a SOM in which each trial can be represented by one node on the output map and, therefore, a clustering of all the trials in the dataset can be visualised more easily. In what follows we will refer to the original SOM as the *phase SOM* and the second SOM as the *trial SOM*.

Table 6: SOM training parameters and quality measures

Parameter	phase SOM	trial SOM
initialisation	*'linear'*	*'linear'*
map size	42×13	9×6
lattice	*'hexagonal'*	*'hexagonal'*
neighbourhood	*'Gaussian'*	*'Gaussian'*
training algorithm	*'batch'*	*'batch'*
rough training		
steps	30	10
radius	$6 \rightarrow 1.5$	$2 \rightarrow 1$
fine-tuning		
steps	500	225
radius	$1.5 \rightarrow 1$	$1.5 \rightarrow 1$
quantisation error	0.226	0.554
topographical error	0.030	0.008

Analysis

We chose to use the U-matrix (Figure 6(a)) to visualise the output of the phase SOM. Trajectories connecting nodes on the U-matrix that best represent the input were used to visualise the multi-segment coordination performed by the participants. The nodes in Region A of the U-matrix represent the preparation phase of the shot. Region B represents the extension phase where the player generates power for the release. Region C represents the final release phase of the movement. Typical movement patterns activate nodes in Region A, ascend up the map through Region B and end at the release phase in Region C. Movements that were patterned uniquely, activated nodes in Region D. Clusters of data can be identified on the U-matrix with blue 'distance cells' which are evidence of similar data among neighbouring nodes. Orange and red distance cells represent larger Euclidean distances between neighbouring nodes and therefore outline borders between clusters.

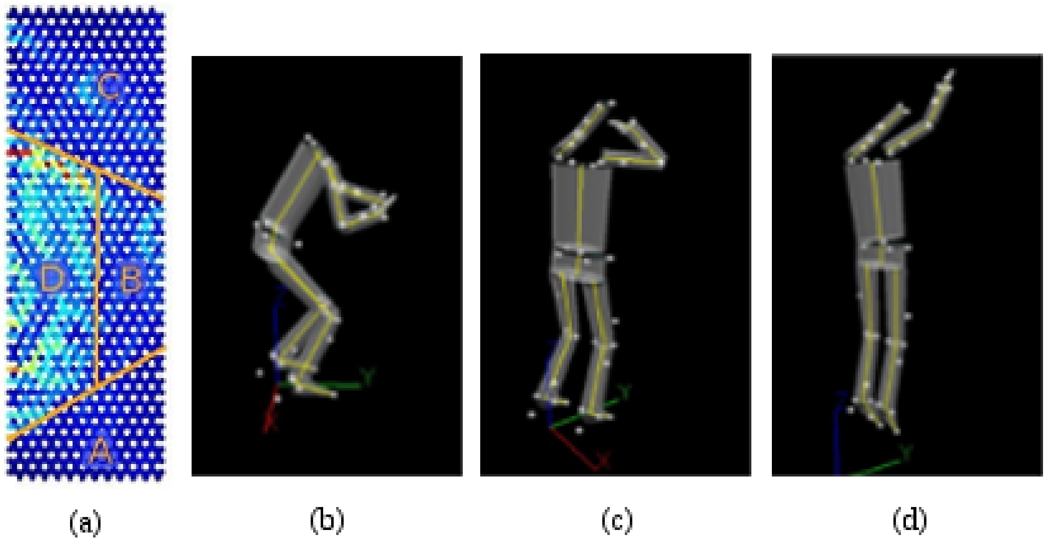

Figure 6: a) U-matrix and movement phases: A Preparation, B Extension, C Release, D Unique coordination; b) Preparation phase; c) Extension phase; d) Release phase.

The phase SOM analysis uses the trajectory of the best matching nodes through the time series of each trial to compare various trials simulated on the same U-matrix visualisation (Lamb, Bartlett, Robins, & Kennedy, 2008). The orange trajectories shown on the U-matrix (Figure 7(a), (c) and (e)) give a representation of the order of the best matching nodes with respect to time. However, the trajectory can potentially be misleading as it gives the impression that the best matching nodes move fluidly through the U-matrix. Visualising trials with just the best matching nodes highlighted in white on black shows the discontinuity on the U-matrix for this dataset. Figure 7 ((b), (d) and (f)) shows these *hit histograms* with best matching nodes shown as white patches with their size increasing as the frequency of hits increases. For these nodes to stand out the rest of the U-matrix is blacked out.

Sammon's mapping was used to visualise the trial SOM because the map size was small with an accordingly small topographical error (Table 6). Each trial in the dataset was assigned a best matching node which was shown on the output map (Figure 11). The text at each node represents the type of shot, the colour of the text identifies the player and the size of the text increases as the hit frequency increases. The lateral connections between nodes represent the Euclidean distance between them.

Results

Phase SOM analysis

The trajectories for the three-point shot and free throw are visually similar in Regions A and C of the U-matrix, suggesting that the coordination patterns in the preparation and release phases were similar. The trajectories differ in the middle area of the map, in Region B, in which the three-point shot moves closer to the right edge of the map (Figure 2(a)) than the trajectories for the free throw (Figure 2(c)). The trajectory for the hook shot (Figures 2(e), (f)) is qualitatively different from the other two shots for Player 1. The main visual difference in the trajectories was seen as the trajectory moves diagonally up and across the U-matrix in Region C.

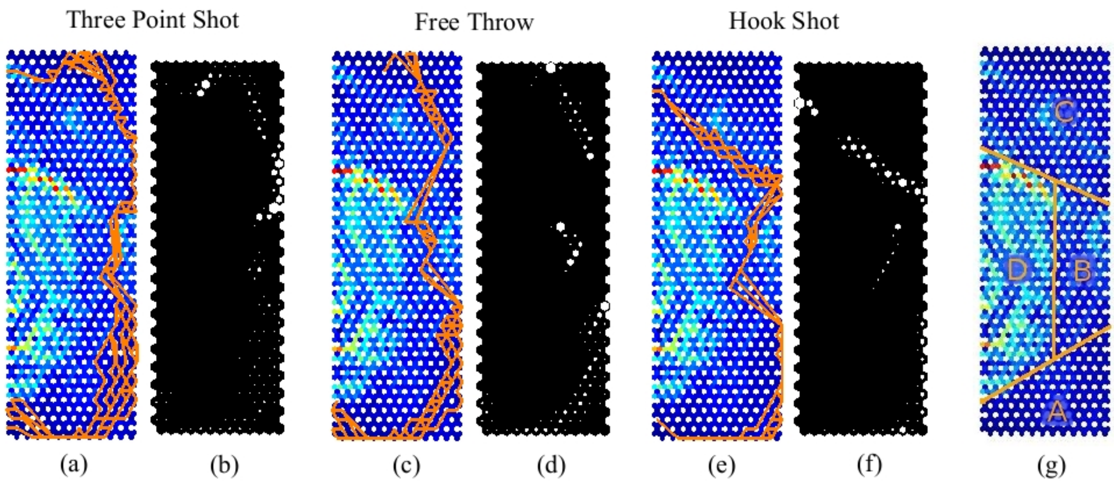

Figure 7: Player 1, a) Three-point shot trajectory, b) Three-point shot hits, c) Free throw trajectory, d) free throw hits, e) hook shot trajectory, f) hook shot hits, g) U-matrix with movement phases.

For Player 2 (Figure 8), the preparation phase for the three-point shot and the free throw are almost identical, occupying many of the same nodes and clustering similarly. During the release phase, the three-point shot moves diagonally up and to the left from the right edge of the map in Region C (Figure 8(a), (b)), similarly to the three-point shot and free throw of Player 1. The diagonal movement on the U-matrix of the free throw is not as long or as consistent as the three-point shot (compare Figure 8(a) with Figure 8(c)). The hook shot (Figure 8(e), (f)) is, again, qualitatively different from the other two shots. Unlike all other shooting conditions for all other players, the best matching node trajectory for the hook shot for Player 2 does not always progress upwards on the U-matrix. The hit histogram in Figure 8(f) shows the best matching nodes for most of the movement are within two brightly coloured borders in Region D of the U-matrix. This is different from any other shot in the dataset.

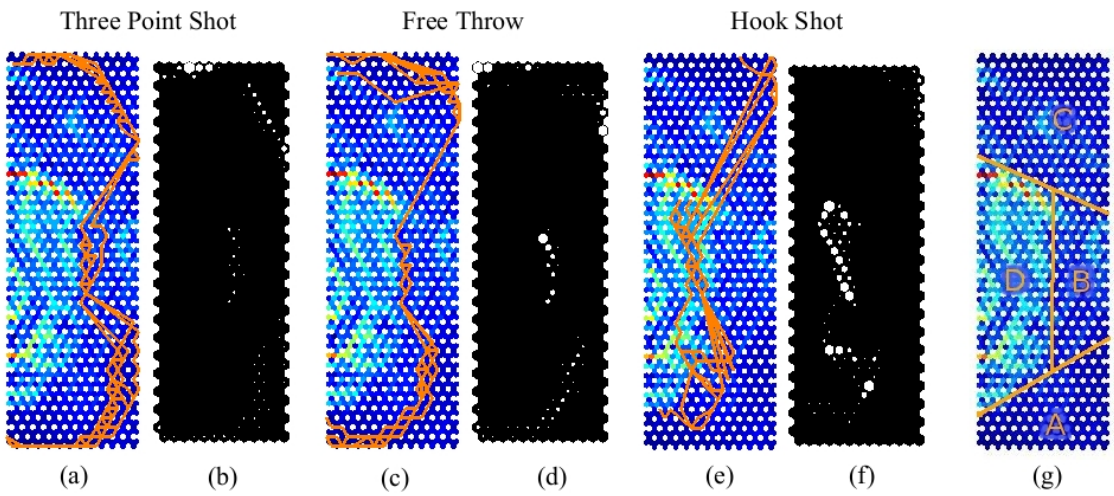

Figure 8: Player 2, a) Three-point shot trajectory, b)) Three-point shot hits, c) Free throw trajectory, d) free throw hits, e) hook shot trajectory, f) hook shot hits, g) U-matrix with movement phases.

The best matching node trajectories for Player 3 are similar for the three-point shot and the free throw (Figure 9(a), (c)). The hit histograms show a large discontinuity as the movement transitions from preparation to release (see Figure 9(b), (d)). The trajectory jumps from Region A to a series of about three different nodes in Region D before jumping into Region C for the release phase of the shot. The jump into Region D is different from any of the other shots in the dataset. The hook shot is visually much different from the three-point shot and the free throw; it stays within Region D, without jumping across any borders, and along a very consistent trajectory of nodes (Figure 9(e)).

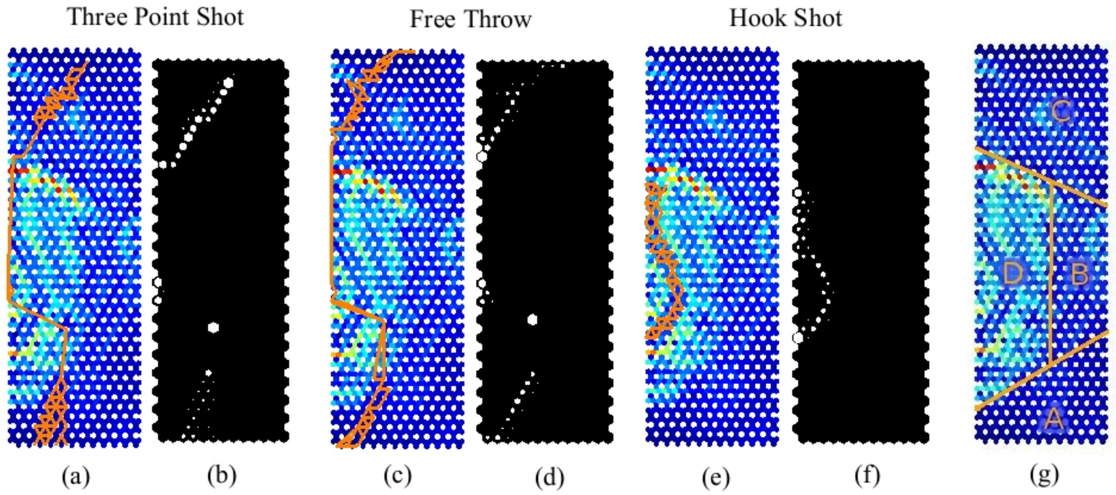

Figure 9: Player 3, a) Three-point shot trajectory, b)) Three-point shot hits, c) Free throw trajectory, d) free throw hits, e) hook shot trajectory, f) hook shot hits, g) U-matrix with movement phases.

For Player 4, the trajectories for the preparation phase of each shot are different. The three-point (Figure 10(a), (b)) and hook shot (Figure 10(e), (f)) best matching nodes were in Region A, as expected, whereas the free throw (Figure 10(c), (d)) began in Region D. In Region B, the three-point shot and hook shot trajectories travel to the left of the bright blue border near the right edge of the U-matrix (highlighted in yellow in Figure 10(g)) whereas the free throw travels to the right of the border. The release, shown in Region C, of the three-point shot and the free throw are quite similar, as shown in Figure 10(a) and (c). The release of all three shots of Player 4 resemble the release of Player 1. The trajectories for the three-point shot and the free throw move above the bright blue border in the middle of Region C, while the trajectory for the hook shot moves below the border.

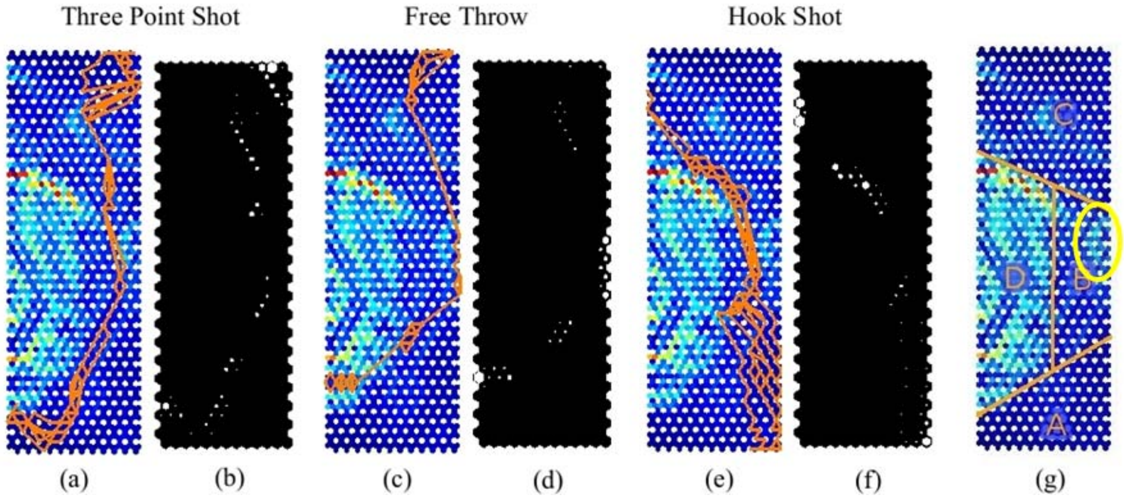

Figure 10: Player 4, a) Three-point shot trajectory, b)) Three-point shot hits, c) Free throw trajectory, d) free throw hits, e) hook shot trajectory, f) hook shot hits, g) U-matrix with movement phases.

Trial SOM analysis

Starting with Player 1 (blue text in Figure 11), the three-point shot and hook shot occupy nodes at the left edge of the map which makes the two shots *second nearest neighbours*. The free throw hits a region toward the bottom of the map, located more closely to different shot types of different players than to other shots by Player 1. As was shown in the previous section in Figure 7 and 3, the coordination patterns for each respective shot for Player 1 and Player 4 (red) are similar. Also the three-point shots and free throws of Player 2 (green) were clustered near the three-point shot of Player 1 (compare Figure 11 with Figure 7 and Figure 8).

The three-point shot and free throw for Players 2 and 3, respectively, are second nearest neighbours with a noticeably short Euclidean distance between them (compare trajectories in Figure 8(a) and (c) and Figure 9(a) and (c)). Most of the hook shots for Player 2 were isolated toward the top right corner of the map. Higher variability within this shooting condition is evident by the distribution of hits across six nodes. Three other shooting conditions occupy more than one node (Player 2 three-point shot and free throw and Player 3 free throw); however, the Euclidean distance spanned by the hook shots of Player 2 show this to be the most variable shooting condition in the dataset.

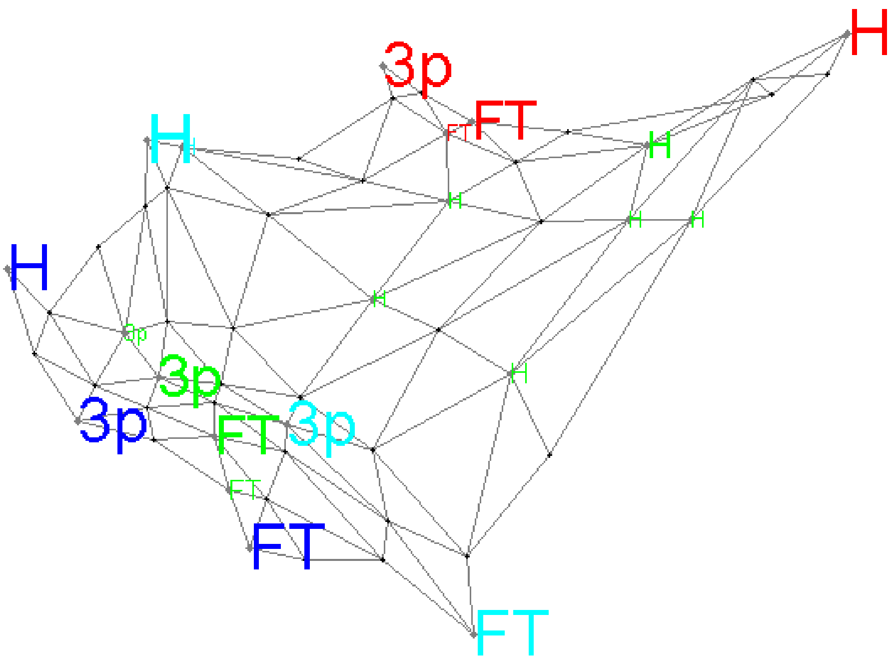

Figure 11: Sammon's mapping of trial SOM. Player 1 is shown in blue, Player 2 in green, Player 3 in red and Player 4 in cyan.

Figure 9 showed the three-point shot and free throw of Player 3 (red) to appear similar to, although distinct from, other shots in the dataset. The hook shot occupied a small area in Region D in Figure 9, which was also distinct from other shots in the dataset. Both of these observations are apparent in Figure 11 (in red). The three-point shot and free throw are separated by only one node and the hook shot is isolated in the top right corner of the map.

The free throw of Player 4 (cyan) is another shot that is clustered away from the rest of the data, in this case the bottom right corner of the map. The three-point and hook shots are shown to be more similar to each other than to the free throw; these shots are also more similar to the three-point and hook shots of Player 1 that they are to the free throw of Player 4. Finally, notice that the three-point shot appears to be the most similar shooting condition among the players, and the hook shot the least similar.

Discussion

The Jump Hook

Qualitatively, Player 1 supported the hypothesis that the three-point shot (Figure 7(a)) and the free throw (Figure 7(b)) would be most similar, but only for the preparation and release phases. Although all time frames of the movement were weighted equally, the trial SOM classified the data for the three-point shot and hook shot in the extension phase to be a larger contributor to overall similarity, partly because of a slight delay at mid-flight between lower and upper body extension in these shots. Overall, the trial SOM showed the lowest variability between the three-point and the hook shots; during the late extension phase and the beginning of the release of the shot, the three-point shot showed more similarity with the hook shot than with the free throw.

For the three-point (Figure 10(a)) and hook (Figure 10(e)) shots, many similar nodes were activated in the extension phase (Region B, Figure 10(g)) for Player 4, adding further evidence that the kinematics involved in the jump in these two shots contribute to the data for each of these shooting conditions being more similar to each other than to the free throw, which does not involve a jump. The release phase of the three-point shot (Figure 10(a)) and free throw (Figure 10(c)) showed more similarity on the U-matrix. This was expected since the three-point shot and the free throw are two-handed shots, whereas the hook shot is a one-handed shot. Computer animations showed that the noticeable difference between the three-point shot and the free throw for Player 4 was the in-phase extension of the upper and lower body; for the free throw the knees and hips reached maximum extension while the upper arms continued to flex and the elbows and ankles continued to extend. The upper arms then stopped, leaving both the ankles and elbows still extending – a somewhat atypical sequence. This sequence is shown on the U-matrix by nodes between the edge of the map and the rightmost brightly coloured border in Region B (Figure 10(c)). Player 4's free throw was the only shot for any of the players to activate these nodes. The overall similarity of the movement patterns used for the three-point shot and the hook shot is verified in Figure 11.

The close proximity of best matching nodes for the release phase of the hook shot for Players 1 and 4 suggest high similarity between these players for the hook shot release. The short Euclidean distance for the hook shots between Players 1 and 4 on the trial SOM (Figure 11) suggests further that the hook shots of these two players are similar. The high dimensionality of the time series data for these throws makes an in-depth, visual analysis of coordination difficult using conventional methods. Research into the information attended to in visual demonstrations has shown that the kinematics of distal segments (arms) has a greater impact than the kinematics of more proximal segments (trunk) in skill acquisition (Hodges et al., 2007). This may be used as evidence suggesting that certain information biases the movement analyst. Since the major difference associated with the hook shot compared to the other two shots is the one-handed release, one could speculate that the movement of the distal segments over-influence the analyst into classifying the hook shot as a completely different movement. If this is the case, the SOM might provide an objective method for analysing human movement for movement analysts and coaches.

The standing hook

Only the shots of Players 2 and 3 were clustered on the trial SOM in support of the hypothesis that the three-point shot and free throw would show less variability between them than when compared to the hook shot. Qualitatively, the three-point shot and free throw, for both Player 2 (Figure 8(a), (c)) and Player 3 (Figure 9(a), (c)), were similar to each other for not only the preparation and release phases of the movement, as for Player 1, but also the extension phase of the movement. The hook shots were qualitatively different for each phase and occupied Region D on the U-matrix (Figure 8(e) and Figure 9(e)). Unique to Players 2 and 3 was that their hook shots lacked a significant jump along with an early release of their three-point shot. The jumping kinematics that separated the three-point shot and the free throw for Players 1 and 4 were much less pronounced for Players 2 and 3, reflected in the short Euclidean distance between the three-point shot and free throw on the trial SOM (Figure 11, Players 2 and 3).

Conclusions

The phase SOM drew our attention to aspects of the movement that were not obvious from more traditional approaches, such as visual analysis of the original movement, or from multiple time series data. Characteristics of the movements found by analysis of the phase

SOM were summarised on a single output map using the trial SOM. In several cases, the SOM output and our natural inclinations as movement analysts did not agree; SOMs thus proved to be a useful tool in our analysis of coordination. The movement analyst might be distracted by visual information in the movement; the SOM might provide a more objective method for explaining movement coordination. In particular, the trial SOM approach may be useful for a gaining a more global representation of the dataset and thus neatly summarise the relationships between a set of coordination patterns.

References

Barton, G. (1999). Interpretation of gait data using Kohonen neural networks. *Gait & Posture, 10*, 85-86.

Barton, G., Lees, A., Lisboa, P., & Attfield, S. (2006). Visualisation of gait data with Kohonen self-organising neural maps. *Gait & Posture, 24*, 46-53.

Bell, A. L., Pedersen, D. R., & Brand, R. A. (1990). A comparison of the accuracy of several hip center location prediction methods. *Journal of Biomechanics, 23*(6), 617-620.

Hodges, N. J., Williams, M. A., Hayes, S. J., & Breslin, G. (2007). What is modelled during observational learning? *Journal of Sports Sciences, 25*(5), 531-545.

Kohonen, T. (2001). *Self-organizing maps* (3rd ed.). Berlin, Germany: Springer-Verlag.

Lamb, P., Bartlett, R. M., Robins, A., & Kennedy, G. (2008). Self-Organizing Maps as a tool to measure movement variability. *International Journal of Computer Science in Sport, 7*(1), 28-39.

Rab, G., Petuskey, K., & Bagley, A. (2002). A method for determination of upper extremity kinematics. *Gait and Posture, 15*, 113-119.

Sammon, J. W. (1969). A nonlinear mapping for data structure analysis. *IEEE Transactions on Computers, C-18*(5), 401-409.

Vesanto, J., Himberg, J., Alhoniemi, E., & Parkankangas, J. (2000). *SOM Toolbox for MATLAB 5* (No. A57). Helsinki, Finland: Helsinki University of Technology.

A Game Theoretic Analysis of Tactics in the Phase of Reception Attack in Volleyball

Nobuyoshi Hirotsu[1], Masamitsu Ito[2], Chikara Miyaji[3], Koji Hamano[1], Azuma Taguchi[4]

[1] Juntendo University, Inba, Japan

[2] Nippon Sport Science University, Tokyo, Japan

[3] Japan Institute of Sports Sciences, Tokyo, Japan

[4] Chuo University, Tokyo, Japan

Abstract

In this paper, we analyze tactical conflicts between attacking formations and blocking formations in the phase of reception attack in volleyball, using a zero-sum game model. In this model, we categorize the attacking formations into 9 patterns which consist of 3 moving patterns of forward players and 3 positions (right, center and left) from which the ball can be spiked. We also categorize the blocking formations into 3 formations: "spread", "bunch" and "dedicate". The conflicts are formulated as a zero-sum game by tabulating these formations, and analyzed by calculating the equilibrium points together with the value of the game. Following this formulation we have developed a game analysis system with Visual Basic programming code for solving the game. The solution gives us minimax strategies with the ratio of successful blocks. Here, we try an application of game theoretic analysis, using the empirical data taken from an intercollegiate women's league in 2004. We estimate the values of the game in the matches, and illustrate a possible improvement in terms of the allocation of attacking and blocking formations used in the matches from the macro-view of game theoretic analysis. This approach could hopefully provide a new standpoint of the analysis of real volleyball matches.

KEYWORDS, GAME THEORY, TACTICS, RECEPTION ATTACK, VOLLEYBALL

Introduction

Together with the recent enhancements in information technology, a variety of computer systems have been developed to analyze the performance in sporting activities. In terms of volleyball, some game analysis systems have been used for recording game data and providing statistical information to coaches and players for tactical support. For example, a well-known program, "Data Volley", is widely used by national teams and club teams to feed back the result of the analysis to coaches and players. Another program, "Touch Volley", (Shigenaga, Ezaki, Yamamoto, & Yamada, 2001; Shigenaga, Ezaki, & Uno, 2002; Shigenaga, Ezaki, Hirotsu, & Miyaji, 2004) has been developed for users to easily input data using laptop computers with a touch sensor.

On the other hand, volleyball will be a possible sport which game theory can be applied in practical analysis. Game theory is a theory of decision-making in conciliation (e.g. Davis, 1983), and has been applied mainly to economic issues rather than to sports, although some applications to sports have been used in textbooks to illustrate the concepts of game theory (e.g. Sadovskii & Sadovskii, 1993; Winston, 1993). In terms of academic research, game theory is applied to analysis on baseball (Weinstein-Gould, 2009; Turocy; 2008), American football (Boronico & Newbert, 1999; Jordan et al., 2009) and soccer (Cowan, 1992; Hirotsu and Wright, 2006; Hirotsu et al.,2009). For volleyball, Yoshida, et al.(1994) applied game theory in order to identify the optimal strategy for use of the four blocking formations, conducting an experiment using intercollegiate players by repeating the attacking-blocking situation. However, there does not until now appear to have been any research published applying game theory to volleyball using real match data.

In this paper, we propose a method for analyzing tactics in volleyball using game theory. Here, we focus on the phase of reception attack, because the tactical conflicts between attacking formations and blocking formations appear in this phase. Firstly, we categorize the patterns of the attacking formations and blocking formations. For the purpose of application of game theory, we separated the attacking formations into 9 patterns of 3 moving patterns of forward players and 3 positions (right, center and left) from which the ball can be spiked. In terms of blocking formations, we separated them into 3 formations: “spread”, “bunch” and “dedicate”. We then formulated the conflict between attack and block as a zero-sum game by tabulating these patterns and analyzed the tactics by calculating the value of the game. Following this formulation we have developed a game analysis system with Visual Basic (VB) programming code for solving the game. The solution gives us minimax strategies with the ratio of successful blocks.

Here, we try an application of game theoretic analysis, using the empirical data taken from an intercollegiate women’s league in 2004. We estimate the game values in the matches and illustrate a possible improvement of the allocation of tactics from this macro-view of game theoretic analysis. Although there can be a lot of subtle confliction which is too complicated to be analysed in each phase of real matches, this approach has an advantage of quantifying the confliction as a game value and we can discuss the tactics based on the empirical data.

This research will be a first step to provide a practical application of game theory to real volleyball matches. We hope that this method may help coaches or players to analyse tactics quantitatively in volleyball matches.

Methods

Modeling the confliction in the phase of reception attack

We now describe how to model a tactical conflict in volleyball, which consists of a series of plays starting off with a service. Here, the phase of reception attack (i.e. the first attack after a serve-receive) can be considered as one tactical conflict between attacking formations and blocking formations. To model this conflict, we tried to categorize the patterns of the attacking formations and blocking formations.

Here, we separated the attacking formations into 9 patterns which consist of 3 moving patterns of forward players and 3 positions (right, center and left) from which the ball can be spiked. Figure 1 shows the 3 moving patterns of forward players for attacking. The patterns are named using the similarly shaped Roman numeral. In terms of Pattern III shown in Figure

1(a), three forward players move without crossing toward the net for attacking. In terms of Pattern XI and IX, two of three forward players cross toward the net for attacking as shown in Figure 1(b) and (c), respectively. By taking into account 3 positions (right, center and left) from which the ball can be spiked with the above 3 moving patterns, we separate the attacking formations into 9 patterns (= 3 moving patterns × 3 positions).

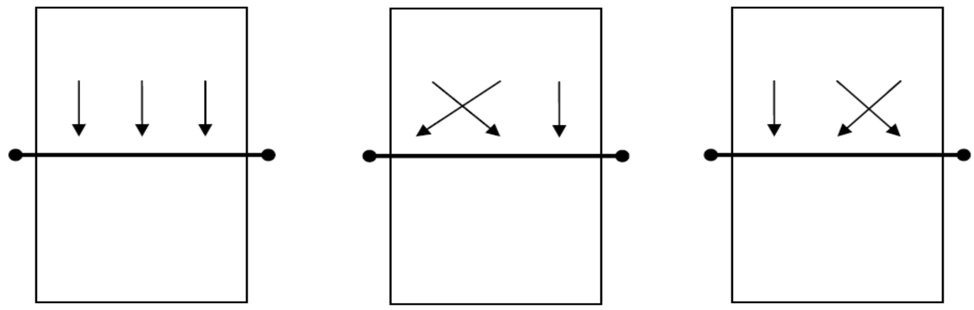

(a) Pattern III (b) Pattern XI (c) Pattern IX

Figure 1. Three moving patterns of forward players for attacking

In terms of blocking formations, we also separated them into 3 formations: "spread", "bunch" and "dedicate" (Figure 2).

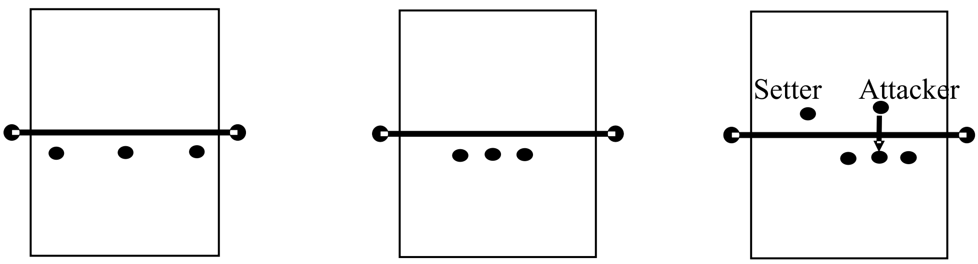

(a) Spread (b) Bunch (c) Dedicate

Figure 2. Three blocking formations

We look at the situations which are categorized in the above patterns, and analyse the ratio of successful blocks. Regarding to the judgment of success or fail of blocks, we define the successful blocks as the case that blocking team gets the blocking point, touch the ball to help the dig or return the ball by blocking. We note that we do not include the number of the mistake of attacks or feint as the number of attacks.

Although this analysis may not reflect the real intention of tactics because we estimate the tactics by watching the players' movement or even players can move without being aware of it, we would like to propose a way of modeling the tactical confliction in volleyball, especially a method for analysis of attacking-blocking situation in this paper. Application of this proposed method will become more practical and informative for coaches and players if the tactics or patterns considered into this macro-view of game theoretic analysis are set based on teams' needs or aims.

The mathematical formulation

We now briefly explain how we formulated the conflicts between the attacking formations and the blocking formations in the phase of reception attack using the above patterns. Here, we formulated it as so called (two-person) zero-sum game, in which two teams play a game and both teams cannot get any points at the same time— if one team gets a point, then the other team loses and the gain of the ratio of successful blocks of one team should be equal to the loss of the ratio of successful attacks of the other team. Actually, this situation can be formulated by tabulating the patterns.

Let a_{ij}, be the ratio of successful blocks in the case of attacking pattern $i \in$ {III R, III C, III L, XI R, XI C, XI L, IX R, IX C, IX L} and blocking formation $j \in$ {S,B,D} as follows:

$$a_{ij} = s_{ij} / n_{ij} \qquad i \in \{\text{III R, III C, III L, XIR, XIC, XIL, IXR, IXC, IXL}\}, \quad j \in \{\text{S, B, D}\} \quad (1)$$

where n_{ij} is the observed number of the combination that attacking i and blocking j occurred. s_{ij} is the observed number of successful blocks in this combination. For example, a_{IIIRS} be the ratio of successful blocks in the case of attacking pattern III with a spike from the right position and blocking formation "spread". In this way, we define matrix A=(a_{ij}), $i \in$ {III R, III C, III L, XI R, XI C, XI L, IX R, IX C, IX L}, $j \in$ {S,B,D}, as a payoff matrix as shown in Table 1.

Table 1. Payoff matrix for the phase of the reception attack in the formulation of zero-sum game

				Blocks	
	Moving pattern	Attacked position	Spread (S)	Bunch (B)	Dedicate (D)
Attacks	Pattern III	Right (R)	a_{IIIRS}	a_{IIIRB}	a_{IIIRD}
		Center (C)	a_{IIICS}	a_{IIICB}	a_{IIICD}
		Left (L)	a_{IIILS}	a_{IIILB}	a_{IIILD}
	Pattern XI	Right (R)	a_{XIRS}	a_{XIRB}	a_{XIRD}
		Center (C)	a_{XICS}	a_{XICB}	a_{XICD}
		Left (L)	a_{XILS}	a_{XILB}	a_{XILD}
	Pattern IX	Right (R)	a_{IXRS}	a_{IXRB}	a_{IXRD}
		Center (C)	a_{IXCS}	a_{IXCB}	a_{IXCD}
		Left (L)	a_{IXLS}	a_{IXLB}	a_{IXLD}

In a zero-sum game, each team chooses a tactic that enables the team to do the best it can. That is, if both teams play rationally, the attacking team chooses a tactic that provides the smallest ratio of successful blocks in row of the matrix. On the other hand, the blocking team will choose its tactic that provides the largest ratio of successful blocks in column of the matrix. Following this type of inference, if this matrix satisfies the condition that the largest minimum of the rows equals to the smallest maximum of these columns (i.e. max (row minimum) = min (column maximum)). That is, if

$$\max_{j}\min_{i} a_{ij} = \min_{i}\max_{j} a_{ij} \qquad i \in \{\text{IIIR,IIIC,IIIL,XIR,XIC,XIL,IXR,IXC,IXL}\}, j \in \{\text{S,B,D}\} \quad (2)$$

holds, it is said to have a saddle point and this value is called the value of the game. A saddle point can also be thought of as an equilibrium point, in the sense that even if one team were to change from this tactic, it will not increase their gain (here, the ratio of successful attacks or blocks).

If there are not any saddle points, then the game is solved as mixed strategies, in which each team selects its tactics with a probability. Let the attacking team choose tactic i among m tactics with a probability p_i ($i=1,\dots,m$). In the same manner, the blocking team choose tactic j among n tactics with a probability q_j ($j=1,\dots,n$). Here, by defining probability vector $\boldsymbol{p}=(p_1, p_2, \dots, p_m)$ and $\boldsymbol{q}=(q_1, q_2, \dots, q_n)$, let $E(\boldsymbol{p}, \boldsymbol{q})$ be the expected payoff taken by blocking team, this is expressed by

$$E(\boldsymbol{p}, \boldsymbol{q}) = \sum_{i}^{m} \sum_{j}^{n} a_{ij} p_i q_j \tag{3}$$

Now in terms of the expected payoff there will be an equilibrium point. That is, $\min_{\boldsymbol{p}} \max_{\boldsymbol{q}} E(\boldsymbol{p},\boldsymbol{q})$ for the attacking team is equal to $\max_{\boldsymbol{q}} \min_{\boldsymbol{p}} E(\boldsymbol{p},\boldsymbol{q})$ for the blocking team,

$$\max_{\boldsymbol{q}} \min_{\boldsymbol{p}} E(\boldsymbol{p},\boldsymbol{q}) = \min_{\mathrm{p}} \max_{\mathrm{q}} E(\boldsymbol{p},\boldsymbol{q}) \tag{4}$$

holds□In this way, if mixed strategies are allowed, it can be shown that this type of zero sum game has an equilibrium point, the value of the game can be obtained. In practice, for example, by solving the following linear programming problem, the value of the game v with tactic i and probability p_i can be calculated.

$$\begin{aligned} &\min \quad v \\ &\textit{subject to} \quad a_{1j} p_1 + a_{2j} p_2 + \cdots + a_{mj} p_m \le v \quad (j = 1,2,\dots, n) \\ &\qquad\qquad\qquad p_1 + p_2 + \cdots + p_m = 1 \\ &\qquad\qquad\qquad p_1, p_2, \cdots, p_m \ge 0 \end{aligned} \tag{5}$$

The System For Identifying Minimax Strategies

Data Input

Following the above formulation, we have developed a game analysis system with VB code for solving the zero-sum game. The solution gives us minimax strategies with the ratio of successful blocks. In this section, we briefly explain this system.

For the practical use of this system, we can input not only real-time data on the site and analyze tactics immediately during a game, but also the past data by watching a recorded scene on the screen after a match and analyzing tactics. Through this input operation, the observed number of the combination of attacking i and blocking j and the number of successful blocks are obtained, and we calculate the ratio based on expression (1).

In practice, the user watches a recorded scene on “Streaming screen” in Figure 3 and clicks buttons on “Data input frame” in the following order:

- Select a moving pattern and click the button
- Select a blocking formation and click the button

- Evaluate the quality of the block and click the button

Then the calculation results are appeared on “Data analysis frame”.

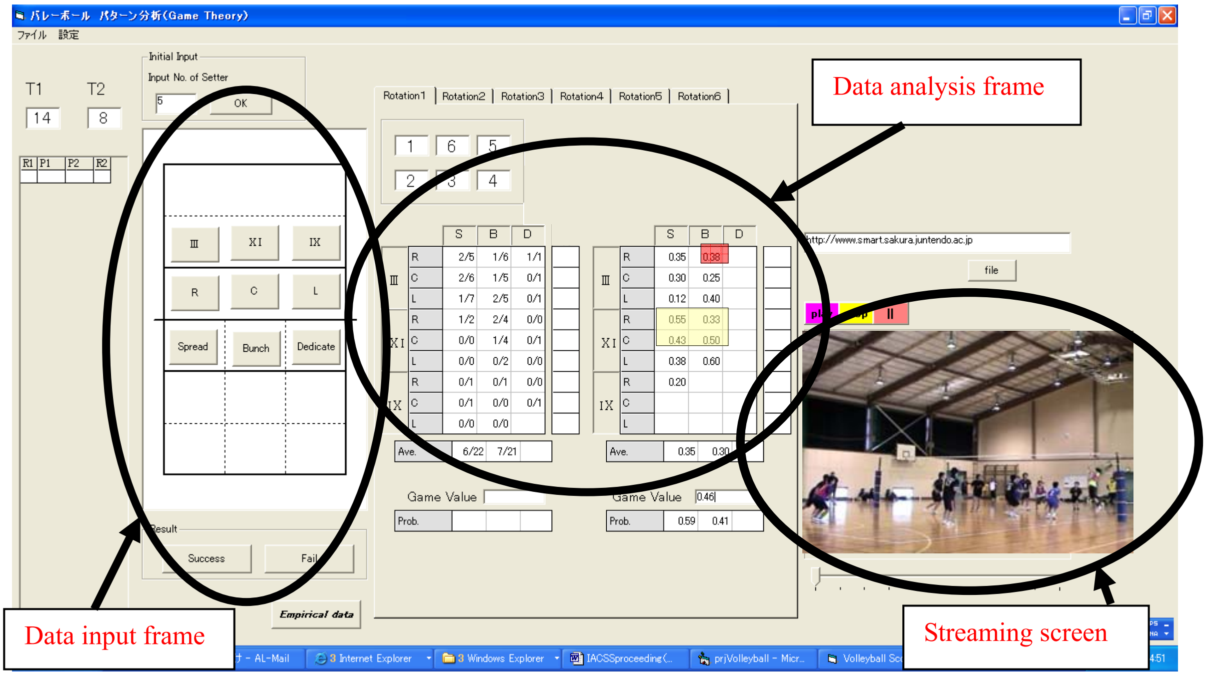

Figure 3. The layout of the frames for a user to input data in this system

Calculation for Identifying Minimax Strategies

Using these calculated ratios, we can make the matrix in the form of Table 1, and the game can be solved based on expression (5) with the help of the VB code. This calculation starts every time after user inputs the data and then clicks “Success” or “Fail” button in data input frame on the screen as shown in Figure 3. This calculation is finished less than a few seconds, and the entries corresponding to minimax strategies for attacking and blocking are highlighted in the matrix on the screen, as also shown in Figure 3. If the game is solved as mixed strategies, the probabilities for realizing the minimax strategies are presented in the lower textbox on the screen. Here, we note that data is summarized depending on each attacking team’s rotation. The result of calculation is aggregated separately for the case that the setter of attacking team is in the front positions or in the back positions and displayed in the right table in the frame for data analysis in Figure 3.

The Data

In this analysis we use the data taken from 32 matches of Division 1 of the Kanto intercollegiate women’s league in the fall of the 2004 season. In the league there were 8 teams and we here name the teams as A,B,...,H in order of final standings of the season. We took the data by watching recorded scenes after the matches and observed each play. We analyzed the 1830 cases of the successful service-receive i.e. the setter gets the received ball without moving his position in the phase of reception attack. We finally selected 1753 cases for this analysis by excluding the mistakes of an attack or a feint, and count the number of successful blocks with regard to the situations of attacking formations and blocking formation.

Result of the Analysis

Overall result

We firstly describe the explanatory statistics for this analysis. Table 2 represents the frequency and the ratio of the situations which have occurred in the 9 attacking patterns (3 moving patterns of forward players and 3 positions from which the ball can be spiked). We separate the case of the attacking teams' setter being in backward position from the case of the setter being in forward position, and in this paper we focus on the former case i.e. attacking teams' setter being in backward position. This is because actual movements of players in the case of setter in backward position are more clearly categorized into the above 3 moving patterns than that in the case of setter in forward position which looks more complicated, and the former case will be enough to illustrate the analysis method proposed in this paper.

As shown in table 2, III and XI were used 63% and 27%, respectively, but IX was used just around 10% in total. With regard to the positions from which the ball was spiked, C is used more (41%) than L (26%) but there looks not so much difference in distribution.

Table 2. Frequency of the attacks with regard to moving patterns and positions.

	R		C		L		Total	
Ⅲ	225	(22%)	246	(24%)	179	(17%)	650	(63%)
X I	95	(9%)	121	(12%)	62	(6%)	278	(27%)
I X	28	(3%)	51	(5%)	25	(2%)	104	(10%)
Total	348	(34%)	418	(41%)	266	(26%)	1032	(100%)

Table 3 represents the relationship between attacking patterns and blocking formations. According to this table, 99.3% of all blocking formations are categorized into the 3 blocking formations (S,B and C), and mostly into S and B.

Table 3. Relationship between attacking patterns and blocking formations.

	Frequency of Attacks		Frequency of Blocks			
	Freq.	Ratio	S	B	D	Others
Ⅲ,R	225	21.8%	91	130	4	0
Ⅲ,C	246	23.8%	71	167	7	1
Ⅲ,L	179	17.3%	71	96	9	3
X I ,R	95	9.2%	27	67	1	0
X I ,C	121	11.7%	21	88	12	0
X I ,L	62	6.0%	11	46	2	3
I X,R	28	2.7%	10	17	1	0
I X,C	51	4.9%	19	32	0	0
I X,L	25	2.4%	9	14	2	0
Total	1032	100.0%	330	657	38	7
Ratio			32.0%	63.7%	3.7%	0.7%

Table 4 shows the detail of Table 3 by adding the information of the success ratio of blocks. The value of the success ratio of blocks should be reliable in some extent. So we exclude the combination of attacking patterns and blocking formations which occurred less than 10 times in the calculation of the success ratio of blocks, and make it as a blank in Table 4.

Table 4. Success ratio of blocks

Attacking		Success ratio of blocks					
			Breakdown				
Pattern	Ratio	Average	S	B	D	Row Max.	
Ⅲ,R	21.8%	0.418	0.330	0.492		0.492	
Ⅲ,C	23.8%	0.290	0.254	0.305		0.305	(0.75)
Ⅲ,L	17.3%	0.386	0.338	0.448		0.448	
XⅠ,R	9.2%	0.295	0.296	0.299		0.299	
XⅠ,C	11.7%	0.298	0.429	0.273	0.250	0.429	(0.25)
XⅠ,L	6.0%	0.492	0.273	0.522		0.522	
ⅠX,R	2.7%	0.464	0.500	0.471		0.500	
ⅠX,C	4.9%	0.412	0.211	0.531		0.531	
ⅠX,L	2.4%	0.400		0.500		0.500	
Total	100.0%	0.361	0.312	0.393	0.237	0.393	
		Column Min.	0.211	0.273	0.250		
			(0.16)	(0.84)		Game value	0.297

As shown in Table 4, pattern “III,C” was used most frequently (23.8%) and its success ratio of blocking is small (0.290). That is, the attacking is not bad because the attacking was done at the least average success ratio of blocks. However, “III,R” was also used frequently (21.8%) although its average success ratio of blocking is quite high (0.418). So, in general the allocation of the attacking patterns seems not to be efficient.

We can obtain the value of the game based on Table 4. The smallest maximum of these rows is 0.299 and the largest minimum of these columns is 0.273. We calculated the value of the game as 0.297, which is realized by the combination of “Pattern III C” in 0.75 and “Pattern XI C in 0.25 for the attacking teams. This implies that if the attacking teams had used the tactics of “III C” in 0.75 and “III C” in 0.25 as a mixed strategy, it could have reduce the success ratio of blocks to 0.297.

Result for each team

In the above we represented overall result of the league. Now in this section we describe the result for each team separately as shown in Table 5. Note that in Table 5 each team’s data is summarized such that each team is considered as a blocking team, and other 7 teams are aggregated as an attacking team against team A. We also exclude the combination of attacking patterns and blocking formations which occurred few times and make it as a blank in Table 5.

Here, for example, team A have the minimum average success ratio of blocks 0.268 against the attacking pattern “III,C”, which was highly used 26.8%. That is, team A was frequently attacked by the patterns which has relatively low success ratio of blocks, although “III,R” of the average success ratio of blocks 0.472 was used 22.9%.

We can also obtain the value of the game based on Table 5. For example, as the smallest maximum of these rows is 0.417 and the largest minimum of these columns is 0.214. We obtained the value of the game as 0.315, which is realized by the combination of “III, C” in 0.58 and “III, L in 0.42 for the attacking teams. This implies that if the attacking teams had used the tactics of “III C” in 0.58 and “III L” in 0.42 as a mixed strategy, it could have reduced the success ratio of blocks to 0.315. We also represent the other 7 teams in Table 5 and each team can be analyzed in the same manner.

Discussion

Overall evaluation of the league

We now discuss the result of overall tendency of the plays by looking over the whole league data. As shown in Table 4, in general, “III,C” which realized small average success ratio of blocks was used most frequently by attacking teams, but “III,R” which realized high average success ratio of blocks was also used frequently. Thus, the attacking patterns seem not to be used efficiently. From the game theoretic point of view, as the value of the game is 0.297 which is smaller than the average success ratio of blocks, the attacking teams could decrease the average success ratio of blocks by changing the allocation of the attacking patterns.

Result for each team

Similar to the overall result in the league as discussed in the above, the attacking teams could decrease the average success ratio of blocks by changing the allocation of the attacking patterns. For example, team A has the value of the game as 0.315 and it could be realized by the combination of “III, C” in 0.58 and “III, C in 0.42 for the opponent attacking teams as a mixed strategy.

Until now, we have analyzed the data from the standpoint of the blocking team, i.e. the team we focused is a blocking team. But, we can look at the situation from the standpoint of the attacking team by changing the aspect of the data. In Table 6, we considered team A, for example, as an attacking team and other 7 teams are aggregated as a opposing team against team A. From this aspect, team A have the minimum average success ratio of opponent blocks 0.243 against team A’s attacking pattern “XI,C”, which was used 23.1% as shown in Table 6. On the other hand, “XI, L” against the success ratio of opponent blocks 0.650 was used 12.5%. That is, team A frequently attacked with the patterns which has low average success ratio of opponent blocks. The value of the game as 0.295 is realized by the combination of “III, L” in 0.92 and “XI, C in 0.08. This implies that team A could still have reduced the success ratio of opponent blocks to 0.295. That is, by changing the allocation of attacking patterns of team A, it could decrease the success ratio of blocking by 0.346－0.295=0.051. We also represent the other 7 teams in Table 6 and each team can be analyzed in the same manner.

Table 5. The data from the standpoint of each team’s blocking formations

	Freq. of Attacks		Freq. of Blocks				Success ratio of blocks					
	Freq.	Ratio	S	B	D	Others	Total	S	B	D	Row Max.	
Team A												
Ⅲ,R	36	22.9%	14	22	0	0	0.472	0.429	0.500		0.500	
Ⅲ,C	42	26.8%	12	28	1	1	0.268	0.417	0.214		0.417	(0.58)
Ⅲ,L	41	26.1%	17	22	2	0	0.317	0.176	0.455		0.455	(0.42)
XI,R	5	3.2%	1	4	0	0	0.600					
XI,C	8	5.1%	1	7	0	0	0.750					
XI,L	3	1.9%	1	2	0	0	0.333					
IX,R	6	3.8%	0	5	1	0	0.500					
IX,C	10	6.4%	1	9	0	0	0.400		0.444		0.444	
IX,L	6	3.8%	0	5	1	0	0.833					
Total	157	100.0%	47	104	5	1	0.404	0.319	0.452		0.452	
			29.9%	66.2%	3.2%	0.6%	Column Min.	0.180	0.214			
								(0.35)	(0.65)		Game Value	0.315
Team B												
Ⅲ,R	35	23.8%	6	28	1	0	0.543	0.333	0.607		0.607	
Ⅲ,C	33	22.4%	7	25	1	0	0.273	0.143	0.280		0.280	
Ⅲ,L	28	19.0%	8	18	1	1	0.444	0.625	0.389		0.625	
XI,R	14	9.5%	5	9	0	0	0.357	0.400	0.333		0.400	
XI,C	13	8.8%	2	11	0	0	0.385	0.500	0.364		0.500	
XI,L	7	4.8%	1	6	0	0	0.571					
IX,R	4	2.7%	0	4	0	0	0.500					
IX,C	8	5.4%	3	5	0	0	0.500					
IX,L	5	3.4%	1	4	0	0	0.200					
Total	147	100.0%	33	110	3	1	0.418	0.424	0.418		0.424	
			22.4%	74.8%	2.0%	0.7%	Column Min.	0.14	0.28			
											Game Value	0.280
Team C												
Ⅲ,R	36	22.4%	4	32	0	0	0.528	0.750	0.500		0.750	
Ⅲ,C	38	23.6%	4	32	2	0	0.421	0.000	0.469		0.469	
Ⅲ,L	23	14.3%	4	18	1	0	0.435	0.000	0.556		0.556	
XI,R	24	14.9%	0	24	0	0	0.250		0.250		0.250	
XI,C	20	12.4%	0	18	2	0	0.200		0.222		0.222	
XI,L	14	8.7%	0	14	0	0	0.500		0.500		0.500	
IX,R	0	0.0%	0	0	0	0						
IX,C	6	3.7%	1	5	0	0	0.500					
IX,L	0	0.0%	0	0	0	0						
Total	161	100.0%	13	143	5	0	0.404	0.231	0.427		0.427	
			8.1%	88.8%	3.1%	0.0%	Column Min.	0.000	0.222			
											Game Value	0.222
Team D												
Ⅲ,R	27	25.0%	1	26	0	0	0.444		0.462		0.462	
Ⅲ,C	30	27.8%	0	29	1	0	0.300		0.310		0.310	
Ⅲ,L	16	14.8%	1	14	1	0	0.250		0.286		0.286	
XI,R	13	12.0%	2	11	0	0	0.308		0.364		0.364	
XI,C	16	14.8%	1	15	0	0	0.125		0.067		0.067	
XI,L	4	3.7%	0	4	0	0	0.500					
IX,R	0	0.0%	0	0	0	0						
IX,C	1	0.9%	0	1	0	0	0.000					
IX,L	1	0.9%	0	1	0	0	1.000					
Total	108	100.0%	5	101	2	0	0.315		0.327		0.327	
			4.6%	93.5%	1.9%	0.0%	Column Min.		0.067			
											Game Value	0.067
Team E												
Ⅲ,R	26	20.3%	21	3	2	0	0.423	0.476	0.333		0.476	
Ⅲ,C	31	24.2%	14	17	0	0	0.323	0.357	0.294		0.357	
Ⅲ,L	18	14.1%	13	5	0	0	0.389	0.308	0.600		0.600	
XI,R	11	8.6%	5	5	1	0	0.364	0.400	0.400		0.400	
XI,C	13	10.2%	5	8	0	0	0.231	0.200	0.250		0.250	
XI,L	8	6.3%	1	6	0	1	0.286					
IX,R	6	4.7%	5	1	0	0	0.500					
IX,C	9	7.0%	5	4	0	0	0.556					
IX,L	6	4.7%	4	1	1	0	0.333					
Total	128	100.0%	73	50	4	1	0.370	0.370	0.400		0.400	
			57.0%	39.1%	3.1%	0.8%	Column Min.	0.200	0.250			
											Game Value	0.250
Team F												
Ⅲ,R	31	23.1%	17	13	1	0	0.355	0.353	0.385		0.385	
Ⅲ,C	32	23.9%	14	18	0	0	0.250	0.214	0.278		0.278	
Ⅲ,L	19	14.2%	10	8	0	1	0.500	0.500	0.500		0.500	
XI,R	8	6.0%	4	4	0	0	0.125					
XI,C	19	14.2%	3	13	3	0	0.421	0.667	0.385		0.667	
XI,L	10	7.5%	3	7	0	0	0.500	0.000	0.714		0.714	
IX,R	4	3.0%	1	3	0	0	0.500					
IX,C	7	5.2%	2	5	0	0	0.429					
IX,L	4	3.0%	1	3	0	0	0.250					
Total	134	100.0%	55	74	4	1	0.361	0.309	0.405		0.405	
			41.0%	55.2%	3.0%	0.7%	Column Min.	0.000	0.278			
											Game Value	0.278
Team G												
Ⅲ,R	13	14.9%	10	3	0	0	0.077	0.000	0.333		0.333	
Ⅲ,C	15	17.2%	6	9	0	0	0.200	0.000	0.333		0.333	(0.40)
Ⅲ,L	15	17.2%	7	6	1	1	0.429	0.429	0.500		0.500	
XI,R	5	5.7%	1	4	0	0	0.000					
XI,C	16	18.4%	2	11	3	0	0.250	0.500	0.273		0.500	(0.60)
XI,L	12	13.8%	3	5	2	2	0.600	0.333	0.600		0.600	
IX,R	6	6.9%	2	4	0	0	0.500					
IX,C	5	5.7%	3	2	0	0	0.200					
IX,L	0	0.0%	0	0	0	0						
Total	87	100.0%	34	44	6	3	0.286	0.235	0.318		0.318	
			39.1%	50.6%	6.9%	3.4%	Column Min.	0.000	0.273			
								(0.11)	(0.89)		Game Value	0.297
Team H												
Ⅲ,R	21	19.1%	18	3	0	0	0.190	0.167	0.333		0.333	(0.63)
Ⅲ,C	25	22.7%	14	9	2	0	0.200	0.286	0.111		0.286	
Ⅲ,L	19	17.3%	11	5	3	0	0.368	0.364	0.400		0.400	
XI,R	15	13.6%	9	6	0	0	0.333	0.444	0.167		0.444	
XI,C	16	14.5%	7	5	4	0	0.250	0.286	0.000		0.286	(0.37)
XI,L	4	3.6%	2	2	0	0	0.500					
IX,R	2	1.8%	2	0	0	0	0.000					
IX,C	5	4.5%	4	1	0	0	0.200					
IX,L	3	2.7%	3	0	0	0	0.000					
Total	110	100.0%	70	31	9	0	0.255	0.257	0.226		0.257	
	110		63.6%	28.2%	8.2%	0.0%	Column Min.	0.167	0.000			
								(0.74)	(0.26)		Game Value	0.21

Table 6. The data from the standpoint of each team' attacking patterns

	Freq. of Attacks		Freq. of Blocks				Success ratio of blocks					
	Freq.	Ratio	S	B	D	Others	Total	S	B	D	Row Max.	
Team A												
Ⅲ,R	28	17.5%	7	21	0	0	0.357	0.000	0.476		0.476	
Ⅲ,C	26	16.3%	11	12	3	0	0.346	0.182	0.417		0.667	
Ⅲ,L	20	12.5%	7	10	2	1	0.263	0.286	0.300		0.300	(0.92)
XI,R	29	18.1%	4	25	0	0	0.310	0.500	0.280		0.500	
XI,C	37	23.1%	5	30	2	0	0.243	0.400	0.233		0.400	(0.08)
XI,L	20	12.5%	2	18	0	0	0.650	0.500	0.667		0.667	
IX,R	0	0.0%	0	0	0	0						
IX,C	0	0.0%	0	0	0	0						
IX,L	0	0.0%	0	0	0	0						
Total	160	100.0%	36	116	7	1	0.346	0.250	0.379		0.379	
			22.5%	72.5%	4.4%	0.6%	Column Min.	0.000	0.233			
								(0.37)	(0.63)		Game Value	0.295
Team B												
Ⅲ,R	43	32.8%	18	24	1	0	0.419	0.278	0.542		0.542	
Ⅲ,C	37	28.2%	10	26	1	0	0.216	0.300	0.192		0.300	
Ⅲ,L	27	20.6%	12	12	3	0	0.111	0.083	0.167		0.167	
XI,R	10	7.6%	4	6	0	0	0.200	0.250	0.167		0.250	
XI,C	6	4.6%	3	3	0	0	0.667					
XI,L	2	1.5%	1	1	0	0	0.500					
IX,R	2	1.5%	0	2	0	0	0.500					
IX,C	4	3.1%	2	2	0	0	0.500					
IX,L	0	0.0%	0	0	0	0						
Total	131	100.0%	50	76	5	0	0.298	0.280	0.329		0.329	
			38.2%	58.0%	3.8%	0.0%	Column Min.	0.083	0.167			
											Game Value	0.167
Team C												
Ⅲ,R	21	15.6%	7	13	1	0	0.333	0.571	0.231		0.571	
Ⅲ,C	26	19.3%	6	19	0	1	0.360	0.333	0.368		0.368	
Ⅲ,L	20	14.8%	6	12	2	0	0.400	0.167	0.583		0.583	
XI,R	11	8.1%	5	6	0	0	0.364	0.200	0.500		0.500	
XI,C	20	14.8%	4	14	2	0	0.250	0.250	0.286		0.286	(0.90)
XI,L	7	5.2%	2	4	1	0	0.571				1.000	
IX,R	6	4.4%	1	4	1	0	0.333				1.000	
IX,C	13	9.6%	4	9	0	0	0.385	0.250	0.444		0.444	
IX,L	11	8.1%	4	6	1	0	0.273	0.500	0.167		0.500	(0.10)
Total	135	100.0%	39	87	8	1	0.351	0.333	0.379		0.379	
			28.9%	64.4%	5.9%	0.7%	Column Min.	0.167	0.167			
								(0.33)	(0.67)		Game Value	0.274
Team D												
Ⅲ,R	32	23.4%	15	17	0	0	0.375	0.267	0.471		0.471	
Ⅲ,C	37	27.0%	14	22	1	0	0.162	0.214	0.136		0.214	
Ⅲ,L	31	22.6%	17	12	1	1	0.533	0.529	0.500		0.529	
XI,R	3	2.2%	0	3	0	0	0.000					
XI,C	2	1.5%	0	2	0	0	0.000					
XI,L	3	2.2%	1	2	0	0	0.333					
IX,R	10	7.3%	3	7	0	0	0.700	0.667	0.714		0.714	
IX,C	13	9.5%	3	10	0	0	0.462	0.333	0.500		0.500	
IX,L	6	4.4%	2	3	1	0	0.333					
Total	137	100.0%	55	78	3	1	0.368	0.345	0.372		0.372	
			40.1%	56.9%	2.2%	0.7%	Column Min.	0.214	0.136			
											Game Value	0.214
Team E												
Ⅲ,R	30	26.3%	16	14	0	0	0.400	0.250	0.571		0.571	
Ⅲ,C	44	38.6%	8	34	2	0	0.273	0.250	0.294		0.294	(0.86)
Ⅲ,L	12	10.5%	5	7	0	0	0.583	0.800	0.429		0.800	
XI,R	6	5.3%	2	4	0	0	0.333					
XI,C	17	14.9%	2	9	6	0	0.353	0.500	0.222		0.500	(0.14)
XI,L	4	3.5%	1	3	0	0	0.500					
IX,R	1	0.9%	1	0	0	0	1.000					
IX,C	0	0.0%	0	0	0	0						
IX,L	0	0.0%	0	0	0	0						
Total	114	100.0%	35	71	8	0	0.368	0.371	0.366		0.371	
			30.7%	62.3%	7.0%	0.0%	Column Min.	0.250	0.222			
								(0.23)	(0.77)		Game Value	0.284
Team F												
Ⅲ,R	26	21.3%	14	12	0	0	0.462	0.500	0.417		0.500	
Ⅲ,C	25	20.5%	13	12	0	0	0.240	0.385	0.083		0.385	(0.59)
Ⅲ,L	10	8.2%	5	5	0	0	0.400	0.200	0.600		0.600	
XI,R	21	17.2%	6	15	0	0	0.286	0.167	0.333		0.333	
XI,C	12	9.8%	3	9	0	0	0.333	0.000	0.444		0.444	(0.41)
XI,L	7	5.7%	1	5	0	1	0.333					
IX,R	6	4.9%	4	2	0	0	0.167					
IX,C	12	9.8%	8	4	0	0	0.250	0.250	0.250		0.250	
IX,L	3	2.5%	3	0	0	0	0.000					
Total	122	100.0%	57	64	0	1	0.314	0.281	0.344		0.344	
			46.7%	52.5%	0.0%	0.8%	Column Min.	0.000	0.083			
								(0.48)	(0.52)		Game Value	0.228
Team G												
Ⅲ,R	13	19.1%	2	10	1	0	0.692	1.000	0.700		1.000	
Ⅲ,C	8	11.8%	0	8	0	0	0.375					
Ⅲ,L	23	33.8%	6	16	1	0	0.435	0.500	0.438		0.500	
XI,R	5	7.4%	2	3	0	0	0.400					
XI,C	10	14.7%	1	9	0	0	0.300		0.333		0.333	
XI,L	6	8.8%	1	5	0	0	0.500					
IX,R	0	0.0%	0	0	0	0						
IX,C	3	4.4%	1	2	0	0	0.333					
IX,L	0	0.0%	0	0	0	0						
Total	68	100.0%	13	53	2	0	0.456	0.538	0.453		0.538	
			19.1%	77.9%	2.9%	0.0%	Column Min.	0.000	0.333			
											Game Value	0.333
Team H												
Ⅲ,R	32	19.4%	12	19	1	0	0.438	0.333	0.526		0.526	
Ⅲ,C	43	26.1%	9	34	0	0	0.419	0.111	0.500		0.500	
Ⅲ,L	36	21.8%	13	22	0	1	0.429	0.231	0.545		0.545	
XI,R	10	6.1%	4	5	1	0	0.300	0.250	0.400		0.400	
XI,C	17	10.3%	3	12	2	0	0.294	0.667	0.250		0.667	
XI,L	13	7.9%	2	8	1	2	0.273	0.000	0.250		0.250	
IX,R	3	1.8%	1	2	0	0	0.333					
IX,C	6	3.6%	1	5	0	0	0.667					
IX,L	5	3.0%	0	5	0	0	1.000					
Total	165	100.0%	45	112	5	3	0.420	0.267	0.491		0.491	
			27.3%	67.9%	3.0%	1.8%	Column Min.	0.000	0.250			
											Game Value	0.250

Here, we summarize the difference between the average success ratio of blocks and the value of the game in Table 7.

Table 7. Success ratio of blocks

		Standpoint of Blocks	Standpoint of Attacks	①−②	Standpoint of Blocks	①−③	Standpoint of Attacks	②−⑤	④−⑥
		Success ratio	Success ratio		Game Value		Game Value		
		①	②		③	④	⑤	⑥	
1	Team A	0.404	0.346	0.058	0.315	0.089	0.295	0.051	0.038
2	Team B	0.418	0.298	0.120	0.280	0.138	0.167	0.131	0.007
3	Team C	0.404	0.351	0.053	0.222	0.182	0.274	0.077	0.105
4	Team D	0.315	0.368	-0.053	0.067	0.248	0.214	0.153	0.095
5	Team E	0.370	0.368	0.002	0.250	0.120	0.284	0.084	0.036
6	Team F	0.361	0.314	0.047	0.278	0.083	0.228	0.086	-0.003
7	Team G	0.286	0.456	-0.170	0.210	0.076	0.333	0.123	-0.047
8	Team H	0.255	0.420	-0.165	0.210	0.045	0.250	0.170	-0.125
	Total	0.361	0.361		0.297	0.064	0.297	0.064	

In Table 7, firstly we look at the difference of the success ratio of blocks between the standpoint of blocking and attacking. For example, as shown Table 7 team A has the average success ratio of blocks 0.404 as the blocking team. This value corresponds to the value in Table 5. As an attacking team, team A faces the opponent blocks as the average success ratio of 0.346, which corresponds to the value in Table 6. Here the difference 0.404−0.346=0.058 is considered to be a superiority of average blocking ability by team A to average ability being blocked by other 7 teams.

On the other hand, team A has the difference between the average success ratio of blocks and the value of the game in blocking such that 0.404−0.315=0.089. This is considered to be a potential gain comes from the tendency that other 7 teams do not use suitable allocation of attacking patterns. In other words, if other 7 teams change the allocation of attacking patterns, team A could decrease the success ratio of blocks by 0.089. (i.e. Team A seems to get benefit 0.089 from other 7 teams' inefficiencies.)

Team A also has the difference between the average success ratio of opponent blocks and the value of the game in terms of attacking such that 0.346−0.295=0.051. This is considered to be a potential loss of team A which does not use suitable allocation of attacking patterns. In other words, if team A change the allocation of attacking patterns, team A could decrease the average success ratio of opponent blocks by 0.051. (i.e. Team A seems to lose benefit 0.051 from other 7 teams by team A's inefficiencies.)

In total, team A gets benefit of 0.089 and lose 0.051, so it gets 0.089−0.051=0.038 as shown in the right column of Table 7. The other 7 teams are analyzed in the same manner.

We plot these values shown in Table 7 on Figure 4. As illustrated in Figure 3, this macro-view of the game theoretic analysis shed the light on the characteristics of teams. In this figure, x-axis represents the difference of success ratio of blocking between the standpoint of blocking and attacking, which is observed just by the statistical data represented by the heading "①−②" in Table 7. Y-axis represents the difference of potential benefit, which is estimated by this game theoretical analysis represented by "④−⑥" in Table 7. Therefore, the teams plotted in the upper right area are considered that they are relatively not only superior in average success ratio of blocks but also get potential benefit form other teams' poor allocation of attacking patterns. On the other hand the team located in the lower left area are relatively inferior in average success ratio of blocks but also lose potential benefit by its own poor allocation of patterns.

Not surprisingly, the top 3 teams of the league (teams A, B and C) locate in the upper right area. Here, team C get the highest potential benefit by the allocation of attacking patterns from the standpoint of this game theoretic analysis. The bottom 2 teams (teams G and H) locate in the lower left area. Team D is not good in the sense of its relative success ratio of blocks but it seems to get quite large benefit by allocation of attacking patterns. These results are of particular interest since they give insights which could in no way be ascertained without help of game theory.

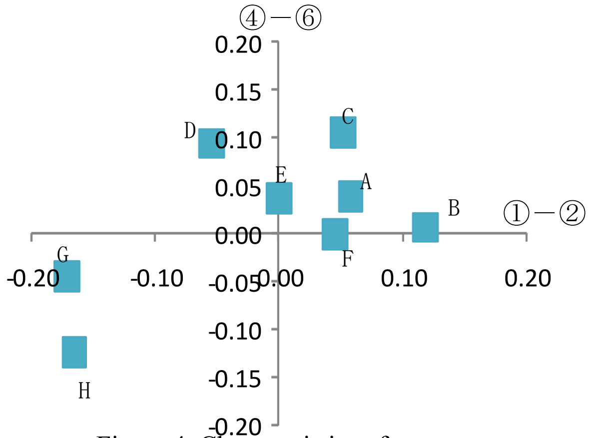

Figure 4. Characteristics of teams

Conclusions

We have presented a method for analyzing tactics in volleyball using game theory, focusing on the phase of reception attack. We have formulated the conflict between attacking formations and blocking formations as a zero-sum game by tabulating these patterns of formations, and have analyzed the tactics by calculating the value of the game with the game analysis system developed on VB. We have also shown an example of a macro-view of game theoretic analysis, using the data taken from the intercollegiate women's league in 2004. Here, we have estimated the game values for the league and show a possible improvement of the allocation of attacking patterns. We have also tried to illustrate the characteristics of teams from the point of success ratio of blocks and allocation of attacking patterns.

Although we have used the empirical data of the intercollegiate women's league in the situation that the setter's position in backward, we will analyze the situation that the setter's position in forward which will be more complicated to model the tactics. We can also state that we should extend our analysis from the women's league to other level and modifying the mathematical model of the pattern of attacking and blocking suitable for the level of play in practice.

This research is just a first step to provide a practical application of game theory to real volleyball matches, but this approach could provide a new standpoint of the macro-view of the volleyball match analysis. Further, this type of game theoretic analysis could be also applicable to other sports by formulating a confliction in each sport, and could hopefully give us new insights into the game.

Acknowledgments

We thank Dr. K. Nemoto, in Faculty of Sport Science at Nippon Sport Science University, for allowing us to refer to the video tapes and giving us practical advice. This research is supported by Grant-in-aid for Scientific Research (C), #17510144 and #21510159.

References

Boronico, J.S. and Newbert, S.L. (1999). Play calling strategy in American football: game-theoretic stochastic dynamic programming approach. *Journal of Sport Management, 13*, 103-113.

Cowan, R. (1992). The Allocation of Offensive and Defensive Resources in a Territorial Game. *Journal of Applied Probability*, *29*, 190-195.

Davis, M. D. (1983). *Game Theory - A Nontechnical Introduction.* NewYork :Dover Publications Inc.

Hirotsu, N., Miyaji, C., Ezaki, N., Shigenaga, T., & Taguchi, A. (2005). A mathematical method for finding optimal tactics by utilizing statistical data updated in real time during a volleyball game, *Proceedings of the 12th IASI (International Association for Sports Information) World Congress*, 226-234.

Hirotsu, N., & Wright, M. B. (2006). Modeling tactical changes of formation in association football as a zero-sum game. *Journal of Quantitative Analysis in Sports*, *2(2),* Article 4.

Hirotsu, N., Ito, M, Miyaji, C., Hamano, K., & Taguchi, A. (2009). Modeling tactical changes of formation in association football as a non-zero-sum game. *Journal of Quantitative Analysis in Sports*, *5(3),* Article 2.

Jordan, J.D., Melouk, S.H. & Perry, M.B. (2009). Optimizing football game play calling, *Journal of Quantitative Analysis in Sports*, 5*(2),* Article 2.

Sadovskii, L. E., & Sadovskii, A. L. (1993). *Mathematics and sports, Mathematical World Vol.3*. American Mathematical Society, Providence, RI. (Translated from the Russian by S. Makar-Limanov)

Shigenaga, T., Ezaki, N., Hirotsu, N., & Miyaji, C. (2004). Development of TOUCH VOLLEY – volleyball tactical support system -, in Hubbard et al (eds.) *The Engineering of Sports 5*, Vol.2, 589-595.

Shigenaga, T., Ezaki, N., & Uno, S. (2002). Development of the tactical support software in a game of volleyball (II). *Annual Reports of Toba national college of maritime technology*, *25*, 41-50.

Shigenaga, T., Ezaki, N., Yamamoto, C., & Yamada, H. (2001). Development of the tactical support software in a game of volleyball. *Annual Reports of Toba national college of maritime technology*, *24*, 33-44.

Turocy, T.L. (2008). In search of the “last-ups” advantage in baseball: A game-theoretic appraoch, *Journal of Quantitative Analysis in Sports, 4(2),* Article 5.

Winston, W. L. (1993). *Operations Research: Applications and Algorithms.* Belmont, CA: Duxbury Press.

Weinstein-Gould, J. (2008). Keeping the hitter off balance: Mixed strategies in baseball, *Journal of Quantitative Analysis in Sports, 5(2),* Article 7.

Yoshida, S., Noro, S., Sato, M., & Wen, L. (1994). Game Theory of Volleyball (1): Optimal Mixed Strategy for Attacking and Blocking. *Bulletin of the Institute of Sports, Physical Education and Recreation, Senshu University*, *17*, 9-19. (written in Japanese)

Genetic Algorithm Optimization Applied to a Biomechanical Model of Snatch Lift

Shahram Lenjan-nejadian[1], Mostafa Rostami[2]
[1]*Faculty of PE & Sport Sciences, University of Isfahan, Isfahan, Iran*
[2]*Faculty of Biomedical Engineering, Amirkabir University of Technology, Tehran, Iran*

Abstract

Simulating the movement of a snatch weightlifter by means of the dynamic formulation and optimizing this movement using Genetic Algorithm as a soft computing method is the main purpose of this study. The snatch weightlifter is modeled by an open kinematic chain. The problem is defined as the optimization of the movement of this model from the first position to the predefined second position while considering the specific optimum criterion like minimizing the muscular effort. The results are represented in the forms of kinematic and kinetic data like trajectory of barbell and actuating joint torques. Because of some similarities between the results and experimental observations by other researches we conclude that our method can be able to model the real situation. This model can be used to optimize the performance of the weightlifters and it could give us some useful advice about the most effective technique.

KEYWORDS: WEIGHTLIFTING, SIMULATION, SPORT BIOMECHANICS

Introduction

Optimization of sport techniques is one of the main goals of sport biomechanics. Since the increasing coaches' tendency to biomechanical analysis of weightlifting, several biomechanical characteristics have been introduced to categorize the weightlifters' performance. Power produced by weightlifters, barbell trajectory, and velocity of barbell are three examples of these characteristics. Analyzing these parameters introduce some indices for evaluating the lifting performance. The most common is the barbell trajectory which has been investigated over the years by several researchers (Baumann, Gross, Quade, Galbierz, & Schwirtz, 1998; Byrd, 2001; Garhammer, 1985, 1998, 2001; Gourgoulis, Aggelousis, Mavromatis, & Garas, 2000; Hiskia, 1997; Isaka, Okada, & Funato, 1996; Schilling, Stone, O'Brayant, Fry, Cogllanese, & Pierce, 2002; Vorobyev, 1978).

Dividing the optimal barbell trajectories from non-optimal ones is in agreement with the most of above mentioned researchers. They studied the differences between the elite weightlifters' characteristics of motion and then categorized the optimal lifting motion patterns. After all, they introduced several optimal trajectories for snatch weightlifting. Vorobyev (1978) suggested three barbell movement patterns for snatch weightlifting roughly depicted in Figure 1. The vertical lines in this Figure indicate the x-component of initial position of barbell and consequently demonstrate its inward-toward motion during the snatch lift. Garhammer (1998) showed that the pattern type A is the best trajectory according to his investigation among the elite weightlifters. Bauman et al. (1998) reported some results which showed the type B is the best, but Hiskia (1997) who studied a large number of weightlifters concluded that the type C is more common than the other types. Byrd (2001) and Bartonietz (1996) also published some results which showed the pattern type B in their experimental observations.

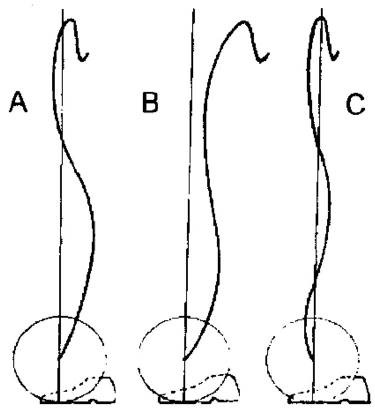

Figure 1. Three types of barbell trajectory in snatch weightlifting (Vertical line demonstrates the inward-toward motion of barbell during the snatch lift)

One of the reasons to this inconsistency for choosing the best type is this idea that the selected criterion by above researchers might not be appropriate. Their criterion was the weightlifters' success percentage to do the snatch. Considering none of the mechanical characteristics to introduce the best pattern is the disadvantage of this criterion. Also the researchers accept the dependency of the optimal barbell trajectory to specific personal parameters such as anthropometric and physical characteristics (Campos, 2006). On the other hand these empirically optimal patterns have not the ability to improve the performance of elite weightlifters themselves, because you cannot compare a good pattern with itself to reach to better performance.

According to above mentioned deficiencies, the necessity for developing a pure mechanical model which considers the specific characteristics of each individual will be obvious. Theoretically this model will be able to lead us to the best ideal technique by using the mechanical principles. The mechanical models have been used to evaluate each technique and to facilitate the procedure of optimization by using the mathematical approach. To do this, we use a five-link model in sagittal plane which is used for lifting task modeling by several researchers (Chang, Brown, Bloswick, & Hsiang, 2001; Lin, Ayoub, & Bernard, 1999; Park, Martin, Choe, Chaffin, & Reed, 2005). The movement of this model can be optimized by minimizing specific mechanical criteria like time, actuating joint torques, and energy consumption (Rostami & Bessonnet, 2001). In recent years, some researchers (Chang et al., 2001) used actuating joint torque as a mechanical criterion to introduce optimal patterns for lifting tasks.We prefer the same because of its relation to injuries (Chang et al., 2001). Optimization of lifting tasks was done by some researchers (Gruver, Ayoub, & Muth, 1979; Hsiang, Chang, & McGorry, 1999; Lin et al, 1999; Salaami et al, 2008; Javadi, Arshi, & Shirzad, 2007) who obtain the optimal movement by using some pre-defined trajectory for each joint. The optimization algorithm minimizes the selective criterion by changing the coefficient of these above mentioned trajectories. Each trajectory should be defined by user and it will be varied if the number of constraints is changed. Another restriction of their optimizing approach is dimensional problem of dynamic programming which is used by them. Chang et al. (2001) believed that this approach is not suitable and use spacetime optimization method to produce better solution for manual lifting task. We believe that although the sequential quadratic programming which is used by him is a good approach and it has some attractive features but also it represents some problems. The Hessian matrix containing the second order derivatives and the solution often requires inversion or factorization of it which is time consuming and it is not easy also. Therefore we want to introduce a suitable and easy to use approach which will be able to predict the optimal movement in snatch weightlifting technique.

Let us summarize the problem as finding the most effective technique while considering the motion equations, the specific mechanical criterion, and the dynamic constraints simultaneously. To formulate this problem we encounter with a set of motion equations should be solved together with minimizing an equation representing the optimization criterion. This situation forms a problem in optimal control domain. There are two different methods to solve this problem. First, the mathematical indirect approach which gives us a unique solution (Nejadian & Rostami, 2007; Lenjan Nejadian, Rostami, & Towhidkhah, 2008) and the second, direct search approach between all solutions of motion equations to reach a solution which fulfills the criterion equation (Lenjan Nejadian & Rostami, 2007). We choose the latter because of its easy modeling and applying and also its faster response. But the direct search without any specific patterns is not suitable or even applicable in this special problem. There are many algorithms to conduct the search approach and one of them is genetic algorithm. In the recent past, genetic algorithm (GA) has been increasingly applied to various optimization problems, including engineering and sciences. It has the advantage of broad applicability, ease of use, and global perspective. In this study, we use a five-link biomechanical model to evaluate the different snatch motions and to predict the optimum barbell trajectory which minimizes the specific mechanical criterion by using genetic algorithm (GA) which is a valid approach to problems requiring efficient and effective searches. The validity of this model can be obtained by comparing its results and experimental observations. But we expect some differences because of two main reasons; first, the intrinsic simplicity of our model and the second, the deviation of each weightlifter from the perfect optimal technique.

Methods

To build a biomechanical model of a weightlifter we should translate the physical property of human into the mathematical one. It means that we should convert the body to appropriate model of links with proper length, mass and moment of inertia. For this purpose, we can use the anthropometric models developed by several researchers. A few comprehensive models have been described by Chaffin and Anderson (1991). By using the proper model, we have a multi-segment model that contains information about mass, center of gravity, length and moments of inertia of each segment which represents the whole body. In this model, the body segments convert into solid links and the body joints convert into simple revolute joints. We simplify this model to a two-dimensional model in sagittal plane which can be used for modeling the weightlifting or other general lifting activities. This is a common assumption that has been used by several researchers (Chang et al., 2001; Menegaldo, Fleury, & Weber, 2003; Park et al., 2005). Now we should make a decision about the number of links we like to use and hence the number of degrees of freedom (DOF) which is the main factor that affects the complexity of model, and therefore it has a direct effect on time and cost of computing and solving the problem. The best model is the one that minimizes the complexity and simultaneously offers a good approximation of the whole motion. Several researchers (Chang et al., 2001; Menegaldo et al., 2003; Park et al., 2005) used five-link model to analyze lifting tasks. Therefore we use the five degrees of freedom model.

Equations of Motion

Using the five-link planar model enables us to extract its motion equations. In Figure 2 the schematic diagram of this model at initial time can be observed. This model is made by five links by which shin, thigh, trunk, upper arm and forearm are represented, respectively named L1 to L5. Also, five body joints: ankle, knee, hip, shoulder and elbow are represented O1 to O5 respectively.

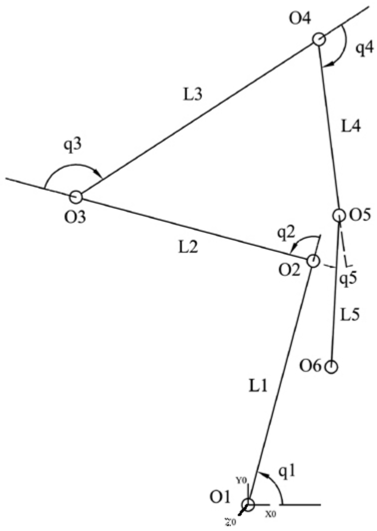

Figure 2. Biomechanical model of a weightlifter at initial position.

Consider a coordinate system ($\mathbf{X}_0\mathbf{Y}_0\mathbf{Z}_0$) which is locked at ankle joint. The model motion can be described by the five relative joint coordinates which are defined by:

$$q_i = (\mathbf{X}_i , \mathbf{X}_{i-1})_{\mathbf{Z}_0} \qquad i = 1, \dots , 5 \quad (\mathbf{Z}_0 = \mathbf{X}_0 \times \mathbf{Y}_0) \tag{1}$$

The vector $\mathbf{X}_i$ indicates the direction of link L_i and $\mathbf{Z}_0$ indicates the positive direction of angular parameters.

Let us add the following complementary notations:

$\mathbf{q} = (q_1 ,\dots, q_5)^{\mathrm{T}}$, vector of joint coordinates

$\dot{\mathbf{q}} = (\dot{q}_1 ,\dots, \dot{q}_5)^{\mathrm{T}}$, vector of joint velocities

$\ddot{\mathbf{q}} = (\ddot{q}_1 ,\dots, \ddot{q}_5)^{\mathrm{T}}$, vector of joint accelerations

where $\dot{q}_i = \mathrm{d}q_i / \mathrm{d}t$, $\ddot{q}_i = \mathrm{d}^2 q_i / \mathrm{d}t^2$.

According to Figure 2, we define the dimension and inertia characteristics of the model by:

$\mathbf{O}_i\mathbf{O}_{i+1} = r_i\, \mathbf{X}_i\, , i = 1,\dots,5;\ \ r_i$, length of link L_i

$\mathbf{O}_i\mathbf{G}_i = a_i\, \mathbf{X}_i\, ,\ \ i = 1,\dots,5$

In which, G_i is center of gravity of link L_i and a_i is its distance from proximal joint.

m_i , mass of link L_i

I_i^z , moment of inertia of L_i with respect to the joint axis $(O_i\,,\,\mathbf{Z_0})$

Numerical values of these dimensional parameters are calculated based on body weight and height of the weightlifter using the models described before (Chaffin and Anderson 1991). For obtaining the equations of motion the Lagrangian of the model is written as:

$$L(\mathbf{q},\dot{\mathbf{q}}) = T(\mathbf{q},\dot{\mathbf{q}}) - U(\mathbf{q}) \tag{2}$$

where U is the potential energy and T is the kinetic energy defined by:

$$T(\mathbf{q},\dot{\mathbf{q}}) = 1/2\,\dot{\mathbf{q}}^T\mathbf{M}(\mathbf{q})\,\dot{\mathbf{q}} \tag{3}$$

$\mathbf{M}$ is the mass matrix of the kinetic chain which its componets are complex function of m_i and I_i^z. Equations of motion may be derived by Lagrange's formula:

$$\frac{d}{dt}\left(\frac{\partial L}{\partial \dot{q}_i}\right) - \frac{\partial L}{\partial q_i} = Q_i^d + Q_i^a \quad , i = 1, \ldots, 5 \tag{4}$$

The right hand term is generalized force which is, due to the definition of virtual work in rotational movements, convert to applied torques. Q_i^a represents the joint actuating torque exerted by L_{i-1} on L_i at O_i and Q_i^d is joint dissipative torque. We neglect the Q_i^d term because it is very small by comparison with Q_i^a.

Constraints

The initial and final conditions specify the conditions of model at start position and at the end of second pulling phase (i.e. start of moving the barbell as a projectile) respectively. The initial conditions are primarily formulated by:

$$t = 0 \quad \begin{cases} q_i\,(t) = q_i^{initial} \quad i = 1,\ldots,5 & a \\ \mathbf{V}(O_6)\cdot\mathbf{X}_0\,(t) = 0 & b \\ \mathbf{V}(O_6)\cdot\mathbf{Y}_0\,(t) = 0 & c \end{cases} \tag{5}$$

$\mathbf{V}(O_6)$ is the velocity of barbell which is labled as O_6 in Figure 2. The first equation (5a) defines the position of each link and consequently the mass center of barbell and the last two equations (5b, c) indicate that barbell has no initial velocity in horizontal and vertical direction at the beginning of motion, i.e., "Lift-off" phase. We formulate the final conditions as below:

$$t = t_{final} \quad \begin{cases} \mathbf{O}_1\mathbf{O}_6\cdot\mathbf{Y}_0\,(t) = H & a \\ \mathbf{V}(O_6)\cdot\mathbf{X}_0\,(t) = V_{xd} & b \\ \mathbf{V}(O_6)\cdot\mathbf{Y}_0\,(t) = V_{yd} & c \end{cases} \tag{6}$$

The first equation (6a) is the vertical position of barbell at the end of second pulling phase and the last two equations (6b, c) indicate the horizontal and vertical velocities of the barbell at this point. These final conditions should be selected appropriately to allow the weightlifter completing the snatch. It means that the projectile motion of barbell should be started in appropriate height and velocity to give weightlifter sufficient time for completing the snatch.

The total time between two above mentioned state conditions is fixed to a certain value which is obtained approximately from experimental results. In order to respect joint stops, to prevent counter-flexion and to moderate total joint coordinate variations, we have to prescribe bounds on the joint coordinates, defined by the below constraints:

$$t \in [t^i, t^f], \quad i \le 5\ , \quad q_i^{\min} \le q_i(t) \le q_i^{\max} \tag{7}$$

In which the t^i and t^f are the initial and final times and the $q_i^{\min}$ and $q_i^{\max}$ are specified values (Lin et al., 1999). In addition to state or kinematics constrains, we use control constraints in the form of the inequalities defining limitation on torques acting on the mechanical system. Muscles produce joint torques with limited values in each angular position (Chaffin & Anderson, 1991). Therefore we can write:

$$t \in [t^i, t^f], \quad Q_i^a(t) \le Q_i^{a,\max}(t) \tag{8}$$

Another constraint is balance maintenance. At each instant the mass center of entire system, including weightlifter and barbell, should be in acceptable range or base of support limits.

$$t \in [t^i, t^f], \quad Lower\ Limit \le COM_{body+barbell}(t) \le Upper\ Limit \tag{9}$$

COM means "center of mass" which was considered for a system comprised body and barbell. Finally, the avoidance of collision between body segments themselves and between barbell and body segments is considered as an important constraint. At each instant we calculate the line representing each segment and then find the intersection of each two lines. If this intersection point is located in the range of both two supposed line, it shows that the criteria is not satisfied. According to above mentioned constraints we should specify that whether a solution is admissible or not. If it is not admissible we can remove that solution or we can impose a penalty for the solution by additional virtual cost.

Criteria Functions

We want to generate an optimal motion by minimizing a performance criterion or dynamic cost. As mentioned before, there are various options to be selected as the optimization criteria. Minimizing the summation of actuating joint torques (Chang et al., 2001; Lin et al., 1999; Rostami & Bessonet, 2001) and minimizing the total power consumption are two options which were used before. To uniform the effect of all joints in these criteria, we divide each joint torque or joint produced power to its maximum permissible value. Sometimes the former is called muscular effort. Therefore the criterion based on muscular effort is written as:

$$J = \sum_{i=1}^{5} \int_{t^i}^{t^f} \left(\frac{Q_i^a(t)}{Q_i^{\max}(t)}\right)^2 dt \tag{10}$$

and the criterion based on power consumption is:

$$J = \sum_{i=1}^{5} \int_{t^i}^{t^f} \left(\frac{Q_i^a(t)\,\omega_i(t)}{Q_i^{\max}(t)\,\omega_i^{\max}}\right)^2 dt \tag{11}$$

In above equations Q_i^a is actuating joint torque, $Q_i^{\max}$ is maximum of actuating joint torque, ω_i is joint angular velocity, and $\omega_i^{\max}$ is maximum of joint angular velocities. Therefore the first equation (10) describes the summation of normalized joint torque and the second (11) describes the summation of normalized joitn power during the specified movement. We extract the cost of each solution by using the functions (10) or (11) separately. To do this, we should solve the equations of motion (4) to compute the actuating joint torques. This is performed by using inverse dynamics approach. We employ the specific trajectory, vector of joint coordinates during the whole motion, and use the finite difference method to calculate the vectors of joint velocities and joint accelerations numerically. Once we have these data, it could be possible to calculate the actuating joint torques or power consumption at each instant.

Optimization Algorithm

Genetic algorithm (GA) is a general purpose search algorithm that used principle inspired by natural population genetics to evolve solution to problems. It was first proposed by Holland (1975) and has been well described in other text books (Cordón, Herrera, Hoffmann, & Magdalena, 2001). GA provides robust search in complex problems. It operates on a population of several individual solutions, called chromosomes, and improves this population towards a better solution. This procedure is performed by means of selection the better chromosomes according to their scores and employ them to make the next generation via GA operators. The classic operators are crossover and mutation which the former hybridize two chromosomes, parents, to make new child and the latter mutate some children to maintain the diversity of population. In other words, crossover is used to effectively explore search space and mutation is used to extend initial search space defined by initial chromosome's population. To solve a particular optimization problem using a GA, we should define a genetic representation of candidate solutions (chromosomes), create an initial population of solutions, and then assess the quality of each individual via computing the criterion function. Then we should select the best solutions (elitism), using them for producing the next generation, and repeat this algorithm until the specific stop criteria is fulfilled. Figure 3 shows this algorithm schematically.

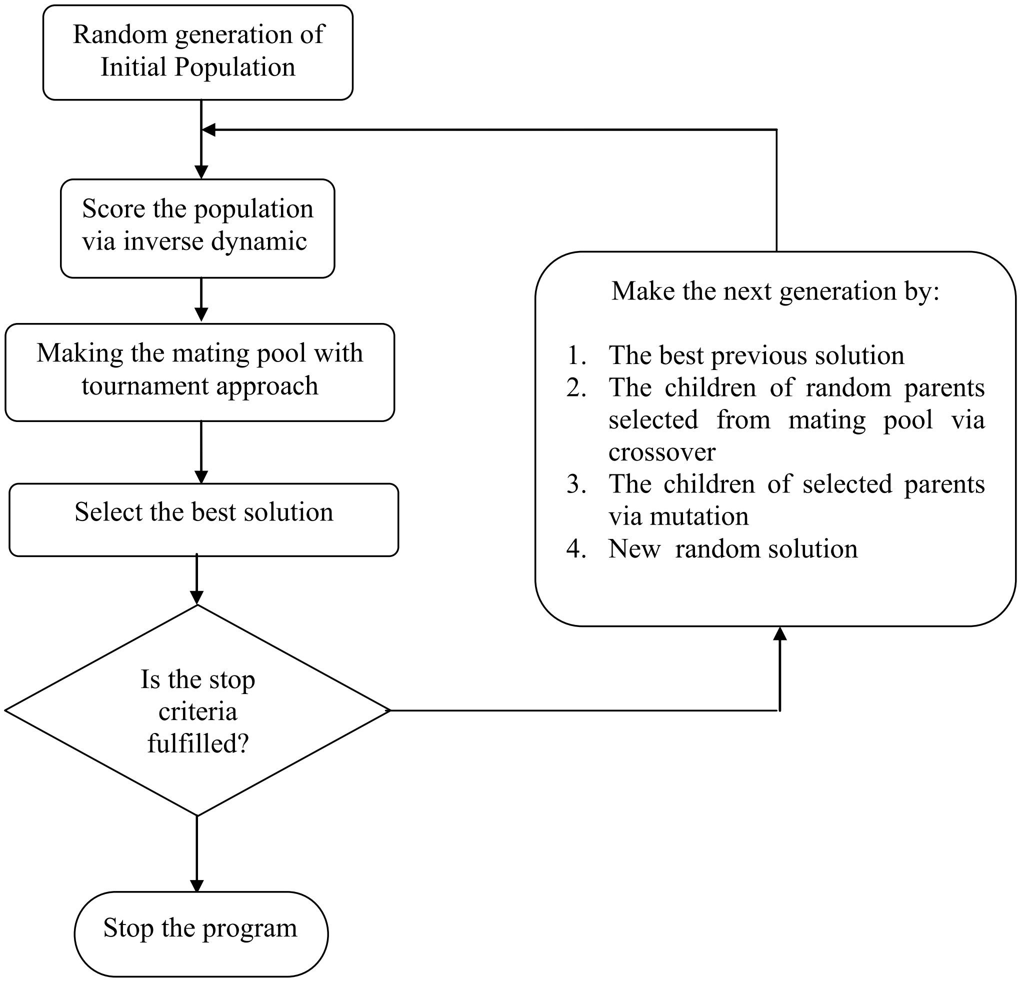

Figure 3. The GA algorithm.

The success of a GA strongly depends on a proper genetic representation of candidate solutions. Binary-coded strings for the representation of candidate solutions historically tend to dominate in research and application of GA. More recently, some authors (Hu & Yang, 2004) proposed that using non-binary representations in GA is more adequate for a certain class of optimization problems. Using a real number representation seems particularly natural for optimization problems in the continuous domain. The chromosome in real-coded genetic algorithms (RCGAs) is a vector of floating point numbers, $C = (x_1, ..., x_n)$, which its size equals the dimension of the continuous search space, or in other words each gene x_j corresponds to a particular parameter of the problem. RCGAs offer the advantage that the continuous parameters can gradually adapt to the fitness landscape over the entire search space whereas parameter values in binary implementations are limited to a certain interval and resolution (Cordón et al., 2001). Therefore we use a vector of floating point numbers, indicating the sequences of joint angles during snatch lift. We employ a five-link model with five degrees of freedom (DOF) and use the below pattern to represent each individual solution, chromosome, as a sequence of these five DOFs during the whole snatch time:

$$Qini(1), Qinv1(1), ..., QinvN(1), Qfin(1), \; ... \;, Qini(5), Qinv1(5), ..., QinvN(5), Qfin(5) \quad (12)$$

Where $Qini(i)$ and $Qfin(i)$ indicate the initial and final position of each angle (five joints in this specific problem) and $Qinv1(i),...,QinvN(i)$ indicate the N interval angles between the initial and final positions. Therefore each chromosome consists of $5\times(N+2)$ genes. The first two, initial and final angles of each joint (totally $5\times 2=10$ genes), are defined as boundary conditions. The rest interval angles (totally $5\times N$) are produced randomly at the start of execution and then modified by GA to the best sequence of motion which minimizes our selected criterion. To evaluate each chromosome we need to solve an inverse dynamics problem. To reduce the coarse variation of joint angles, actual angles are obtained using a cubic polynomial curve fitting to above angles. Then we differentiate numerically by using finite difference method to calculate the angular velocities and accelerations. Now the actuated joint torques can be calculated easily by using the motion equations.

The first population is made randomly and then a ranking selection mechanism is used. Ranking selection is based on the ranking of the population according to their fitness score which is obtained according to selected criterion. A randomly chosen of individuals compete in a tournament and among them, only the best-score individual is selected for mating pool. This tournament is repeated until the mating pool is filled (Cordón et al. 2001). The next generation is divided into three groups: the best individual of the previous generation (elitist selection mechanism), the newly random population, and the children who made from mating pool by using the crossover and mutation operators. Simple crossover is equivalent to the conventional one-point crossover in swapping the parent tail segments starting from a randomly chosen crossover site. But one-point crossover operator has the drawback of a positional bias, in that genes located at both ends of the chromosomes are disrupted more frequently than those in the centre (Cordón et al. 2001). Two-point crossover avoids this positional asymmetry in cutting the chromosome at two locations rather than one and swapping the middle segments in the offspring. We use these two methods alternatively with same probability to produce the offspring. In random mutation, the mutated gene is drawn randomly, uniformly from the specific intervals which the user defines as the lower and upper limits of each parameter or gene.

The most important step to produce the next generation is the selection of the elite parents according to their scores. This step is different in each specific problem. According to our approach to minimize the muscular effort or power consumption, we should give the best score to the solution which has the minimum corresponding value. For doing this procedure, we must first calculate the actuating torques of each individual solution. The trajectory is known by each individual and we must solve the equations of motion via inverse dynamic method.

Starting with the first random population; we score them by solving the equations of motion and computing the integral cost for each individual. Then we select the best individuals by tournament method and store them in mating pool. Reproducing of the next generation is done by crossover and mutation operators applying to mating pool. The next generation is evaluated in the same manner. This procedure continues until the stop criterion fulfilled. The population size, the maximum iteration and the number of interval points (N) between initial and final positions are some inputs of our algorithm.

A Simple Example

To demonstrate the efficiency of this algorithm, we solved a simple problem of finding the minimum distance of two points. This is an optimization problem similar to finding the trajectory of snatch but, with different criteria function. Since the result of this problem was obvious, the answer was found by GA algorithm, ensured correct working of this algorithm. Suppose 100 points in a 10×10 network which is started from 1 to 10 in each x and y direction. The problem is defined as travel from point A to point B with minimum distance. The procedure of solving this problem is similar with the weightlifter problem. We define a vector of 8 interval points between the points A and B as an individual solution. The program starts with a random population and continues toward an optimal solution. You can see the results of one sample run from point A with coordinates (3, 8) to point B with coordinates (8, 2) in Figure 4.

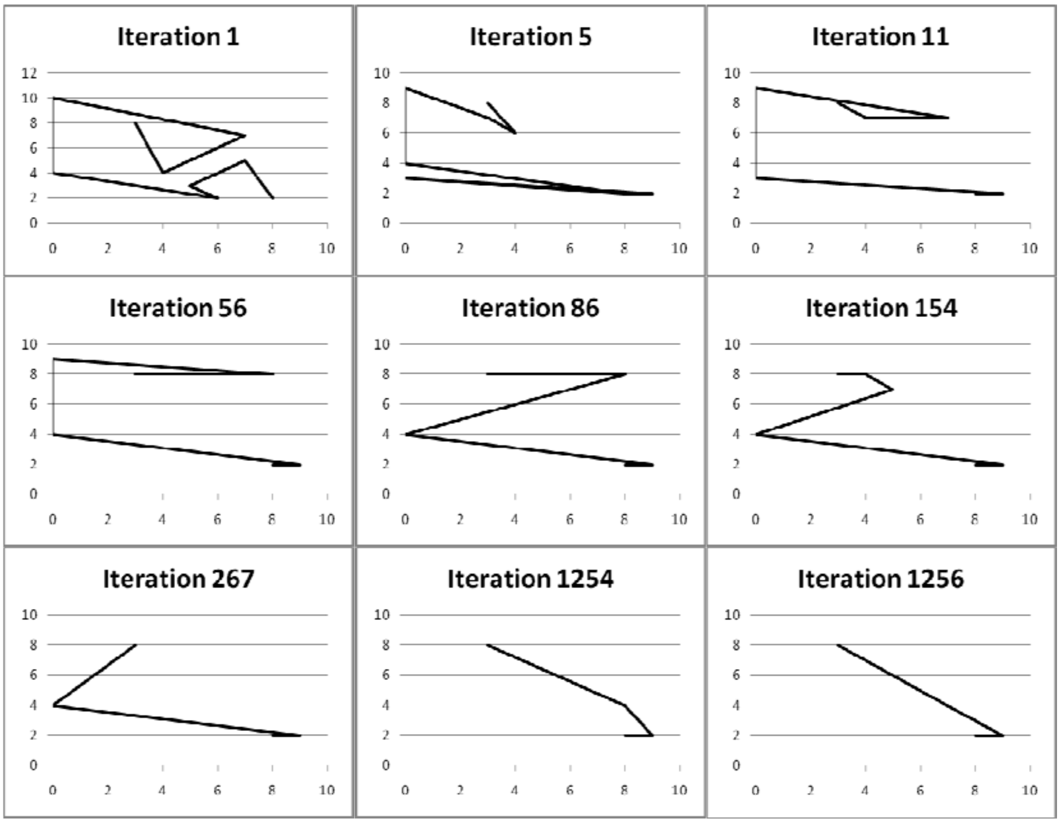

Figure 4. The result of sample problem to validate our algorithm: travel from point A (→) to point B (←).

Snatch Weightlifting Technique

We solved four different problems for a weightlifter with 80 (kg) mass and 1.8 (m) height who lifts 180 (kg) and 100 (kg) barbell by snatch technique. Other parameters for solving this problem are listed in Table 1.

Table 1. Some parameters used for optimization

Item No.	Description	Value
1	Relative joint angles at initial time (deg)	(80, 85, -155, -110, 0)
2	Upper limits of relative joint angles (deg)	(95, 90, 0, -90, 0)
3	Lower limits of relative joint angles (deg)	(75, 0, -155, -170, 0)
4	Height at final time (m)	1
5	Total duration time and time intervals (sec)	0.7, 0.01
6	Maximum permissible joint torques (Nm)	(250, 350, 500, 150, 100)
7	Min. and Max. limits for base of support (m)	(0, 0.25)

We selected two performance criteria; the first one is the muscular effort and the second one is the total power consumption which both were described before by (10) and (11). We solved our problem between two points representing the start of snatch and the start of catch phase respectively. Considering the snatch description by Derwin (1990) states "the basic principle of the snatch quite simply as vertically accelerating the barbell to a sufficient height, enabling the lifter to rapidly move beneath the bar and support it in an overhead full squat position", the start of catch phase has been selected in a manner that the barbell had a good condition to continue its motion and the weightlifter could move under the bar quickly. At first generation of random solutions we are able to apply the constraints directly, but for next generations which are produced by means of genetic operators, we use the penalty method to apply the above mentioned constraints.

Results

The Figure 5 shows the barbell trajectories during the snatch lift for 180 (kg) and 100 (kg) barbell while considering both muscular effort and total power consumption as optimizing criteria. These trajectories have been plotted from the time just prior to when the barbell left the floor ("lift-off") until just after the bar reached at the end of second pull. At this point the barbell continues to move as a "projectile" and it allows the athlete to complete "move under the bar" to catch it. According to experimental observations, the typical form of trajectory described by Garhammer (2001) shows that when the barbell is lifted from the "lift-off" phase, it moves toward the athlete during the first pull, then away from the athlete, and finally toward him again as it begins to descend during the catch phase. Only one trajectory of four trajectories depicted in Figure5 shows this typical form. This trajectory obtained for 180 (kg) barbell when the optimizing criterion is based on muscular effort. One can see the similarity between this optimized trajectory and experimental results of trajectory type B recommended by Baumann (1988) and shown in Figure 1.

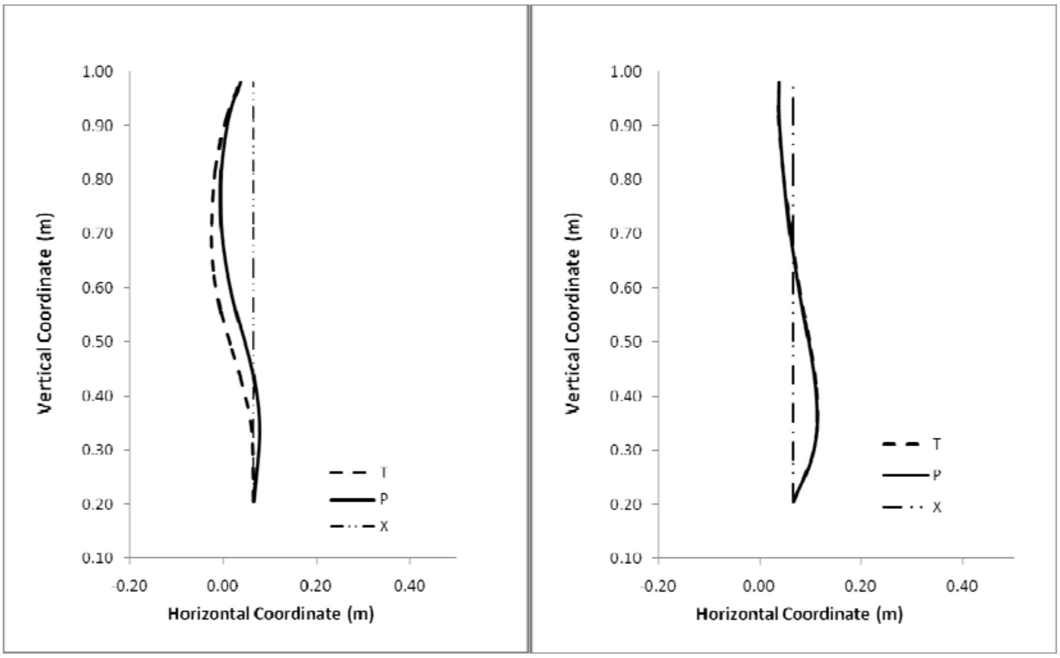

Figure 5: Optimized Barbell Trajectory for 180 kg barbell (left) and 100 kg barbell (right) when optimization criteria are muscular effort (T) and power consumption (P), (line X indicates the initial x-coordinates of barbell)

The sequences of snatch motions by considering both optimizing criteria (i.e. muscular effort and total power consumption) are depicted in Figure 6 which shows that the collision avoidance constraint has been satisfied well by using penalty method.

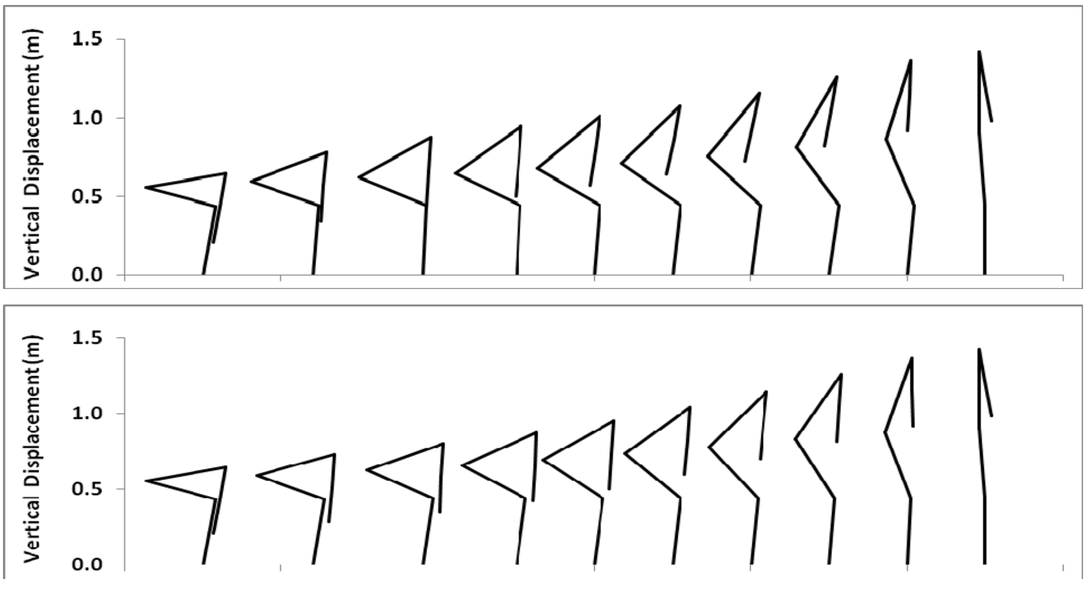

Figure 6. Optimized motion of model with minimum muscular effort for 180 kg barbell (upper) and 100 kg barbell (lower)

Figure 7 shows the variations of actuating joint torques for ankle, knee, and hip between initial and final positions. The contribution of each joint in making a complete snatch lifting motion can be realized by these diagrams. For instance it shows that the actuated torques in hip joint is more than other joints during the snatch lift and hence the hip joint has the greater importance to produce this movement. One can see that all the values for actuating joint torques are in the permissible range that we enter as the kinetic constraints.

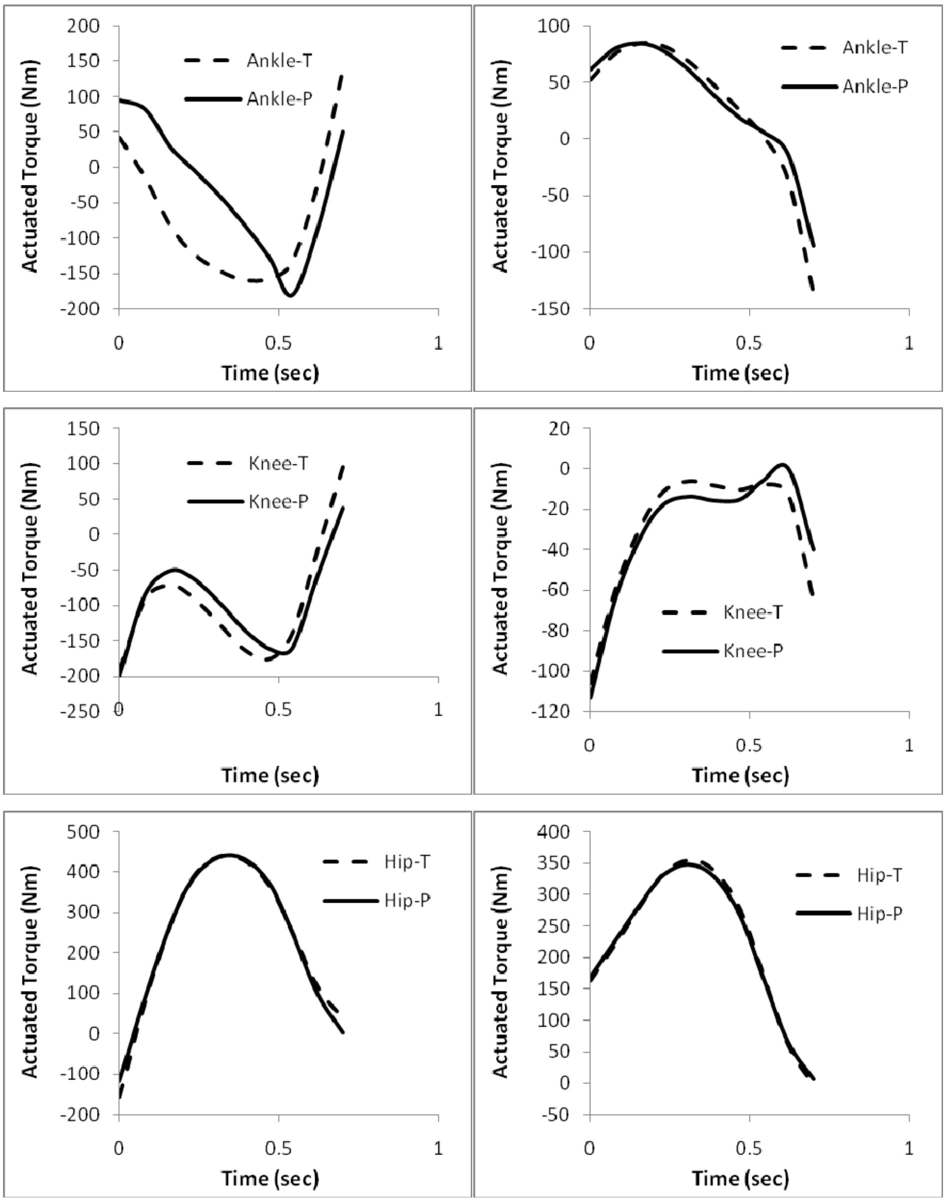

Figure 7: Optimized actuating torques in ankle, knee, and hip joints for 180 kg (left column) and 100 kg (right column) barbell weights; criteria functions are muscular effort (T) and power consumption (P)

Discussion

Barbell trajectory for 180 (kg) barbell mass which is optimized for minimizing the muscular effort shows the typical inward-toward form that we can see in experimental data. Since we obtain this optimized trajectory by using dynamic motion equations considering the proper kinetic constraints, we sure that according to mechanical point of view this trajectory can be produced by a weightlifter, although we may encounter to some other difficulties like the training method or something else. But this similarity to well-known inward-toward trajectory is not seen in trajectories which are optimized by power consumption and also it is not seen for 100 (kg) barbell even when the optimizing criterion is muscular effort. Therefore we can conclude that for heavy barbells if the criterion function changes, the trajectory will change also. According to our results when the optimizing criterion changes from muscular effort to total power consumption, the initial inward motion has never seen anymore. But for lighter barbell (100 kg), there are no sensible differences between two optimizing criteria. If we accept that the movements of human, especially the elites, are according to some optimizing criteria, then it seems that the muscular effort shows the better agreement than power consumption. Therefore the relative success to predict the optimal motion will depend on the selective criterion. However selecting the best criteria to improve the performance of weightlifters requires more studies and it could consist of more than one criterion combined together during the full snatch. Since there are no similarities between our optimal barbell trajectory and experimental observations in the case of lighter barbell, we conclude that we have different optimal trajectories depending on the barbell mass. Comparing to experimental optimal trajectories for heavy barbell mass, it seems that the muscular effort criterion suggests a trajectory which is similar to pattern type B (see Figure 1) and the total power consumption criterion lead us to optimal trajectory which is similar to pattern type C. Another advantage of this theoretical model is the ability to obtain the best trajectory for each individual weightlifter. As mentioned before, the researchers have accepted that the optimal trajectory is individual depended. The optimal trajectory according to the weightlifters' experiences neglects this dependency and hence we would not be able to advise the resultant pattern to another weightlifter with different anthropometric or physical characteristics. Therefore our above suggestions are only valid for the specific weightlifter with 80 (kg) mass and 1.8 (m) height.

The actuating joint torques are good parameters to show us the practical differences between an actual snatch motion of a weightlifter and the ideal optimized one which he could achieve. We can reduce these differences by advising the weightlifter about the strength training he should do to compensate the weakness of particular joint. As anyone expects, these actuating torques will reduce when the barbell mass decreases. Figure 7 shows that the hip joint plays the greater role to complete the snatch movement.

The results of this optimization may help us to train weightlifters according to optimized kinematics and kinetics parameters. Comparing the actual parameters of the weightlifter with optimized one may guide us to achieve these useful comments. The determination of optimal motion during the whole motion of snatch lift may help coaches to train weightlifters on a more systematic manner.

The above mentioned notes are related to the advantages of this model, but we like to describe the advantages of our selected approach too. We know that the search space may have more than one local optimal solution. It means that when we use the mathematical solution approach (e.g. Pontryagin Maximum Principle), we should start our solution routine with an initial guess. The final optimal solution is affected by this initial guess and because of this problem we called our solution as local optimal one. On this situation we encounter with some local optimal solutions that resulted from several runs with different initial guess. This is the common problem between almost all mathematical methods. Therefore traditional methods are not good candidates as efficient optimization algorithms for this nonlinear problem and using GA technique can alleviate the above difficulty and may constitute an efficient optimization tool. The genetic algorithm provides the global optimal solution without any dependency to initial starting point. Also, because there is no need to compute the sophisticated gradient of criteria or other functions (e.g. mass matrix), this algorithm is very easy and fast. Also the divergence of solution is a common problem of mathematical approaches when the initial guess was not suitable or when the problem is highly nonlinear, but in GA we don't encounter with this problem.

The good results obtained from optimization problem shows that this method is reliable. The fair success of this model encourages us to continue our approach and improve our model by the models which have more degrees of freedom in the near future.

References

L Bartonietz, K.E. (1996). Biomechanics of the snatch: toward a higher training efficiency. *Strength and Conditioning, 18*(3), 24-31.

Baumann, W., Gross, V., Quade, K., Galbierz, P., & Schwirtz, A. (1988). The snatch technique of world class weightlifters at the 1985 world championship. *International Journal of Sport Biomechanics, 4*, 68-89.

Byrd, R. (2001). Barbell trajectories: three case study. *Strength and Health (on-line publication of York Barbell Company), 3*, 40-42.

Campos, J., Poletaev, P., Cuesta, A., Pablos, C., & Carratala, V. (2006). Kinematical analysis of the snatch in elite male junior weightlifters of different weight categories. *Journal of Strength and Conditioning Research, 20*(4), 843-850.

Chaffin, D.B., & Anderson, G.B.J. (1991). Occupational Biomechanics. John Wiley.

Chang, Ch., Brown, D.R., Bloswick, D.S., & Hsiang, S.M. (2001). Biomechanical simulation of manual lifting using spacetime optimization. *Journal of Biomechanics, 34*, 527-532.

Cordón, O., Herrera, F., Hoffmann, F., & Magdalena, L. (2001). *Genetic fuzzy systems: evolutionary tuning and learning of fuzzy knowledge bases*. World Scientific.

Derwin, B.P. (1990). The snatch: Technical description & periodization program. *National Strength & Conditioning Journal. 12*, 80-81.

Garhammer, J. (1985). Biomechanical profiles of Olympic weightlifters. *International Journal of Sport Biomechanics, 1*, 122-130.

Garhammer, J. (1998). Weightlifting performance and techniques of men and women. In conference book of *First international conference on weightlifting and strength training*, 89-94, Lahti, Finland.

Garhammer, J. (2001). Barbell trajectory, velocity, and power changes: six attempts and four world records. *Weightlifting USA, 19*(3), 27-30.

Gourgoulis, V., Aggelousis, N., Mavromatis, G., & Garas, A. (2000). Three-dimensional kinematic analysis of the snatch of elite Greek weightlifters. *Journal of Sports Sciences, 18*(8), 643-652.

Gruver, W.A., Ayoub, M.M., & Muth, M.B. (1979). A model for optimal evaluation of lifting tasks. *Journal of Safety Research, 11*, 61-67.

Hiskia, G. (1997). Biomechanical analysis of world and Olympic champion weightlifters performance. Proceedings of the *IWF Weightlifting Symposium*, 137-158, Ancient Olympia, Greece.

Holland, J.H. (1975). *Adaptation in natural and artificial systems*. Ann Arbor: University of Michigan Press.

Hsiang, S.M., Chang, C.C., & McGorry, R.W. (1999). Development of a set of equation describing joint trajectories during para-sagittal lifting. *Journal of Biomechanics, 32*, 871-876.

Hu, Y., & Yang, S.X. (2004). A knowledge based genetic algorithm for path planning of a mobile robot. Proc. IEEE: *International Conference on Robotics and Automation*, 4350-4355, New Orleans, LA.

Isaka, T., Okada, J., & Funato, K. (1996). kinematics analysis of the barbell during the snatch movement of elite Asian weightlifters. *Journal of Applied Biomechanics, 12*, 508-516.

Javadi, A.H., Arshi, A.R., & Shirzad, E. (2007). Snatch technique validation using computational methods: A genetic algorithm approach. Proceedings of *XXV ISBS Symposium*, 67-70, Ouro Preto, Brazil.

Lenjan Nejadian, Sh., Rostami, M., & Towhidkhah, F. (2008). Optimization of barbell trajectory during the snatch lift technique by using optimal control theory. *American Journal of Applied Sciences, 5*(5), 524-531.

Lenjan Nejadian, Sh., & Rostami, M. (2007). Optimization of barbell trajectory during the snatch lift technique by using genetic algorithm, Proc. of *Fifth IASTED International Conference on Biomechanics (Biomech'07)*, 34-39, Honolulu, Hawaii, USA.

Lin, C.J., Ayoub, M.M., & Bernard, T.M. (1999). Computer motion simulation for sagittal plane activities. *International Journal of Industrial Ergonomics, 24*, 141-155.

Menegaldo, L.L., Fleury, A.D.T., & Weber, H.I. (2003). Biomechanical modeling and optimal control of human posture. *Journal of Biomechanics, 36*,1701-1712.

Nejadian, S.L., & Rostami, M. (2007). Mathematical modeling and optimization of snatch lift technique. Proceedings of *XXV ISBS Symposium*, 119-122, Ouro Preto, Brazil.

Park, W., Martin, B.J., Choe, S., Chaffin, D.B., & Reed, M.P. (2005). Representing and identifying alternative movement technique for goal-directed manual tasks. *Journal of Biomechanics, 38*, 519-527.

Rostami, M., & Bessonnet, G. (2001). Sagittal gait of a biped robot during the single support phase. Part 2: Optimal motion. *Robotica, 19*, 241-253.

Salaami, F., Jamshidi, N., Rostami, M., & Najarian, S. (2008). Power enhancement of weightlifters during snatch through reducing torque on joints by particle swarm optimization. *American Journal of Applied Sciences, 5*(12), 1670-1675.

Schilling, B., Stone, M., O'Brayant, H.S., Fry, A.C., Cogllanese, R.H., & Pierce, K.C. (2002). Snatch technique of college national level weightlifters. *Journal of Strength and Conditioning Research, 16*(4), 551-555.

Vorobyev, A.N. (1978). *Weightlifting*. International Weightlifting Federation. Budapest.

Interactivity and e-Learning – An experimental study

Nina Roznawski & Josef Wiemeyer

Institute of Sport Science, Darmstadt University of Technology

Abstract

Interactive features play an important role in e-learning. In this paper we report an experimental pilot study which tested e-learning units with different degrees of interactivity. A specific experimental design adapted to a blended-learning scenario was developed. Participants learned with e-learning units, dealing with different movement analysis concepts (MACs), which differ only in interactive features (different degrees of interactivity). Pretest and posttest measured participants' basic knowledge and knowledge transfer of the MACs. A further measurement of participants' basic knowledge was performed immediately after learning. Moreover participants' experience of activation and interactivity was assessed by a questionnaire. The results show that students could improve their knowledge. However we did not find any significant impact of different degrees of interactivity. This result may be due to confounding problems or a small sample size. In some items the groups who learned interactively or actively rated activation and interactivity higher than the non-active or non-interactive groups. Open-ended questions showed, that when being exposed to non-interactive or non-active e-learning units students complained about the absence of interactive features.

KEYWORDS: E-LEARNING, DEGREES OF INTERACTIVITY, EXPERIMENTAL STUDY

Introduction

Interactivity and interactions are important aspects in e-learning (Sims, 1997). According to Wiemeyer (2008) within an e-learning system complex interactions can be distinguished (interactions between learners, teachers, learning content and learning system). The importance of interactions for the learning process is described by Wagner (1997) who focused on interaction outcomes. According to Wagner (1997, p. 22-23) interactions facilitate active engagement of learners, support individualized learning experiences, enhance understanding, support knowledge transfer and increase motivation. Interactions and interactivity in e-learning can enhance the learning process and have an additional benefit to students only if they are well designed and integrated into a didactical design. In the literature different classifications, concepts, categories and ideas exist how to design interactive e-learning (Chou, 2003; Kettanurak, Ramamurthy & Haseman, 2001; Roblyer & Ekhaml, 2000; Sims, 1997; Wagner, 1997). Different technologies like synchronous communication tools (online-chats, video-conferencing) or asynchronous communication tools (discussion forum, e-mailing, mailing-lists, wikis) as well as specifically designed learning objects (tasks/questions with feedback, simulations, animations and interactive videos) enable interactions. Several studies examined the effects of different degrees of interactivity and interactions on learning outcome in multimedia learning (Evans & Gibbons, 2007; Gao & Lehmann, 2003; Haseman, Polatoglu & Ramamurthy, 2002; Ritter & Wallach, 2006). The studies of Ritter and Wallach (2006) and Gao and Lehmann (2003) showed that students who learned interactively improved their learning outcome significantly more compared to non interactive conditions. The study of Evans and Gibbons (2007) showed an interactivity effect only for an immediate transfer test. No significant impact of interactivity on learning outcome was found by the study of Haseman, Polatoglu and Ramamurthy (2002). These inconsistent results may be due to different implementation of interactivity (different kinds of tasks) and methodological shortcomings (e.g., missing or mismatching pretest, confounding of time on task and interactivity, short retention interval).

In the subproject “Functional movement analysis” of the HeLPS project, a cooperative project of the five Hessian Institutes of Sport Science, interactive e-learning units were designed. The aim was to teach knowledge concerning three different movement analysis concepts (Göhner, 1979; Kassat, 1995; Meinel & Schnabel, 1998) in an interactive way and moreover to practice the application of these concepts. Formative evaluations of the developed e-learning units performed in the winter term 2007/08 and in the summer term 2008 showed, that students liked and appreciated the interactive features and wished more interactive support (Roznawski & Wiemeyer, 2008). To analyze the effects of interactive features within e-learning units on students’ knowledge and motivation, a specific experimental design was developed and tested in a pilot study in the winter term 2008/09.

Hypotheses

The primary aim of the experimental field study was to gain detailed knowledge about learning with interactive e-learning units within a blended-learning scenario. The study focused on two main aspects: first students’ learning outcome (achievement) and second students’ experience of activation and interactivity when learning with interactive e-learning units. The following hypotheses were tested.

Hypothesis 1: Students who learn with the interactive or the active versions of the e-learning units achieve better learning outcomes in the knowledge tests than students who learn with the non-interactive or the non-active version of the e-learning units.

Hypothesis 2: Students who learn with the interactive or active version of the e-learning units experience higher activation and interactivity than students who learn with the non-interactive or non-active versions of the e-learning units.

Methods

The pilot study was performed in the course “How do movements work?”. A sample of 12 students (9 males, 3 females, mean age: 24.4 years) participated and completed the course. This course was organized based on a blended-learning concept with alternating online working phases and phases of physical presence. The online working phases were supported by ILIAS, a web-based open-source learning management system. We used ILIAS for providing the online learning units, communication with the students (chat and discussion forum) and online-tests. Altogether three online phases took place. During these phases participants worked on e-learning units for one week, dealing with the movement analysis concepts (MACs) of Meinel and Schnabel (1998; MAC-MS), Göhner (1979; MAC-G) and Kassat (1995; MAC-K). In the following two phases of physical presence students applied these concepts to selected sport movements. In the first lesson students discussed how to apply the concepts in small groups. Discussions were moderated by experts and supported by prepared checklists which illustrated the procedure of the MACs. In the second lesson the results of the teamwork were presented and discussed in a plenary session.

The experimental design and tests

The experimental design was adapted to the course structure. For testing the differences between varying levels of interactivity we used an experimental pre-post design with two experimental groups. The participants' knowledge was assessed by five tests: a pretest, three immediate tests and a posttest. At the beginning and at the end of the experiment the participants had to answer a questionnaire to assess their motivation and attitude towards e-learning. Furthermore the participants completed a short online survey after each immediate test to evaluate their attitude towards and perception of the e-learning units (only selected results will be reported).

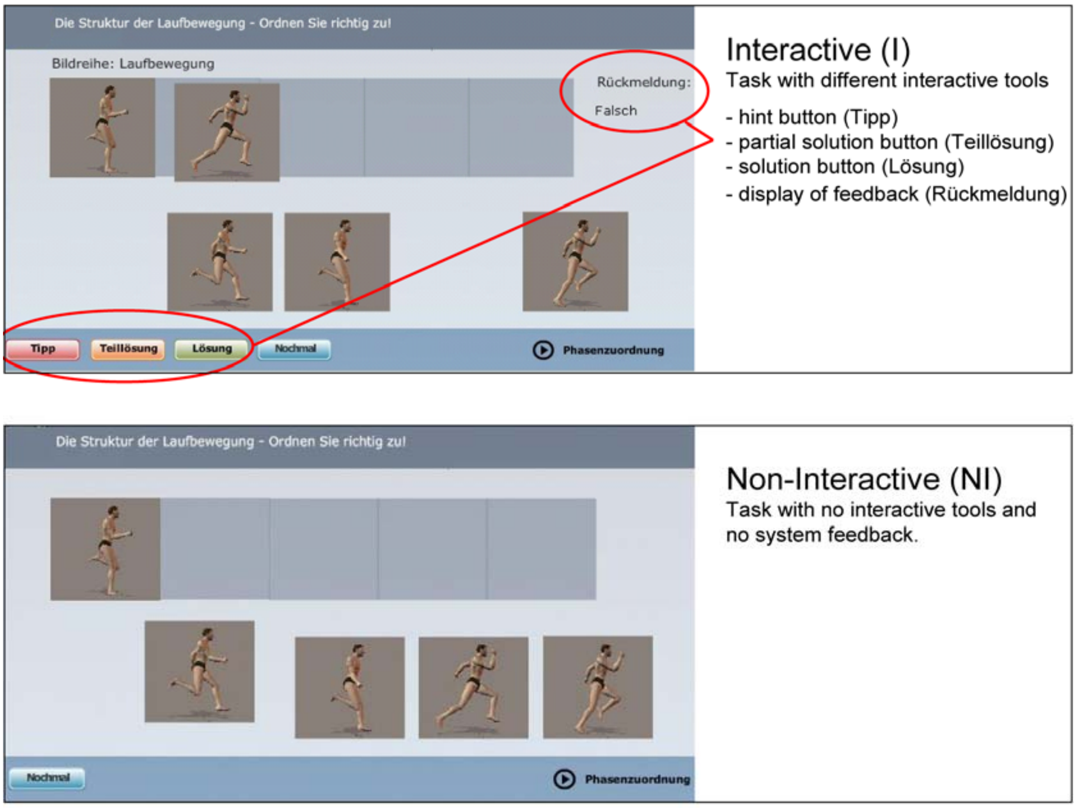

Figure 1. Interactive task (I) for Meinel and Schnabel (1998) with system feedback and non-interactive task (NI) without system feedback

Experimental treatment

Based on pretest performance participants were assigned to the experimental groups (matching method). During each online working phase the experimental groups worked on an e-learning unit with identical content. The e-learning units only differed in interactive features or the active engagement. Interactive units (I) consisted of tasks and questions including system feedback, whereas non-interactive units (NI) did not deliver any system feedback. Figure 1 shows an example of an interactive and non-interactive task in the e-learning unit dealing with MAC-MS. Active units (A) required active engagement with tasks and questions, whereas non-active units (NA) did not contain tasks and questions. Figure 2 shows an example of an active task (drag and drop) which supported active engagement with the learning content and the same learning content which is represented as tabular form and supported less active engagement.

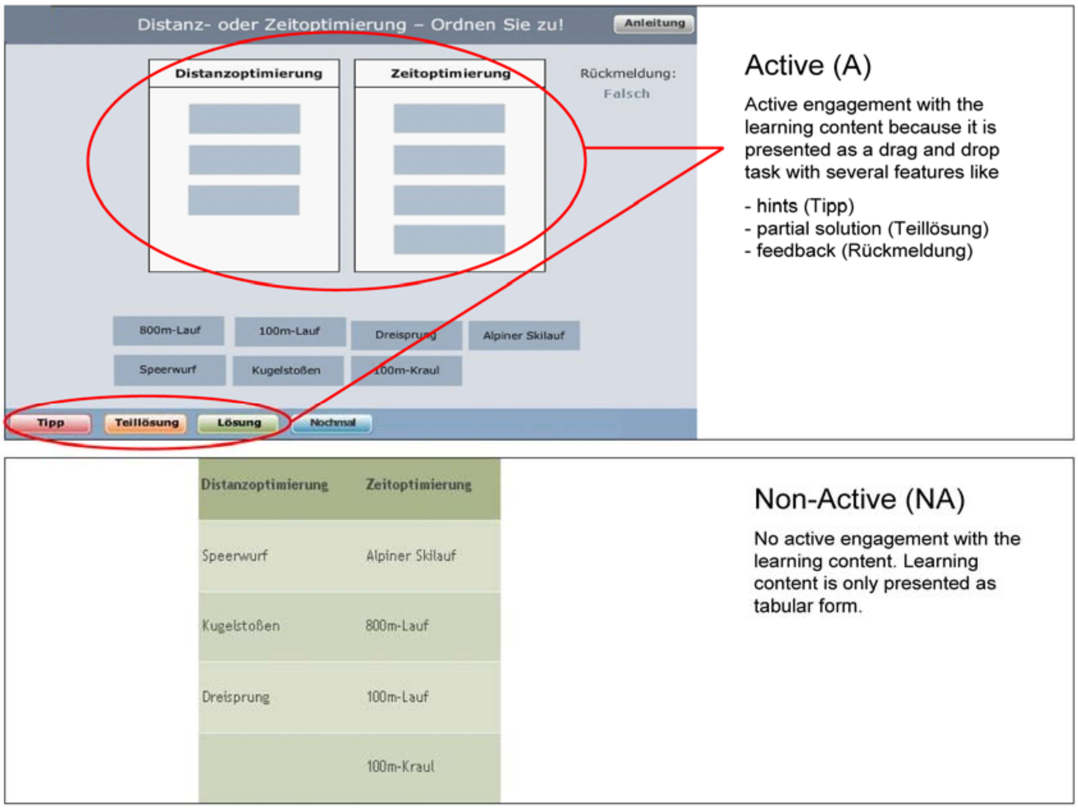

Figure 2. Active unit (A) for Göhner (1979) with active engagement and non-active unit (NA) without active engagement

The following table (Table 1) provides an overview and explains the experimental treatment and the differences of the treatment groups in more detail. The MAC-MS units (I/NI) only differ in the existence of interactive tools (i.e., hints and feedback) but they have an identical number of tasks and questions. The MAC-G and MAC-K units (A/NA) differ in the way they support active engagement. Active units (A) assist active engagement with the learning content because of tasks and questions, whereas non active units (NA) do not contain any tasks and questions.

Table 1: Differences of experimental conditions in the three e-learning units

Learning unit	**Differences of experimental conditions**	**Number of Questions**	**Number of Tasks**
MAC-MS (U1)	I (with interactive tools)	6 (hints etc.)	12 (hints etc.)
	NI (without interactive tools)	6	12
MAC-G (U2)	A (with active engagement)	3	21
	NA (without active engagement)	None	None
MAC- K (U3)	A (with active engagement)	1	10
	NA (without active engagement)	None	None

Figure 3 illustrates the treatment for the experimental groups. The groups learned with e-learning units which differ only in the degrees of interactivity. In the first online phase group 1 learned interactively about the MAC-MS (U1 I), in the second online-phase they learned non-actively about the MAC-G (U2 NA), and in the third online phase they learned actively about the MAC-K (U3 A). Conversely, group 2 first learned non-interactively in the first online phase about the MAC-MS (UI NI), actively in the second online phase about the MAC-G (U2 A) and in the last online phase non-actively about the MAC-K (U3 NA). Each online working phase was followed by an immediate knowledge test performed online. One week after the last session of the course a posttest addressing all three MACs followed. Whereas the results of the knowledge pretest and the three specific knowledge tests did not count for the course grade the results of the final knowledge test contributed 50% to the final course grade.

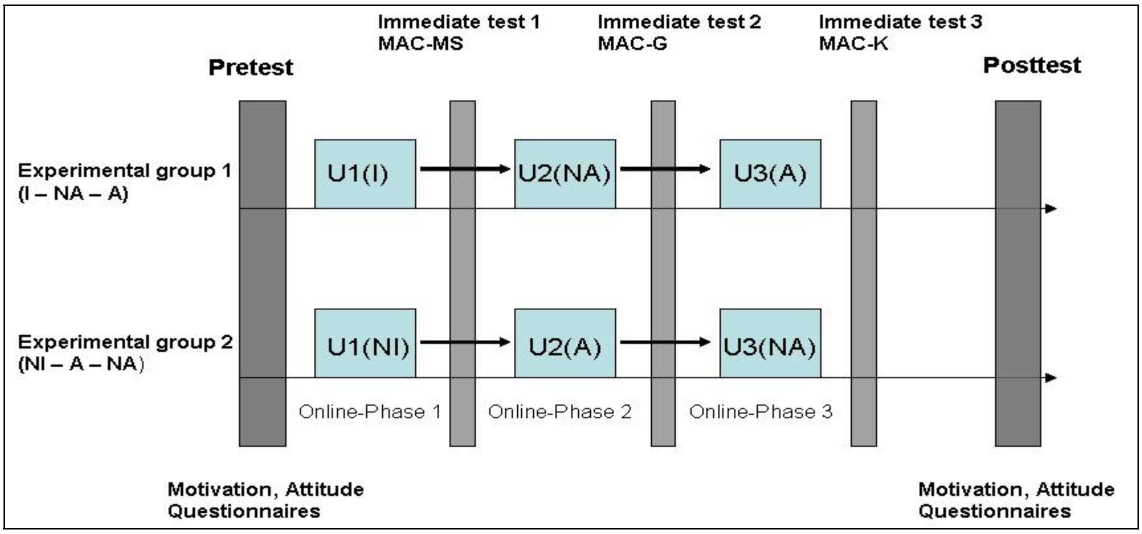

Figure 3. Experimental Design (U – Unit, I – Interactive, NI – Non-Interactive, A – Active, NA – Non-Active; MAC-MS, MAC-G, MAC-K – movement analysis concepts of Meinel & Schnabel (1998), Göhner (1979) and Kassat (1995), respectively).

Tests

Knowledge tests (Pretest and Posttest)

Pretests and posttests covered each of three MACs and were structured identically; the first part assessed basic knowledge and the second part tested knowledge transfer. Altogether both tests consisted of 30 basic knowledge questions (10 for each MAC) and 12 knowledge transfer questions for all MACs. In order to avoid recognition effects questions were different in pretest and posttest. The basic knowledge questions were selected from a pool consisting of 145 questions. Students were asked if short statements dealing with the different MACs were correct or wrong and how confident they were with their answers (five-point scale: 'highly sure, that the statement is right', 'rather sure that the statement is right', 'I don´t know', 'rather sure that the statement is wrong', 'highly sure that the statement is wrong'). The design of the knowledge transfer tests was adapted to the procedure of the different MACs and the developed checklists. Students were asked to apply the three MACs to sport movements (i.e., butterfly stroke, high jump and kip on the high bar).

Immediate tests

Each of the three immediate knowledge tests addressed basic knowledge about one of the studied MACs. These questions (short statements) were also taken from the above-mentioned question pool and the options to answer the questions were the same as in the pretest and posttest. The immediate knowledge tests were performed using the ILIAS survey tool and have been carried out after each online working phase.

Questionnaires

Altogether two different types of questionnaires were applied in the study. The first questionnaire measured students' motivation and attitude towards e-learning, e-learning experience, computer literacy and use of computers. In order to notice changes in attitude students answered this questionnaire at pretest and posttest.

The second questionnaire measured use, experience, and attitude (utilization, design and structure of tasks and questions, learning, comprehensibility, experience of activation and interactivity) towards the e-learning units with a four-point scale ('strongly agree' to 'strongly disagree'). Open-ended questions at the end gave students the opportunity to mention positive and negative aspects of the e-learning units.

Procedure

Pretest

In the second lesson of the course students performed the pretest to measure students' existing basic knowledge and knowledge transfer concerning the three MACs (MAC-MS, MAC-G, MAC-K). The test was performed as a paper-and-pencil test in the classroom at usual course time and took 45 minutes. Students were informed that pretest results did not count for the course grade. Furthermore they were instructed to answer the test to the best of their knowledge. Based on pretest performance students were assigned to the experimental groups. Furthermore students answered the questionnaire which measured students' motivation and attitude towards e-learning, e-learning experience, computer literacy and use of computers which took about 15 minutes.

Online phases - learning the MACs

After a further lesson held by the teacher three online learning phases followed. The same procedure was applied at all online phases. First the groups learned with the e-learning units concerning the different concepts (first phase: MAC-MS, second phase: MAC-G, third phase: MAC-K) which only differed in the degrees of interactivity at the learning management system ILIAS. The phase of online self-study ended with an online session where all students met at the learning management system to perform the immediate online knowledge tests dealing with the different MACs (first phase: MAC-MS, second phase: MAC-G, third phase: MAC-K). Additionally the groups answered questionnaires about the learning units. Altogether students had 20 minutes time to complete the test and the questionnaire. Students were instructed to answer the test to the best of their knowledge and without any help (e.g., consult a book, look up the e-learning units) in order to measure the learning achievement. Furthermore students were informed that the results did not count for their final grade. Immediately after passing the test and questionnaire an online chat lesson followed. In the chat lesson students applied the concepts to selected sport movements with the assistance of the lecturer.

Phases of physical presence – applying the concepts

At the end of each online phase, two phases of physical presence followed. In the first lesson students applied the concepts in small groups to selected sport movements using checklists and in the following lesson their results were discussed in a plenary session.

Posttest

One week after finishing the last MAC the posttest was performed as a paper-and-pencil test in the classroom at the usual course time. Similar to pretest procedure students had 45 minutes to answer the questions for each concept. This time the results counted for the final grade. Again students answered the questionnaire which measured motivation and attitude towards e-learning, e-learning experience, computer literacy, and use of computers.

Results

Statistical data analysis was performed using SPSS Statistics version 17.0.0. The applied statistical tests are specified in the respective sections.

Knowledge tests

The total scores of the pretest and posttest were analyzed using a 2 (groups) × 2 (tests) ANOVA with repeated measures on the factor tests. ANOVA yielded a significant main effect of knowledge test (F (1,10) = 124.14, $p < .001$) indicating a gain from pretest to posttest (see Figure 4). The analysis yielded no significant main effect of experimental groups (F (1,10) = .001, $p = .975$) and no groups × tests interaction (F (1,10) = .002, $p = .965$).

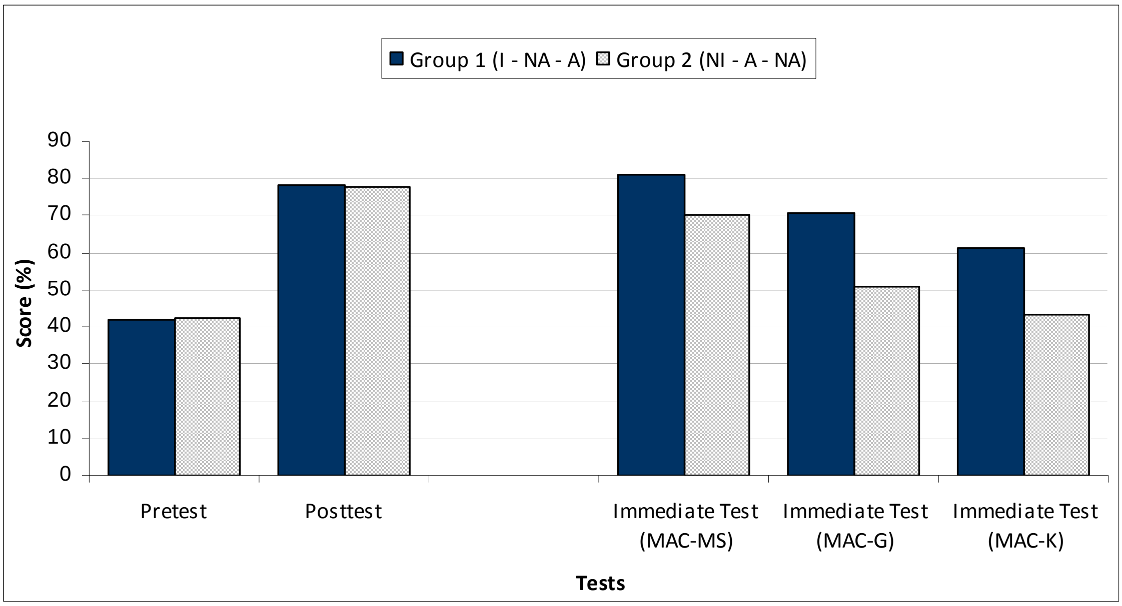

Figure 4. Means of total knowledge score (%) of the two experimental groups in different tests

Furthermore participants' *basic knowledge* at pretest, immediate test and posttest was analyzed (Table 2). The 3 (MACs) × 2 (groups) × 3 (tests) ANOVA with repeated measures on the factor tests yielded a significant main effect of MACs (F (1, 13) = 65.70, p <. 001). There was also a significant main effect of tests (F (2, 18) = 6.26, p < .01). The MACs × tests interaction was also significant (F (3,25) = 3.51, p < .05).

Table 2. Results of 3 (MACs) × 2 (groups) × 3 (tests) ANOVA for differences in basic knowledge

Effects	***df***	***F***	***p***
Main Effects			
MACs	1,13 $^{\varepsilon_1}$	65.70	< .001
Tests	2,18	6.26	< .01
Groups	1,9	.56	.48
Two-way interaction			
MACs × Groups	2,18	1.72	.21
Tests × Groups	2,18	.86	.44
MACs × Tests	3,25 $^{\varepsilon_2}$	3.51	< .05
Three-way interaction			
MACs × Tests × Groups	4,36	.22	.92

$^{\varepsilon_1}$, $^{\varepsilon_2}$ Adjusted with Greenhouse-Geisser: ε1 = .696, ε2 =.686

Figure 5 shows the relative basic knowledge scores of the two experimental groups in the different tests. Wilcoxon tests revealed that participants continuously increased performance at each test for each MAC. Comparing the MACs Wilcoxon tests showed, that the concept of MAC-MS was significantly easier than the concepts of MC-G and MC-K at the immediate tests. Furthermore there was a significant difference between the concepts of MC-MS and MC-K at posttest indicating greater difficulty of MAC-K.

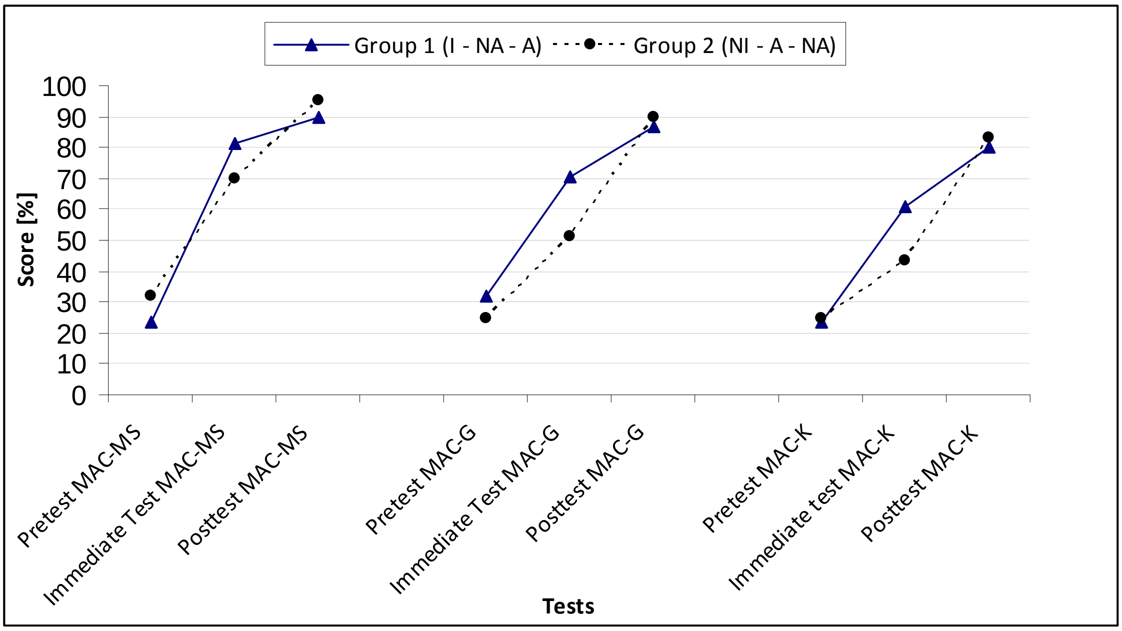

Figure 5. Basic knowledge scores (%) of the two experimental groups at different tests

The participants' *knowledge transfer* of each MAC at pretest and posttest was analyzed using a 3 (MACs) × 2 (groups) × 2 (tests) ANOVA with repeated measures on the factor tests (Table 3). We found a significant main effect of MACs (F (2, 20) = 17.09, p < .001). Furthermore ANOVA yielded a significant main effect of tests (F (1, 10) = 8.67, p < .001) indicating knowledge gain from pretest to posttest. Wilcoxon tests revealed significant differences between all MACs at posttest. At pretest there was only a significant difference between MAC-MS and MAC-K. Furthermore Wilcoxon tests showed that from pretest to posttest students significantly improved their knowledge transfer of MAC-MS and MAC-K but not for MAC-G.

Table 3. Results of 3 (MACs) × 2 (groups) × 2 (tests) ANOVA for differences in knowledge transfer

Effects	***df***	***F***	***p***
Main Effects			
MACs	2,20	17.09	< .001
Tests	1,10	8.67	< .05
Groups	1,10	.38	.55
Two-way interaction			
MACs × Groups	2,20	.48	.63
Tests × Groups	1,10	.20	.66
MACs × Tests	2,20	.34	.72
Three-way interaction			

MACs × Tests × Groups	2,20	.13	.88

Figure 6 shows the relative knowledge transfer scores for each MAC at pretest and posttest. Hypothesis 1 was not supported. Students learning with the interactive or active e-learning units did not achieve better learning outcomes.

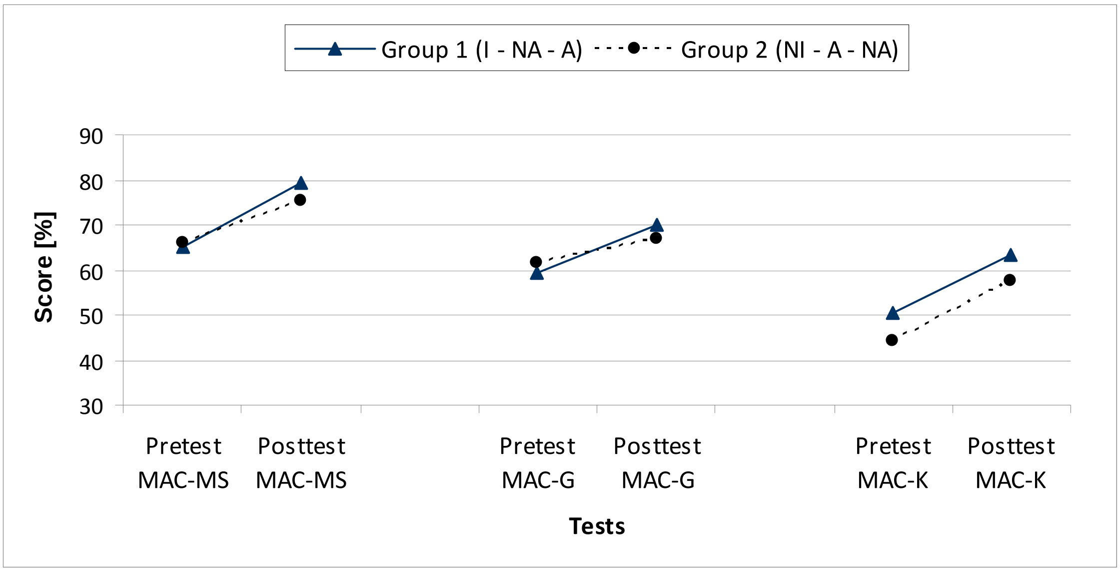

Figure 6. Knowledge transfer scores (%) of the two experimental groups at pretest and posttest

Confidence in answering questions

The originally used five-point scale was transformed to a three-point scale. This transformed confidence score reflects how sure students were with their answers ('I don´t know', 'rather sure' and 'highly sure'). If they selected 'highly sure' in all questions they gained 30 points at pretest and posttest for each MAC and 20 points at each immediate test. The confidence in answering questions at pretest and posttest was analyzed using a 2 (groups) × 2 (tests) ANOVA with repeated measures on the factor tests. There was a significant main effect of tests at MAC-MS (F (1,10) = 162.89, p < .001), MAC-G (F (1,10) = 232.68, p < .001) and MAC-K (F (1,10) = 129.48, p < .001) indicating an increase of confidence in answering the questions (Figure 7) from pretest to posttest. No significant group effects were found for MAC-MS (F (1,10) = .88, p = .37), MAC-G (F (1,10) = .24, p = .63) and MAC-K (F (1,10) = .26, p = .62). The groups × test interactions were also not significant for MAC-MS (F (1,10) = .69, p = .43), MAC-G (F (1,10) = 1.09, p = .32) and MAC-K (F (1,10) = .60, p = .46).

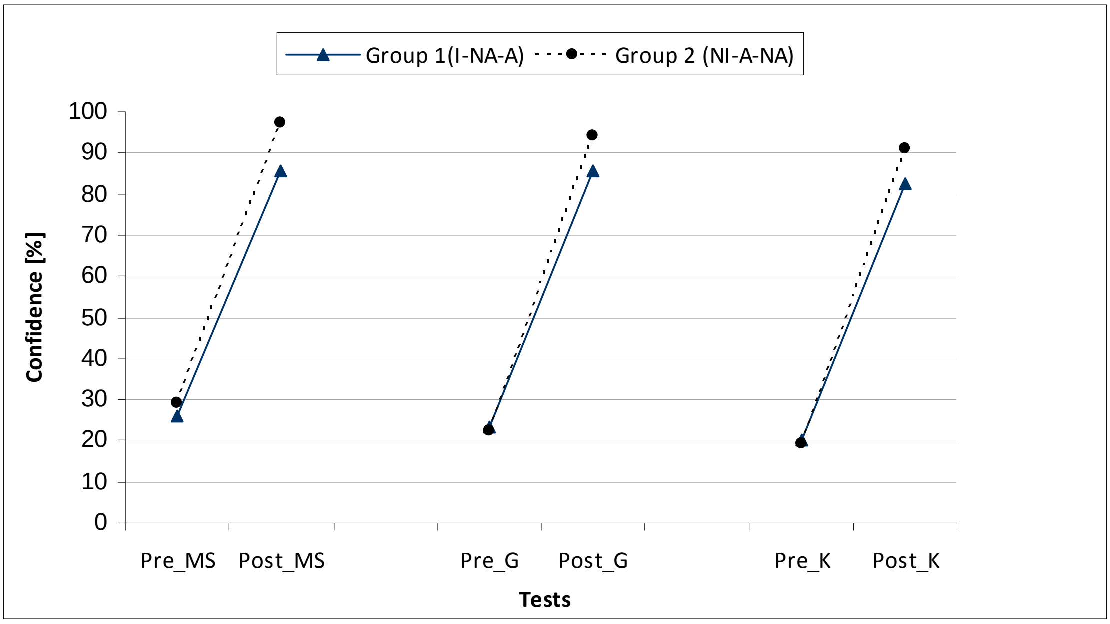

Figure 7. Relative mean confidence scores at pretest (Pre_) and posttest (Post_) for all concepts (MS – Meinel & Schnabel, G – Göhner, K – Kassat)

Confidence scores of immediate tests were analyzed using a 2 (groups) × 3 (MACs) ANOVA with repeated measures on MACs. ANOVA yielded no main effect of groups (F (1,9) = 1.05, p = .33). The main effect of MACs was significant (F (2,18) = 8.31, p < .01). The interaction groups × MACs was not significant (F (2,18) = .29, p = .75). Wilcoxon tests revealed that the MAC-MS was significantly easier than the MAC-G and MAC-K.

Again, hypothesis 1 was not supported.

Questionnaire (Activation and Interactivity)

The experience of activation and interactivity was measured with a four-point scale (4 – ‘strongly agree’, 1 – ‘strongly disagree’). Activation and interactivity of the MAC-MS, MAC-G and MAC-K questionnaire were analyzed using a 3 (MACs) × 2 (groups) × 9 (items) ANOVA with repeated measures on the factor items (Table 4). The analysis yielded a significant main effect of groups (F (1,9) = 9.69, p < .05). There was also a significant interaction of MACs × groups × items (F (16,144) = 2.26, p < .01). Because we were interested in group differences, U-test follow up analyses were calculated.

Table 4. Results of 3 (MACs) × 2 (groups) × 9 (items) ANOVA for differences in perception of activation and interactivity

Effects	***df***	***F***	***p***
Main Effects			
MACs	2,18	2.19	.14
Groups	1,9	9.69	<.05
Items	3,24 $^{\varepsilon}$	1.55	.23
Two-way interaction			
MACs × Groups	2,18	2.10	.15
MACs × Items	16,144	1.30	.21
Groups × Items	8,72	1.22	.30
Three-way interaction			
MACs × Items × Groups	16,144	2.26	<.01

$^{\varepsilon}$ Adjusted with Greenhouse-Geisser ε = .336

U-tests for MAC-MS (Figure 8) confirmed significant group differences concerning the variables 'respond to actions', 'deep learning' and 'self determined learning'.

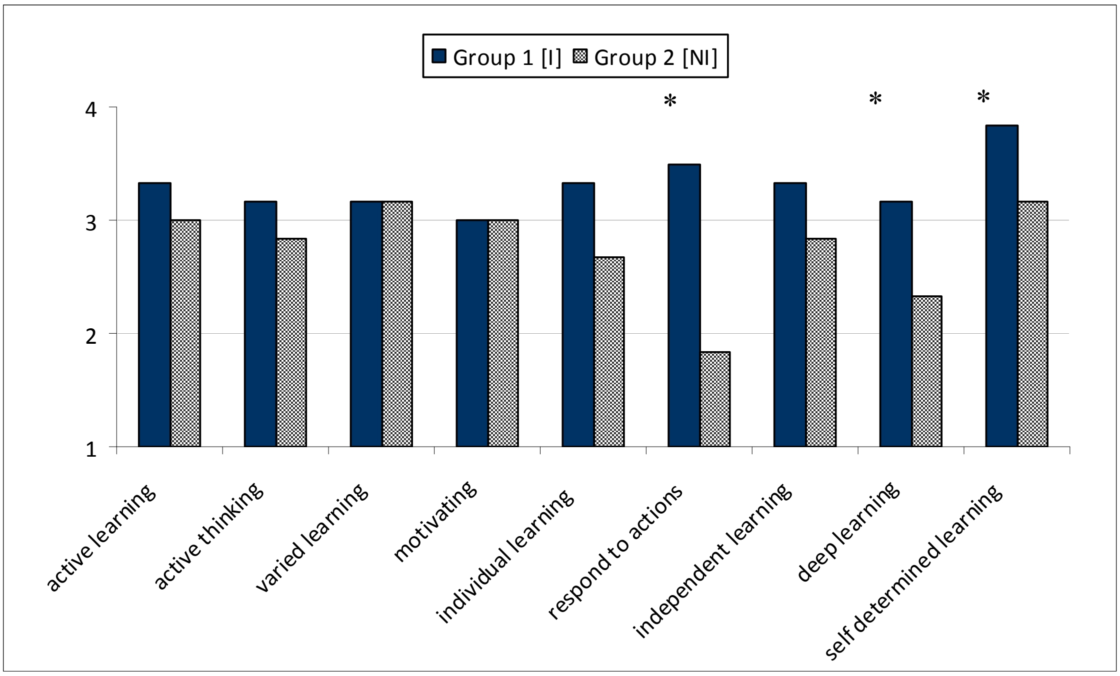

Figure 8. Experienced activation and interactivity of the e-learning unit dealing with the MAC of Meinel & Schnabel (1998) (4 – 'strongly agree' , 1 – 'strongly disagree')

U-tests for MAC-G confirmed significant group differences concerning the variables 'individual learning' and 'self determined learning'. U-test for MAC-K did not show any significant group differences. Hypothesis 2 was supported only for selected variables. Students learning with the interactive or active e-learning units experienced higher activation and interactivity concerning response to actions, deep learning, self-determined learning and individual learning.

Results of open-ended questions

Open-ended questions at the end of the questionnaires showed that participants clearly recognized the differences between the different degrees of interactivity of the e-learning units. Students who learned with the interactive e-learning unit for example mentioned that 'the tasks and questions demonstrated what I have learned' and that they liked the combination of text, video and pictures. Students who learned with the non-interactive e-learning unit complained about 'the lack of direct feedback' or the 'lack of solutions'. Students who learned actively appreciated the interactivity of the units, 'the tasks, which demonstrated what I have learned' and 'the questions which introduced a new topic'. Conversely when learning with the non-active e-learning units they complained about the lack of tasks and questions and that they had 'no opportunity to test what I have learned with the e-learning unit'.

Discussion and Conclusions

The reported pilot study served to test an experimental design for examining different degrees of interactivity and to measure knowledge achievement, motivation, and attitude towards e-learning.

The results reveal various learning effects. A total effect refers to the whole course and a specific effect to the e-learning units. Both experimental groups could improve their knowledge of the three different MACs during the course. Compared to pretest results the results of the immediate tests showed that both experimental groups improved their basic knowledge of each concept after learning with the e-learning units. Altogether students could improve their knowledge continuously until the posttest (no ceiling effect).

Comparing the immediate knowledge test scores of all MACs, these scores showed, that both groups scored best at MAC-MS, second best at MAC-G and worst at MAC-K. This is probably caused by the degree of difficulty of the three concepts, because difficulty and complexity of the concepts are increasing from MAC-MS to MAC-K. Furthermore it is noticeable that group 2 received lower scores than group1 in all immediate tests and that they only performed comparably well in the posttest. A reason for this can not easily be identified. Presumably the students of group 2 were not motivated at the immediate tests.

The students also improved their knowledge transfer concerning MAC-MS and MAC-K from pretest to posttest but there was no effect for MAC-G. A reason for this could be, that the criteria for analysis proposed by Göhner (1979) are comparably abstract. This is consistent with the criticism by Kassat (1995) who states that Göhner (1979) does not deliver clear criteria for analysis.

Contrary to our expectations we did not find any significant differences between the groups who learned with different degrees of interactivity. This could be due to the fact that we only tested small groups (6 participants per group). Furthermore we may not find an interactivity effect because there is a confounding problem. This study tested different degrees of interactivity within a real blended-learning scenario and students are possibly influenced by different factors like chat session, group discussions and team-work after they had learned with the e-learning units. Moreover we could not eliminate or control the impact of potential external factors like using additional support during the online tests. A further reason could be, that despite differences between the interactive and non-interactive version and the active and non-active version of the e-learning units both groups experienced a comparatively enriched learning environment. This may be confirmed by the fact that both groups doubled their knowledge. Maybe more pronounced interactive features within the active and interactive versions of the e-learning units are necessary to show an interactivity effect.

The confidence in answering questions at pretest and posttest shows a similar and even more distinct development as the knowledge test results at pretest and posttest. There is a great increase in confidence from pretest to posttest but no significant differences between the groups. There were also no group differences at the immediate tests for confidence in answering questions. The development of the confidence scores at the immediate tests is also comparable with the immediate knowledge test results. MAC-MS was the easiest concept showing the best knowledge test results and the highest confidence scores, followed by MAC-G and MAC-K.

The variables which measured students' experienced activation and interactivity showed no clear results. The three-way interaction MACs × groups × items indicates that only few variables show differences between groups. The item 'self-determined learning' seems to be particularly sensible, whereas the items 'response to actions', 'individualized learning' and 'deep learning' differentiate only between selected MAC-related e-learning units. An unexpected result occurred with MAC-G. Here group 1 rated the e-learning units as more activating and interactive than group 2, although group 2 received the more activating e-learning unit. Obviously the perception of activation and interactivity of group 1 is generally higher regardless of the real degree of interactivity of the respective e-learning unit. This may be due to a different concept of activation and interactivity.

As a consequence of the inconsistent results the following improvements will be implemented in follow-up research and especially in the next term: First this experiment will be repeated with a larger number of participants to improve validity. A power analysis will be done to determine the sample size needed. To control the impact of potential external factors during the online tests, like using additional support, a time limit will be introduced. The time limit forces students to answer the tests immediately without leaving time to look up solutions or communicate to other persons. Furthermore all test results (except pretest results) will contribute to the final grade. In future research transfer of knowledge should be tested in a broader way using a greater variety of sport movements. Moreover long term retention tests are planned to test whether different degrees of interactivity generate delayed learning effects.

References

Chou, C. (2003). Interactivity and interactive functions in web-based learning systems: a technical framework for designers. *British Journal of Educational Technology, 34* (3), 265-279.

Evans, C. & Gibbons, N. J. (2007). The interactivity effect in multimedia learning. *Computers & Education, 49*, 1147-1160.

Gao, T. & Lehmann, J. D. (2003). The effects of different levels of interaction on the achievement and motivational perceptions of college students in a web-based learning environment. *Journal of Interactive Learning Research, 14* (4), 367-386.

Göhner, U. (1979*). Bewegungsanalyse im Sport*. Schorndorf: Hofmann.

Haseman, W. D., Polatoglu, V. N. & Ramamurthy, K. (2002). An empirical investigation of the influences of the degree of interactivity on user-outcomes in a multimedia environment. *Information Resources Management Journal*, *15* (2), 31-48.

Kassat, G. (1995). *Verborgene Bewegungsstrukturen*. Rödinghausen: fcv.

Kettanurak, V., Ramamurthy, K. & Haseman, W.D. (2001). User attitude as a mediator of learning performance improvement in an interactive multimedia environment: an empirical investigation of the degree of interactivity and learning styles. *International Journal of Human-Computer Studies, 54*, 541-583.

Meinel, K. & Schnabel, G. (1998). *Bewegungslehre – Sportmotorik* (9. Aufl.). Berlin: Sportverlag.

Ritter, S. & Wallach, D. (2006). Interaktivität als Determinante der Lerneffektivität bei der multimedialen Wissensvermittlung. *i-com*, 2, 26-30.

Roblyer, M.D. & Ekhaml, L. (2000). *How interactive are your distance courses? A rubric for assessing interaction in distance learning.* Retrieved July 26, 2009 from http://www.westga.edu/~distance/roblyer32.html

Roznawski, N. & Wiemeyer, J. (2008). Interactivity and interactions in e-learning – Implementation within a blended-learning scenario. *International Journal of Computer Science in Sport*, *7* (2), 52-58.

Sims, R. (1997). Interactivity: a forgotten art. *Computers in Human Behavior, 13* (2), 157-180.

Wagner, E.D. (1997). Interactivity: from agents to outcomes. *New Directions for Teaching and Learning, 71*, 19-26.

Wiemeyer, J. (2008). Multimedia in sport – between illusion and realism. In P. Dabnichki & A. Baca (eds.), *Computers in sport* (pp. 293-317). Southampton: WIT press.